



Escola de Camins

Escola Tècnica Superior d'Enginyeria de Camins, Canals i Ports
UPC BARCELONATECH

2D RIVER FLOOD MODELLING USING HEC-RAS 5.0

Treball realitzat per:

Flotats Palau, Joan

Dirigit per:

Sánchez Juny, Martí

Grau en:

Enginyeria Civil

Barcelona, 20 de juny de 2016

Departament d'Enginyeria Hidràulica, Marítima i Ambiental

TREBALL FINAL DE

2D RIVER FLOOD MODELLING USING HEC-RAS 5.0

Joan Flotats Palau

20/06/2016

Abstract

Flooding may occur as an overflow of water from water bodies, such as a river, lake or ocean, in which the water overtops or breaks levees, resulting in some of that water escaping its usual boundaries. Floods also occur in rivers when the flow rate exceeds the capacity of the river channel.

Floods represent the deadliest natural hazard in Europe, resulting in loss of life, damage to buildings, homes, business and structures such as bridges and roads. Since such consequences are highly undesirable for human beings, the need to avoid or at least control them has become obvious. This led to the appearance of hydrodynamic models, numerical tools able to simulate the flow movement, also in case of flooding. Those models would let us know how the flow behaves in certain situations and how to act in consequence in order to avoid those undesirable effects.

In April 2016, the new two-dimensional version of HEC-RAS has been released, the so-called HEC-RAS 5.0. This version is especially interesting since all previous versions of HEC-RAS had never been able to simulate flows in two dimensions. The main motivation of this document is to analyse the functionality and workability of HEC-RAS 5.0 regarding two-dimensional river flooding. In order to do so, three different work approaches have been carried out, with further analysis of the correspondent results.

First, a detailed intercomparison between the main hydrodynamic models available has been carried out in order to check the features of the new version of HEC-RAS next to another four computational programs.

Second, the same case simulation has been performed at the same time for HEC-RAS 5.0 and for Delft3D. The aim of this is to check the reliability and functionality of HEC-RAS new version regarding to 2D river flood modelling next to an already developed two-dimensional model such as Delft3D is. For this simulation, an ideal created prismatic channel has been chosen in order to work in a basic scenario and two approaches have been analysed: steady non-flooding and unsteady flooding cases.

Finally, and once its workability has been checked, a more complex case has been simulated with HEC-RAS 5.0. In this case, the scenario is a real case study, consisting in a river flood in the Fluvià River, in Catalonia, Spain, with real data of a return period of 50 years, obtained from Agència Catalana de l'Aigua (ACA) in 2009.

The results led to very sensitive output, realistic and similar to the expected and contrasted. Thus, one can conclude that, despite small instabilities were found, HEC-RAS 5.0 is able to perform simple 2D river flood modelling simulations at a similar level of the most advanced two-dimensional programs, such as Delft3D. However, when it comes to very complex simulations, some features, such as combination with transport of substances and water quality or combination with sediment transport and morphological evolution, are not yet available in two dimensions for HEC-RAS 5.0, so one would rather choose a more advanced model.

TABLE OF CONTENTS

1. INTRODUCTION	1
2. THEORY	3
3. METHODOLOGY	7
4. INTERCOMPARISON OF DIFFERENT HYDRODYNAMIC MODELS	8
4.1. ANALYSIS	8
4.2. RESULTS	16
5. SIMULATION PERFORMANCE	18
5.1. SIMPLE IDEALIZED CASE: PRISMATIC CHANNEL	18
5.1.1. CASE DESCRIPTION	18
5.1.2. CONSIDERATIONS	22
5.1.3. PROBLEMS FOUND	24
5.1.4. RESULTS	25
5.1.4.1. HEC-RAS 5.0 SIMULATION	25
5.1.4.2. DELFT3D SIMULATION	31
5.1.5. EXTRA TESTS: M1 AND M2 CURVES	40
5.2. REAL CASE: FLUVIÀ RIVER	42
5.2.1. CASE DESCRIPTION	42
5.2.2. CONSIDERATIONS	46
5.2.3. PERFORMANCE	47
5.2.4. PROBLEMS FOUND	48
5.2.5. RESULTS	49
5.2.6. CONTRAST WITH IBER	58
5.3. OVERVIEW OF THE SIMULATIONS PERFORMED	60
6. CONCLUSIONS	61
7. REFERENCES	64

LIST OF FIGURES

Figure 1.1. a) Flood in Dutch Rhine, 1996. (Blom, 2015) b) Aerial view of the Danube River in Deggendorf, Germany, June 2013. (Blom, 2015)	1
Figure 2.1. Finite volume discretization for a two-dimensional domain. (Bladé, 2010)	5
Figure 2.2. Different mesh examples in detail, for different applications. (Bladé, 2010)	5
Figure 2.3. Example of RAS Mapper interface	6
Figure 3.1. Methodology followed in this paper	7
Figure 4.1.1. Schematic representation of one-dimensional (X), two-dimensional (X,Y) and three-dimensional (X,Y,Z) hydrodynamic models (Cáceres, 2006)	9
Figure 4.1.2. Cross-section example made with HEC-RAS 1D	10
Figure 4.1.3. Example of non-structured mesh composed by triangular elements with IBER (Bladé, 2010)	11
Figure 4.1.4. Schematic approach of Reynolds-averaged Navier Stokes equations. (Blom, 2015)	12
Figure 4.1.5. a) Afferdense waard during a flood. Mild slope, normal flow is subcritical. (Blom, 2015); b) Spillway Para dam US. Steep slope, normal flow is supercritical. (Blom, 2015)	13
Figure 4.1.6. a) Spillway and culvert combination. (The Ras Solution, 2016) b) Bridge structure. (The Ras Solution, 2016)	14
Figure 4.1.7. a) Confluence between Rio Negro and Amazon River, in Brasil, in which sediment transport difference between both rivers is noticeable. (Blom, 2015); b) Amazon River delta, top view. (Blom, 2015)	15
Figure 5.1.1.1. Created channel topography in three-dimensional view, with Delft3D	18
Figure 5.1.1.2. AutoCAD sketch of top and front view of the created channel. Sketch units in meters (m). Please note the sketch is not on scale.	20
Figure 5.1.1.3. AutoCAD Sketch of longitudinal view of the created channel. Sketch units in meters (m). Please note the sketch is not on scale.	20
Figure 5.1.2.1. Rectangular grid created for HEC-RAS 5.0 channel performance	22
Figure 5.1.2.2. Rectangular grid created for Delft3D channel performance	22
Figure 5.1.2.3. Close view of the rectangular grid used in Delft3D, with $25 \times 25 \text{m}^2$ cells	22
Figure 5.1.2.4. Extension of the downstream end boundary condition for the unsteady case (left: steady case; right: unsteady case). Example with Delft3D model	23
Figure 5.1.2.5. HEC-RAS Interface with previous default options and chosen options for the channel	23
Figure 5.1.4.1.1: Channel water depth in steady conditions, with HEC-RAS 5.0	25

Figure 5.1.4.1.2. Location and depth over time graphs for two representative points in the channel reach, for steady conditions, with HEC-RAS 5.0	25
Figure 5.1.4.1.3. Channel water velocity all over the reach for steady conditions, with HEC-RAS 5.0	26
Figure 5.1.4.1.4. Location and velocity over time graph for selected point of the ideal channel, in steady conditions, with HEC-RAS 5.0	26
Figure 5.1.4.1.5. Flooding flow behaviour series of the ideal channel for the unsteady hydrological data created, with HEC-RAS 5.0	27-28
Figure 5.1.4.1.6. Close view of the area at the downstream end of the reach at time 21OCT2008 10:45	28
Figure 5.1.4.1.7. Location, water depth over time graph and velocity over time graph of the two points chosen for analysis in the flooded channel situation, with HEC-RAS 5.0	29
Figure 5.1.4.1.8. Water flow velocity difference between the main channel and the two floodplains in the flooded channel situation (velocity units in m/s), with HEC-RAS 5.0	30
Figure 5.1.4.2.1. Channel water depth all over the reach in steady conditions, with Delft3D	31
Figure 5.1.4.2.2. Channel water level all over the reach in steady conditions, with Delft3D	31
Figure 5.1.4.2.3. Situation of the three observation points for the steady flow performance in the channel, with Delft3D	31
Figure 5.1.4.2.4. Graph showing the two water velocity components over time in the unsteady channel simulation with Delft3D for point (44,28)	32
Figure 5.1.4.2.5. Graph showing the magnitude difference between both velocity components in the unsteady channel simulation with Delft3D for point (44,28)	32
Figure 5.1.4.2.6. Graph showing the two water velocity components over time in the unsteady channel simulation for points (224,29) and (408,28)	33
Figure 5.1.4.2.7. Water depth in the channel for steady flow for the three observation points set	33
Figure 5.1.4.2.8. Graph showing the Froude number all over the reach simulated with Delft3D for the steady channel situation	33
Figure 5.1.4.2.9. Flooding flow behaviour series of the channel for the unsteady hydrological data created, with Delft3D	34-35
Figure 5.1.4.2.10. Situation of observation points over the channel reach and floodplains for unsteady results with Delft3D	36
Figure 5.1.4.2.11. Water depth over time graph of point (224,29) for the flooded channel situation, with Delft3D	36
Figure 5.1.4.2.12. Water depth over time graph of points (224,43) and (224,12) for the flooded channel situation, with Delft3D	36
Figure 5.1.4.2.13. Flow velocity general results for unsteady channel case, with Delft3D	37
Figure 5.1.4.2.14. Close view of flow velocity general results for unsteady channel case, with Delft3D	37
Figure 5.1.4.2.15. Graphs showing the two water velocity components over time and the relation between them, in the unsteady channel simulation, for point (224,43), with Delft3D	38

Figure 5.1.4.2.16. Graphs showing the two water velocity components over time and the relation between them, in the unsteady channel simulation, for point (224,12), with Delft3D	38
Figure 5.1.4.2.17. Graphs showing the two water velocity components over time and the relation between them, in the unsteady channel simulation, for point (224,29), with Delft3D	39
Figure 5.1.4.2.18. Graph showing the Froude number all over the reach simulated with Delft3D for the unsteady channel situation	39
Figure 5.1.5.1. M-type curves (Gutiérrez, 2014)	40
Figure 5.1.5.2. Water depth in the case of M1 curve in the channel. Units in metres.	41
Figure 5.1.5.3. Flow velocity in the case of M2 curve in the channel. Units in metres.	41
Figure 5.1.5.4. Water depth in the case of M2 curve in the channel. Units in metres.	41
Figure 5.1.5.5. Flow velocity in the case of M2 curve in the channel. Units in metres.	41
Figure 5.2.1.1. Fluvià River basin location in Spain (ACA, 2015)	42
Figure 5.2.1.2. Fluvià River reaches and sub basins (ACA, 2015)	43
Figure 5.2.1.3. Domain studied, top view satellite image (Google Maps, 2015)	43
Figure 5.2.1.4. Fluvià hydrograph for T=10 years	45
Figure 5.2.1.5. Fluvià hydrograph for T=50 years	45
Figure 5.2.2.1. a) Thin dam top view (Google Maps, 2015) b) Bridge top view (Google Maps, 2015)	46
Figure 5.2.3.1. Terrain with the mesh and boundaries applied, with HEC-RAS 5.0	47
Figure 5.2.3.2. Mesh and boundaries used for Fluvià River reach, with HEC-RAS 5.0	47
Figure 5.2.3.3. Detailed view for mesh with squared cells used	48
Figure 5.2.4.1. Flooding flow behaviour series of Fluvià River simulation 1 with HEC-RAS 5.0	49-50
Figure 5.2.4.2. Non-flooding flow behaviour series of Fluvià River simulation 2, with HEC-RAS 5.0	51
Figure 5.2.4.3. Flooding flow behaviour series of Fluvià River simulation 3 with HEC-RAS 5.0	53-54
Figure 5.2.4.4. Maximum water depths at Fluvià River reach in Simulation 3, with RAS Mapper interface. Units in metres.	55
Figure 5.2.4.5. Maximum flow velocities at Fluvià River reach in Simulation 3 with RAS Mapper interface. Units in m/s.	55
Figure 5.2.4.6. Location, water depth over time graph and flow velocity over time graph of two points in the main river channel in Fluvià River Simulation 3, with HEC-RAS 5.0	56
Figure 5.2.4.7. Location, water depth over time graph and flow velocity over time graph of two points in the northern floodplain in Fluvià River Simulation 3, with HEC-RAS 5.0	57
Figure 5.2.5.1. Maximum depths in Fluvià River simulation obtained with IBER	58
Figure 5.2.5.2. Maximum water elevations in Fluvià River simulation obtained with IBER	59
Figure 5.2.5.3. Figure X: Maximum velocities in Fluvià River simulation obtained with IBER	59

LIST OF TABLES

Table 2.1. HEC-RAS modelling type and analytic tools evolution. (Bladé, 2015)	6
Table 4.2.1. Intercomparison between different hydrodynamic models results table	17
Table 5.1.1.1. Created channel data, set in a simple Excel file	19
Table 5.1.1.2. Hydrological data created for the purpose of the unsteady flow simulation of the ideal channel	21
Table 5.1.5.1. Boundary conditions set for the M1 and M2 curves in the channel, with HEC-RAS 5.0	40
Table 5.2.1.1. Hydrograph data for T=10 years (ACA, 2009)	45
Table 5.2.1.2. Hydrograph data for T=50 years (ACA, 2009)	45
Table 5.3.1. Overview table of the simulations performed	60

1. INTRODUCTION

Contextualization:

The European Union Floods Directive defines a flood as a covering by water of land not normally covered by water. Flooding may occur as an overflow of water from water bodies, such as a river, lake or ocean, in which the water overtops or breaks levees, resulting in some of that water escaping its usual boundaries. Floods can also occur in rivers when the flow rate exceeds the capacity of the river channel. (European Commission, 2015)

People have traditionally lived and worked by rivers because the surrounding land is usually flat and fertile and because rivers provide easy travel and access to commerce and industry. In consequence, river floods often cause damage to those people, homes and business that are located in the natural flood plains of rivers, consisting in loss of life, damage to buildings and other structures such as bridges, roads, sewerage systems or power systems. (Blom, 2015)

There are many examples of floods that occurred in the past. The deadliest flood in the twentieth century occurred in 1931 in China, in which 70 thousand square miles were flooded and 3.7 million deaths were estimated. The devastating flood also led to starvation for the next months, which would also increase the amount of deaths. But not this only flood occurred in China, five other big floods occurred in the country from 1887 to 1975. However, China is not the only country that suffered the consequences of flooding. In 2004, Indian Ocean Tsunami led to 230000 deaths in Indonesia and surrounding countries, such as Thailand and Sri Lanka, and 100000 people were killed in 1971 in North Vietnam due to the Hanoi and Red River Delta flood. Although the most devastating floods did not happen in Europe, there are also examples of European deadly floods, such as the so-called St. Felix Flood in The Netherlands, in 1530, in which more than 100 thousand people were killed, and more recently, the combination of earthquake, tsunami and fires that happen in Messina in 1908, which ended up killing more than one hundred thousand people. (O'Connor, 2004)

Not only in the past but also today, floods represent the deadliest natural hazard in Europe.



Figure 1.1. a) Flood in Dutch Rhine, 1996. (Blom, 2015)

b) Aerial view of the Danube River in Deggendorf, Germany, June 2013. (Blom, 2015)

Since such consequences are highly undesirable for human beings, the need to avoid or at least control them has become obvious. This led to the appearance of hydrodynamic models, numerical tools able to simulate the flow movement, also in case of flooding. Those models would let us know how the flow behaves in certain situations and how to act in consequence. For example, we could figure out that a certain river is especially dangerous in respect to flooding and we could build a dam in order to control its water flow or, if not possible, could avoid building next to it or create an efficient warning system.

Nowadays, several numerical models are available for flood modelling. Some of them, such as HEC-RAS, Delft3D, IBER, SOBEK and 3Di, will be explained in detail in the next sections, but there is a large number of other models that can fulfil the same objectives.

In April 2016, the new two-dimensional (and combined) version of HEC-RAS has been released, the so-called HEC-RAS 5.0. This version is especially interesting since all previous versions of HEC-RAS had never been able to simulate flows in two dimensions.

Research question

The initial motivation towards this project is the release of the new version of HEC-RAS, namely HEC-RAS 5.0, which, as said, introduces for the first time the two-dimensional approach in this model.

This study aims to analyse the workability, new features and potential of the new version, not only working with it but also comparing to other models to which it aims to be competitive. The main focus will be set on flood simulation, since the second case study shows relevant interest in this aspect.

Two main statements related to the topic are presented:

- First: It is not clear how to choose an appropriate numerical model for flood safety.
- Second: The performance of the new HEC-RAS version is still unknown.

Thus, the main questions that the project aims to answer are the following:

- What are the features of different modelling systems?
- What features are important in order to choose an appropriate model for flooding?
- How does the new HEC-RAS version compare to one of the existing modelling systems?
- To what extent is HEC-RAS 5.0 competitive with other hydrodynamic models, regarding 2D flood modelling?

The first two questions relate to the first statement, while the third and fourth questions relate to the second statement.

In order to solve the first and second questions, which are definitely related, a detailed analysis of the main hydrodynamic models is done. The models studied are: HEC-RAS, Delft3D, IBER, SOBEK and 3Di. A research on which features to analyse in the intercomparison of those models leads to the answer of the first question. Once the intercomparison between the chosen features for each of those models is done, a conclusion leads to the answer of the second question.

Also, the intercomparison results give the keys on how to choose an appropriate model for a practical comparison with HEC-RAS 5.0. The model chosen for this purpose is Delft3D and the arguments for this choice are explained in the intercomparison results section.

The third and fourth question have a more practical approach.

For the purpose of the third and fourth questions, this document shows a study of the hydraulic behaviour of a simple case by means of HEC-RAS 5.0 and Delft3D models, in order to be able to compare and analyse the results and features of two different models and get to relevant conclusions.

Besides, once HEC-RAS 5.0 workability is checked next to Delft3D, a real case study is performed by means of this model. With this more complex and real case study one can check again the reliability of HEC-RAS 5.0 flood simulations.

Those two cases are first, an idealized prismatic channel reach; and second, a real case based on a Fluvià river reach, next to Torroella de Fluvià, in Catalonia, Spain. The objective of the latter is to study the flood extension for hydrological data of a return period of 50 years given by Agència Catalana de l'Aigua (ACA; Catalan Water Agency) in July 2009.

2. THEORY

To be able to understand this document, it is necessary to have a background on the topic. In this section, it is described what hydrodynamic models are, how they work and their most relevant properties.

What is, in fact, a hydrodynamic model?

Let us start from the beginning. Hydrodynamics is the study of motion of liquids and, in particular, the study of motion of water. Thus, a *hydrodynamic model* is a tool to describe or represent in some way the motion of water. Although virtually all hydrodynamic models in use today are computational numerical models, a hydrodynamic model could in fact be a physical model built on scale, as it was before the advent of widely available computer systems.

Since hydrodynamic modelling is part of the larger field of computational fluid dynamics, those models used for coastal ocean and river applications have a lot in common with models developed for meteorology, aerospace and automotive design, ventilation systems, etc. Its common basis is the numerical solution of the governing equations of conservation of momentum and mass in fluid. (NOAA, 2015)

How do hydrodynamic models work?

Computational hydrodynamic models are based on a set of equations that describe fluid motion, the so-called Navier-Stokes equations. Those equations are derived from Newton's laws of motion and describe the action of force applied to a fluid; that is, the resulting changes in flow. This property is called conservation of momentum and is basically Newton's second law, which says acceleration is dependent upon the force exerted and proportional to its mass. The continuity principle is also imposed by computational hydrodynamics. This principle states that mass and momentum are conserved unless they pass out the domain. In hydrodynamic modelling, the Navier-Stokes equations are simplified according to the specific characteristics and properties of the coastal ocean, resulting in the so-called Shallow Water Equations, whose name expresses the fact that the vertical features are neglected over the horizontal. The Shallow Water Equations allow for more efficient numerical solution of flow in the oceans, coastal zones, estuaries, plain rivers and lakes environment, in which the length and width are much more relevant than the depth.

Rivers, estuaries and oceans are usually very complex systems, which impede an analytical solution of the governing equations. Computer development has allowed researchers to address these complex issues through numerical methods. To solve a problem, computers perform discrete calculations of the continuous governing equations for small individual problems (breaking the system into multiple small parts) in order to be able to quickly solve the system. Two classes of approach are commonly used when modelling: structured grid approaches (finite differences and finite volumes algorithms) and unstructured grid approaches (finite element and finite volume methods). To form a grid, the domain is separated into numerous components through a discretization process. Although structured grids provide straightforward and efficient algorithms, their grid's flexibility in solving the system is limited since they usually use quadrilateral cells. Unstructured grid models provide much more flexibility in their grid resolution by means of employing variable triangular elements. In consequence, they tend to be more time consuming to run and more sensitive to numerical errors. Both kinds of numerical methods can be applied to high performance computing systems and are able to simulate complex coastal and river areas at high resolution.

The accuracy of those models is related to the provided input, this is, the topography and meteorological conditions. Data such as river inflow and tidal signals at the boundaries are required in order to run a simulation. (NOAA, 2015)

The hydrodynamic equations in detail

In order to understand how the main models behave, it is advisable to take a look at the general equations for variable regime in two dimensions, this is, the two-dimensional Saint-Venant equations, the so-called *Shallow Water Equations*. These equations are valid for flows with a two-dimensional character: small vertical velocities, small bed slope values and horizontal dimensions generally predominant over vertical dimension.

Those equations are the following:

$$\frac{\partial}{\partial t} \mathbf{U} + \nabla \mathbf{F} = \mathbf{H}$$

Where \mathbf{U} is the flow variables vector, \mathbf{F} is the flow tensor and \mathbf{H} is the independent term, which are expressed as follows:

$$\mathbf{U} = \begin{pmatrix} h \\ hu \\ hv \end{pmatrix} ; \quad \mathbf{F} = \begin{pmatrix} hu & hv \\ hu^2 + g \frac{h^2}{2} & huv \\ huv & hv^2 + g \frac{h^2}{2} \end{pmatrix} ; \quad \mathbf{H} = \begin{pmatrix} 0 \\ gh(S_{ox} - S_{fx}) \\ gh(S_{oy} - S_{fy}) \end{pmatrix}$$

where

- h is water depth
- u and v are velocity components
- S_{ox} and S_{oy} are the geometric slopes in x- and y-direction
- S_{fx} and S_{fy} are the driving slope in x- and y-direction
- g is acceleration due to gravity

As mentioned, the previous equation consists of three terms. The first term shows the local temporal variation of the hydraulic variables (flow depth and flow velocity). The second term represents the special variation of flow of those quantities. Finally, the third term, the so-called independent term, represents the mass and momentum gain or loss per time unit in a differential volume moving with the fluid. Since the mass variation has to be null, the first component of the independent term vector is zero.

The Shallow Water Equations are a specific case of differential equations system in hyperbolic, quasi-linear and independent term partial derivatives. The great utility of the finite volume technique has been proved when developing high-resolution two-dimensional schemes, since the finite volumes allow us discretize the domain by irregular meshes and, therefore, adapted to the contours of each specific case, and uses the integral formulation of the equations.

The finite volumes in the mesh can both be four-sided or triangular, or even combination of them. The mesh can be regular or irregular (and structured or unstructured in the latter case).

In two-dimensional modelling the initial conditions needed to introduce to each volume element are the water depth (or, alternatively, the water height level), and both components of velocity. It is possible to start the calculations with a dry domain (or part of it). For those dry elements, the water depth and the velocity components are considered to be null. (Bladé, 2010)

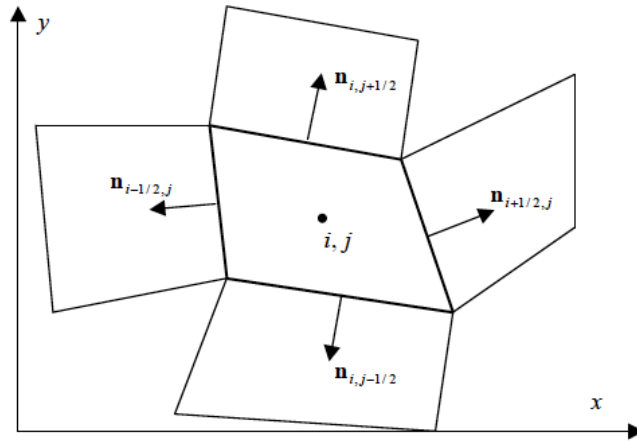


Figure 2.1. Finite volume discretization for a two-dimensional domain. (Bladé, 2010)

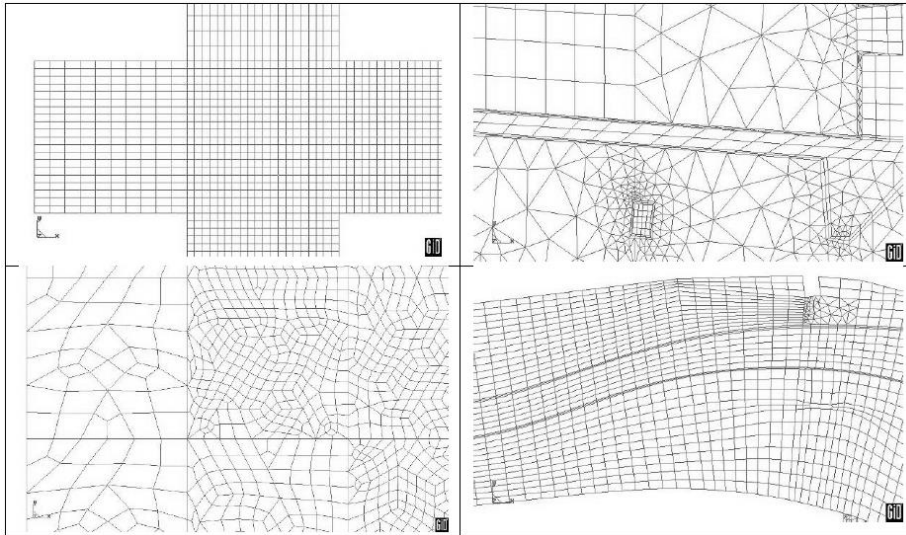


Figure 2.2. Different mesh examples in detail, for different applications. (Bladé, 2010)

About Delft3D

A brief introduction to Delft3D –and also to its FLOW module– is convenient since it takes important part in the case study.

Delft3D has been developed by Deltares (Delft, The Netherlands). This fully integrated software suite provides a multidisciplinary approach and 3D computations for river, coastal and estuarine zones. Delft3D can simulate flows, sediment transports, waves, water quality, morphological developments and ecology; and is designed for both experts and non-experts.

Delft3D is a suite composed of several modules that can be executed independently or in combination with other modules by means of a so-called communication file. Delft3D-FLOW is one of this modules/components. Delft3D-FLOW is a multidimensional (2D or 3D) hydrodynamic and transport simulation program that calculates non-steady flow and transport phenomena that result from tidal and meteorological forcing on a rectilinear or a curvilinear, boundary fitted grid. In 3D simulations, the vertical grid is defined following the σ co-ordinate approach. (Deltares, 2014)

About HEC-RAS

In this document, HEC-RAS is the model that needs the most attention, since its new version is its main motivation origin. HEC-RAS has been evolving for the last years and its latest version –HEC-RAS 5.0.1 version– is capable to simulate the water flow in one and two dimensions –and also both combined–. The following table shows how HEC-RAS has been evolving in relation to the different flow conditions:

Table 2.1. HEC-RAS modelling type and analytic tools evolution. (Bladé, 2015)

Version	1D	Quasi 2D	2D	Permanent flux	Non-permanent flux	Sediment transport	Water quality
2.2	✓			✓			
3.1.3	✓			✓	✓		
4.1.0	✓	✓		✓	✓	✓	✓
5.0	✓	✓	✓	✓	✓	✓	✓

Note: a relevant limitation of HEC-RAS model is that it is not yet capable to apply simulation of sediment transport and water quality in *two* dimensions.

HEC-RAS 5.0 uses the equations of Diffusive wave and Saint-Venant by means of the implicit finite volumes algorithm. The latest version also includes RAS Mapper, an interface window in which the user integrates the digital model of the land, as an initial step for the flow simulation.

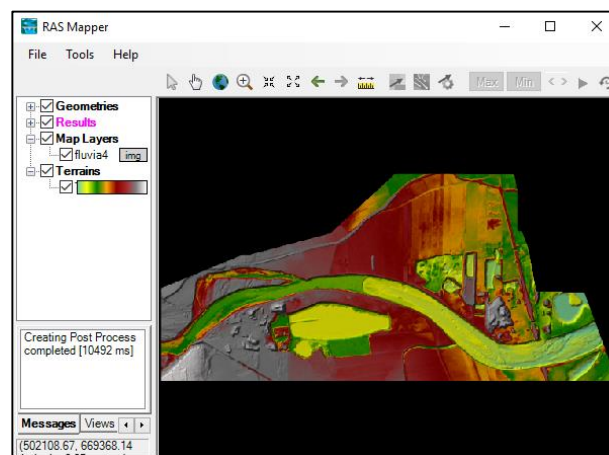


Figure 2.3. Example of RAS Mapper interface

Version 5.0.1 of HEC-RAS includes the following new features (US Army Corps of Engineers, 2016):

1. Two dimensional and combined 1D/2D Unsteady Flow Modelling
2. New HEC-RAS Mapper capabilities and enhancements
3. Automated Manning's n value calibration for 1D unsteady flow
4. Simplified Physical Breaching algorithm for Dam and Levees
5. Breach Width and development time calculator
6. New hydraulic outlet features for inline structures
7. Sediment transport modelling enhancements: including unsteady flow sediment transport analyses, reservoir flushing and sluicing, as well as channel stability using BSTEM integrated within HEC-RAS
8. Completely new 2D User's Manual
9. Several new example applications within the Applications Guide
10. Updates User's Manual, Hydraulic Reference Manual, Applications Guide and Help System

3. METHODOLOGY

The study procedure, this is, the numerical modelling will be carried out by means of two simulation case studies and two different hydrodynamic models: HEC-RAS 5.0 and Delft3D. Those case studies have only been performed in two dimensions and focusing on the river flooding simulation approach.

In order to choose which program to compare to HEC-RAS 5.0, a detailed analysis between the main hydrodynamic models has been first done in the next section. The model finally chosen is, as mentioned, Delft3D.

The next schematic figure gives an idea of the methodology of this document, from the initial motivation to the final method.

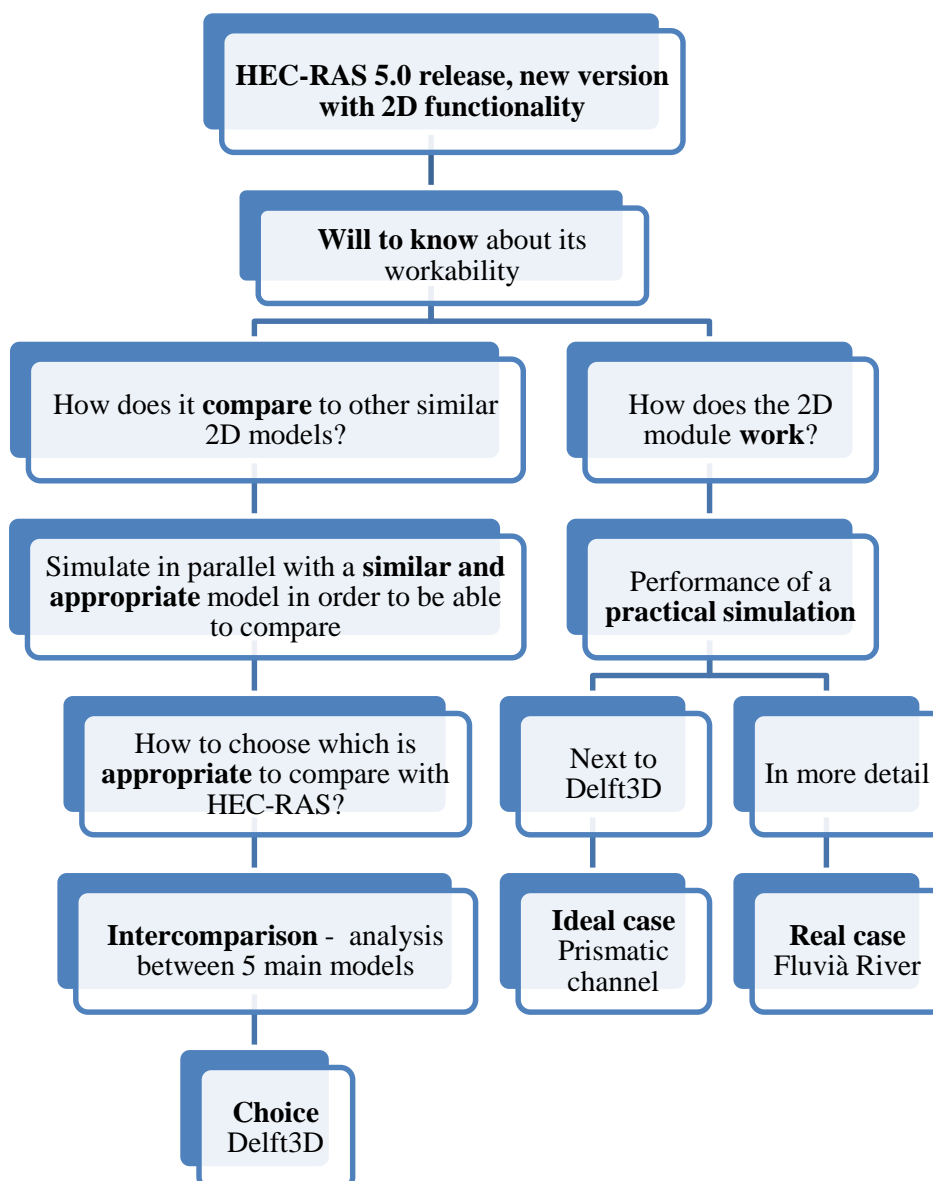


Figure 3.1. Methodology followed in this paper

4. INTERCOMPARISON OF DIFFERENT HYDRODYNAMIC MODELS

4.1. ANALYSIS

For a clear and schematic analysis of the main hydrodynamic modelling systems, one first needs a detailed explanation of the different features. There are several characteristics to describe numerical models. However, the most relevant will be discussed in this section.

Dimensions

Hydrodynamic models can be differentiated between one-dimensional (1D), two-dimensional (2D) and three-dimensional (3D).

On one hand, one-dimensional models are the simplest option. They only need a velocity u and a water depth d to compute the water flow movement. It is assumed that one of the directions, the longitudinal direction along the river axis, prevails above the other directions. Thus, these models are simpler since they do only take into account the longitudinal axis. The hydraulic data is applied through transversal cross-sections, with average values for each cross-section. This means that the full cross-section is represented by a single value of velocity, without consideration of any differential neither horizontally nor vertically. One relevant limitation for one-dimensional models is that they assume the flow is totally perpendicular to the cross-section. This kind of models is applicable to very long reaches, generally twenty or more times larger than the width. (Cáceres, 2006)

One-dimensional models have several advantages, such as:

- They can usually be set up quickly and their computations are fast. Time series simulations and large networks simulations will generally require only some minutes of computer time to run
- Can accurately represent cross-sections area of channels at all stages because they do not require grids to approximate cross-section as two- and three-dimensional models do.
- Little field data is required in order to set up the model
- They generally include more powerful capabilities to describe control structures than two- and three-dimensional models do

But they also have a main disadvantage, based on the inability to describe two-dimensional characteristics such as channel meander, circulation within large water bodies or stratification. (Moffatt and Nichol, 2005)

On the other hand, two-dimensional models are able to describe the movement in two directions and use both components of velocity (u_x, u_y) on the horizontal plane. Those models are usually called shallow water models since they are especially useful for extensive flows (like estuaries or lakes) where the vertical velocity variation is low. They are not recommended for notable vertical velocity variations. Those models can be called 2DH models, while 2DV models have flow velocity components in the vertical plane (one component in the horizontal streamwise direction and one component in the vertical direction). However, in this document, when one speaks about two-dimensional models is only referring to 2DH models. 2DV models are not relevant for the practical part of this document.

A two-dimensional model is indispensable if the problem involves complicated circulation patterns. However, these models require more data and are more time consuming to run. Also, two-dimensional have more numerical stability problems. (Moffatt and Nichol, 2005)

Finally, three-dimensional models are needed when the vertical component of the velocity (u_z) also takes part. The vertical dimension is modelled through a number of layers which is usually from two to ten or even more. 3D models represent the most advanced state of modelling. Those models are capable to calculate the three spatial components of velocity and are therefore applicable to any practical case, although it might not be recommendable when the horizontal dimensions are much larger than the vertical dimensions, for practical reasons.

Three-dimensional models provide the most detailed look at a hydrodynamic system, at a penalty of much longer computer simulation times and the requirement for a substantial amount of field data to capture the complexities of flow in all three dimensions in the most complex cases. (Moffatt and Nichol, 2005)

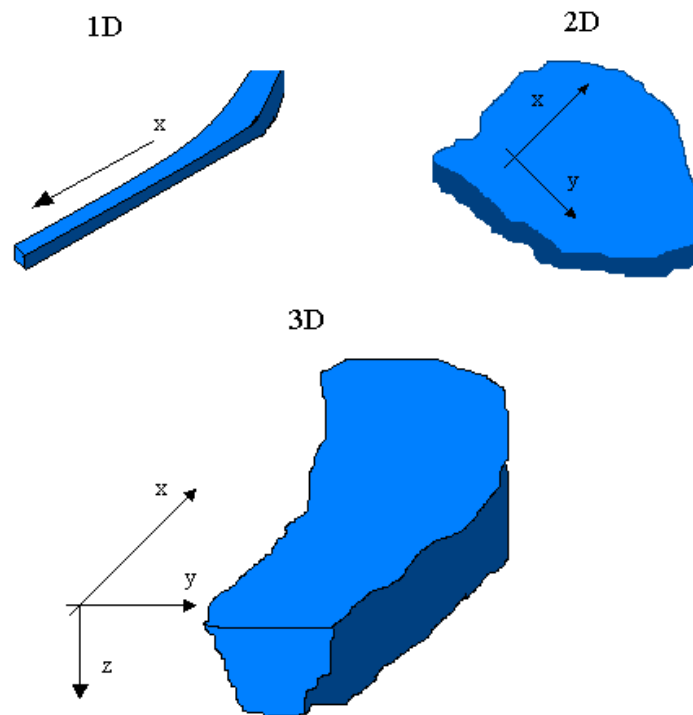


Figure 4.1.1. Schematic representation of one-dimensional (X), two-dimensional (X,Y) and three-dimensional (X,Y,Z) hydrodynamic models (Cáceres, 2006)

While the old version of HEC-RAS is a one-dimensional model, IBER and SOBEK are two-dimensional models and, for instance, Delft3D can fulfil the 3D approach.

Finite difference and finite element models and grid types

Since water is constituted for a quasi-infinite number of particles, it is very hard to solve the water flow behaviour of a determined scenario. The way to deal with it is dividing the water mass in discrete elements with finite size, in order to make management possible for computers.

For the simpler cases of one-dimensional models, such as the previous versions of HEC-RAS, the discretization is performed through transversal cross-sections. The methodology in this case consists on balancing the energy in one section and then proceeding with the next one until finishing all of them. This is a very simple method. Therefore, those programs are generally robust, fast and reliable.

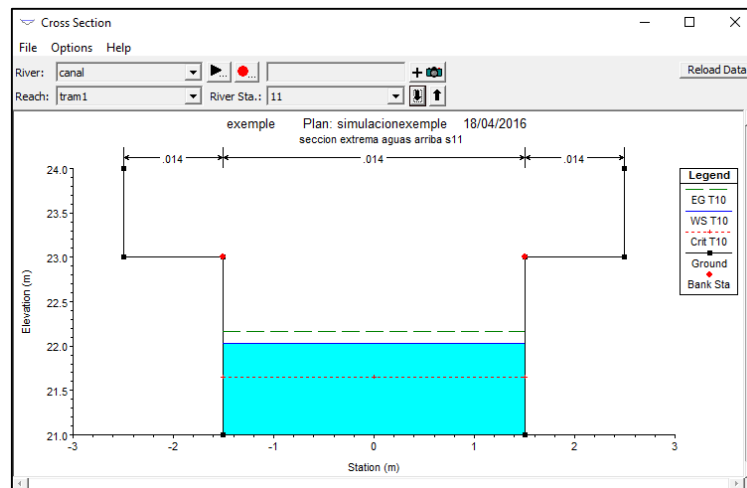


Figure 4.1.2. Cross-section example made with HEC-RAS 1D

Since two- and three-dimensional cases lead to a differential equation process, a more detailed discretization through a computational grid is required. This grid has a determined shape and characteristics that are needed to classify them: structured or unstructured mesh, rectilinear or curvilinear elements, elements of a determined number of sides (squared, quadtrees...), etc.

The different types of grids are the following (Moffatt and Nichol, 2005):

- Rectangular grids: since real river boundaries have curved shapes, these grids suffer from the relevant disadvantage that the contour cells do not match a perfect shape and information is lost (water bodies are represented as stair-step edges). Thus, this requires a fine grid with small cell sizes.
- Curvilinear orthogonal grids: the curvilinear grid can be fitted along boundaries and contours. Thus, these grids are able to represent the configuration of a water body more accurately than rectangular grids do.
- Unstructured grids: sometimes, simulations need to be more detailed somewhere and less detailed elsewhere. Unstructured grids are appropriate in those cases, because they are able to incorporate model elements that vary in size. Complex boundaries and contours can be smoothly fitted. However, they can be very time consuming to set up.

Those grids contain all the elements for which the partial differential equations must be solved. The two main approaches for this purpose are (Moffatt and Nichol, 2005):

- The finite-difference method: for each time step, represents the water levels at a set of discrete points. The typical solution grid is a network of straight or curved lines with nodes at the intersections.
- The finite-element method: the solution domain is divided into a set of triangular or polygonal elements. The water levels and currents are described as linear or quadratic functions across each finite element.

Generally, finite-difference calculations are more computationally efficient than finite-element calculations, for a given network size. However, finite-difference models are generally limited to a rectangular or curved grid, while finite-element grids are more appropriate for irregularly shaped model domains. In conclusion, finite-difference solutions often require finer grids with smaller cell sizes than finite-element solutions when modelling complex shapes. Also, for finite-element solutions, the time step can be longer, which leads to a faster simulation process. (Moffatt and Nichol, 2005)

One should note that the calculation precision is directly related to the used mesh, and the latter to the topography quality. Note that this means that if the same case is applied to two different models with the same cell size and same time step, the level of detail will be exactly the same. However, the accuracy can be different for different programs.

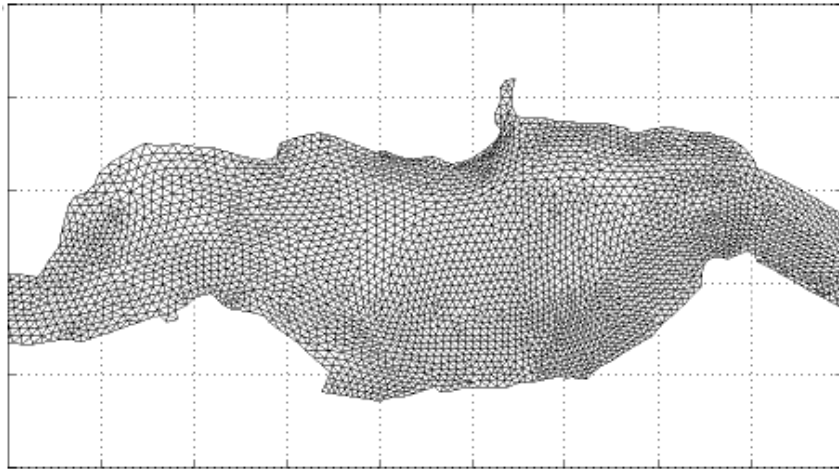


Figure 4.1.3. Example of non-structured mesh composed by triangular elements with IBER (Bladé, 2010)

Hydrodynamic equations

The hydrodynamic equations used for each model is definitely a main feature to consider. The equations used can be divided into two main groups: Reynolds-averaged Navier Stokes equations (RANS) and Horizontal Large-Eddy Simulation equations (HLES).

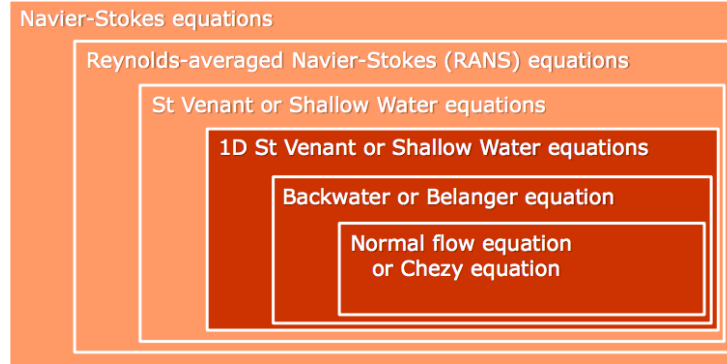


Figure 4.1.4. Schematic approach of Reynolds-averaged Navier Stokes equations. (Blom, 2015)

Reynolds-averaged Navier Stokes equations (RANS) are the most common used in the main hydrodynamic models and the ones which are used in this document simulation.

Although the Navier Stokes equations describe the turbulent flux in rivers and that numerical schemes do exist for its resolution, it is not yet possible to model turbulence flux in an exact manner. This is due to the fact that for such a small scale, a computational capacity that does not exist yet would be required. This limitation motivated the development of certain models based in a statistics approximation in order to model turbulence by means of the so-called Reynolds-averaged Navier-Stokes equations (RANS). Those equations are obtained from the averaging of the Navier-Stokes equations in a bigger scale than the turbulence scale. Thus, RANS equations describe features (velocity, pressure, temperature, et cetera) in average but not the details of the turbulent fluctuations (Pedrozo-Acuña, 2011).

The Reynolds-averaged Navier-Stokes equations are (Pedrozo-Acuña, 2011):

$$\frac{\partial \langle \bar{u}_i \rangle}{\partial x_i} = 0$$

$$\frac{\partial \langle \bar{u}_i \rangle}{\partial t} + \frac{\langle \bar{u}_i \rangle}{n(1+c_A)} \frac{\partial \langle \bar{u}_i \rangle}{\partial x_j} = \frac{1}{(1+c_A)} \left[-\frac{n}{\rho} \frac{\partial \langle \bar{p} \rangle^f}{\partial x_i} - \frac{\partial \langle u_i u_j \rangle}{\partial x_j} + \frac{1}{\rho} \frac{\partial \langle \tau_{ij} \rangle}{\partial x_j} + n g_i \right]$$

$$- \frac{1}{1+c_A} \left[\frac{\alpha(1-n)^2}{n^2 D_{50}^2} \langle \bar{u}_i \rangle + \frac{\beta(1-n)}{n^2 D_{50}} \sqrt{\langle \bar{u}_1 \rangle^2 + \langle \bar{u}_2 \rangle^2} \langle \bar{u}_i \rangle \right]$$

$$\langle a \rangle = \frac{1}{V} \int_V a \, dV$$

$$\langle a \rangle^f = \frac{1}{V_f} \int_{V_f} a \, dV$$

where u_i is the i-component of the velocities vector, ρ is the fluid density, p is the pressure, g_i is the i-component of the acceleration of gravity and τ_{ij} is the tensor of viscosity tensions (Pedrozo-Acuña, 2011).

Only Delft3D can work with Horizontal Large-Eddy Simulation equations (HLES), while the other five cases studied can only perform simulations using Reynolds-averaged Navier Stokes equations (RANS).

Supercritical flow

Sometimes, in a river scenario, one can find that the water depth is higher than the critical water depth. This state is the so-called slow regime or subcritical flow. Also, one can find the opposite: a lower water level than the equilibrium. This state is the so-called fast regime or supercritical flow. Finally, critical flow is the state in which the water depth equals the equilibrium water depth.

The calculation of the Froude number Fr let us know easily if a river is in supercritical or subcritical flow state. The Froude number Fr is defined as the division of the inertia forces over the gravity forces, as follows (Gutiérrez, 2014):

$$Fr = \frac{u}{\sqrt{g \cdot d_e}}$$

where u is the flow velocity, g is the acceleration of gravity and d_e is the equilibrium water depth.

And, depending on its value, one has:

Subcritical flow if	$Fr < 1$
Critical flow if	$Fr = 1$
Supercritical flow if	$Fr > 1$



Figure 4.1.5. a) Afferdense waard during a flood. Mild slope, normal flow is subcritical. (Blom, 2015); b) Spillway Para dam US. Steep slope, normal flow is supercritical. (Blom, 2015)

Subcritical flow, this is, Froude number $Fr < 1$, is generally simple and all models are able to simulate it. However, supercritical flow, this is, Froude number $Fr > 1$, is particularly complex for some numerical models, since a rapidly varied flow caused by hydraulic jumps and crash waves is difficult to model. The most difficult aspect to model is usually the case in which subcritical and supercritical flow are alternatively switching. For this reason, it is an important characteristic of models whether they can run supercritical (or combined) flow or not. (Cáceres, 2006)

In this document, all programs analysed are, to a certain extent, able to model supercritical flow.

Structures

When it comes to real cases, some structures take part of the hydrodynamic scenario. It is usual to find bridges, culverts, lateral structures, sluice gates, pump stations, weirs or porous plates along a river or channel reach. This brings us to the need of hydrodynamic models to adapt to reality; this is, to add those structures to their simulations.

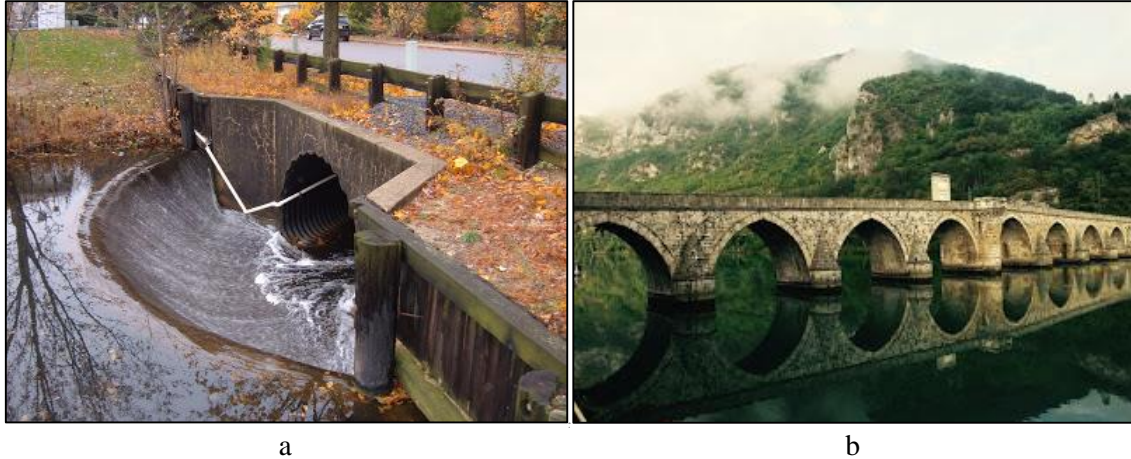


Figure 4.1.6. a) Spillway and culvert combination. (The Ras Solution, 2016)
b) Bridge structure.(The Ras Solution, 2016)

Some models can model most of these structures while others cannot yet. Thus, this is another important aspect to take into account when classifying hydrodynamic models.

Generally, Delft3D, SOBEK and 3Di are capable to model more different kind of structures than HEC-RAS or IBER.

Combination with transport of substances and water quality

Modelling transport of substances and water quality is a useful tool that allows us to predict how poured in water substances will behave by means of numerical models. The aim of this approach is preservation of water quality in the environment and public health.

For instance, Delft3D can provide functionality for transport of substances and water quality, in which the user can add any kind of pollutants and tracers or salinity. However, other models like 3Di do not offer this feature. In case of HEC-RAS, this feature is only present for one-dimensional simulations.

Although this aspect of modelling has its importance, it will not be regarded in the practical of this paper since HEC-RAS does not include it in the two-dimensional approach yet and in order to simplify the problem.

Combination with sediment transport and morphological evolution

One of the greatest aims of river engineering is the prediction of morphological evolution. In practical cases, river bed and water flow interact so that bed elevation can change due to the water flow and vice versa. This feature is important to predict how a bed level will develop in case of construction of new structures in a river or canal reach such as dams, dikes or bridges, but also in case of narrowing or widening. (Blom, 2015)

The models offering this feature are the same as the ones that did for the last section. Again, HEC-RAS can only simulate sediment transport and morphological evolution for one-dimensional cases and 3Di cannot offer this feature at all.

The same reasons as in combination with transport of substances and water quality bring this document to leave this feature aside for the practical sections.



Figure 4.1.7. a) Confluence between Rio Negro and Amazon River, in Brasil, in which sediment transport difference between both rivers is noticeable. (Blom, 2015)
b) Amazon River delta, top view. (Blom, 2015)

Local running availability

Sometimes, the high computational –and economical– costs that a simulation represents are not affordable for a local –standard– computer. This means that, for some models, certain equipment is required. For example, local running is possible with models like HEC-RAS, IBER or Delft3D, but 3Di cannot be ran in a local computer and the purchase of the required equipment to do so is really expensive –about 20.000€–. (3Di Waterbeheer consortium, 2014)

Open source

Some hydrodynamic models allow the user to have access to the source; this is, to the program itself, so that the user can manipulate the program in order to make it more appropriate for his or her work.

For instance, programs developed by US Army Corps of Engineers and Flumen; this is, HEC-RAS and IBER, do not offer an open source, while models like Delft3D, SOBEK and 3Di do.

Others

Many other aspects can be analysed when it comes to hydrodynamic models, such as turbulence submodels, hydraulic roughness origin, source terms (tributary rivers, wind effects, Coriolis forces), real-time control availability, drying and wetting treatment, et cetera.

4.2. RESULTS

All the present features in section 4.1 have been considered for every of the models studied in order to do a proper intercomparison. The results of this model intercomparison are exposed in detail in the next section.

The detailed study of the different features of the five hydrodynamic models of study has been analysed by means of their corresponding user manuals and other papers, all of them referenced at the end of this document.

The intercomparison results have been published in the intercomparison table of features that follows in the next page. In it, one can find the characteristics of every feature analysed for every of the five computational programs studied.

One of the aims of this intercomparison between five hydrodynamic models is to find an appropriate program for the performance of a parallel simulation with HEC-RAS 5.0 for a practical case. Its results considered Delft3D to be a suitable model for a more detailed comparison with HEC-RAS 5.0. In addition, this model was available at Delft University of Technology. Those reasons led to the choice of this program for the performance of a basic ideal case simulation next to HEC-RAS 5.0 in order to analyse both models from a practical point of view. The steps followed for this choice are explained below.

The model chosen needs to fulfil some requirements in order to be appropriate for this paper.

- Two-dimensional workability
- Similar or at least comparable to HEC-RAS 5.0 two-dimensional approach. This is, for instance, capacity to use the same hydrodynamic equations and similar numerical equations method.
- Possibility for local running. This requirement is essential since this study has limited budget. As the table of results show, 3Di model cannot be run in an ordinary computer. For this reason, this program will not be taken into account for the practical case.
- Special interest on the chosen method. This requirement mainly refers not to perform studies that have already been performed. In this case, a very similar study using IBER has already been done (Bladé, 2010), which led us to a lack of interest in repeating the exact same study. Thus, IBER will be deleted from the list of possible choices.

Therefore, the only models left are SOBEK and Delft3D. Although both models are considered appropriate for a practical case simulation in comparison to HEC-RAS 5.0, the latter will be chosen because of the availability reasons mentioned above.

Thus, the ideal channel simulation that follows in the next sections will be performed both by HEC-RAS 5.0 and Delft3D, in a two-dimensional approach, in order to analyse their workability and functionality.

Table 4.2.1. Intercomparison between different hydrodynamic models. Results table

	HEC-RAS 1D	HEC-RAS 5.0	IBER	Delft3D	SOBEK	3Di
Dimensions	1D	1D & 2D	2D	2D & 3D	1D & 2D	1D & 2D
Computational grid	NO GRID	Structured and unstructured	Structured and Non-structured mesh with 3- and 4-side elements	Rectilinear or curvilinear, boundary fitted grid	1D / 2D elements grid	Sub-grid with irregular quadrees
Hydrodynamic equations	RANS 1D Saint-Venant Bernoulli	RANS Saint-Venant Diffusive wave	RANS Saint-Venant	RANS Saint-Venant HLES	RANS Saint-Venant	RANS Saint-Venant
Supercritical flow (suitability for $Fr > 1$)	YES	YES	YES	YES	YES	YES
Turbulence submodules	NONE	NONE	k-ε	k-ε, k-L, algebraic and constant model	NONE	NONE
Numerical equations	Finite volumes, implicit	Finite volumes, implicit	Finite volumes, explicit	Finite volumes, implicit and explicit	Staggered grid (Delft Scheme)	Finite elements, implicit
Hydraulic roughness	Manning-Strickler	Manning-Strickler	Manning-Strickler	Chézy Manning-Strickler White-Colebrook	Chézy Manning-Strickler White-Colebrook	Manning-Strickler
Source terms	Tributary rivers	Tributary rivers, Coriolis forces	Tributary rivers, wind effects, infiltration	Tributary rivers, infiltration, wind shear stress, Coriolis forces	Tributary rivers, wind friction, infiltration	Tributary rivers, wind effects
Structures	Bridges, culverts, lateral structures	Bridges, culverts, lateral structures	Bridges, sluices, culvert and weirs	Gates, bridges, culverts, porous plates and weirs	Manual or automated pumps, sluice gates, weirs, storage tanks	Pump stations, weirs, underflows, culverts and bridges
Real-time control	NO	NO	NO	YES	Only for Rural and Urban modules, not for River module	For 1D
Dike breach	YES	YES	YES	NO	YES	YES
Treatment of drying and wetting	YES	YES	YES	YES	YES	YES
Combination with transport of substances and water quality	YES	Only for 1D	YES	YES	YES	NO
Combination with sediment transport and morphological evolution	2.2 NO 3.1.3 NO 4.1.0 YES	Only for 1D	YES	YES	YES	NO
Input and output	Graphical user interfaces	Graphical user interface	ASCII files	Graph User Interface Binary	Graphical user interface ASCII files	Graphical user interface
Local running availability	YES	YES	YES	YES	YES	NO
Open source	NO	NO	NO	YES	YES	YES
Helpdesk and support	www.hec.usace.army.mil/software/hecras		www.flumen.upc.edu/ca	deltares.nl/en/software-solutions	www.deltares.nl/nl/software/so-bek-suite/	www.3di.nu
User community	http://hecrasmodel.blogspot.nl/		-	oss.deltares.nl/web/delft3d	https://publicwiki.deltares.nl/	-

(RANS = Reynolds-averaged Navier-Stokes; HLES = horizontal large-eddy simulation)

5. ASSESSMENT OF SIMULATION PERFORMANCE

5.1. SIMPLE IDEALIZED CASE: PRISMATIC CHANNEL

5.1.1. CASE DESCRIPTION

Objective

The aim of creating an ideal case for a practical simulation is to work in a simple scenario in order to compare the features and workability of the two hydrodynamic models proposed, HEC-RAS 5.0 and Delft3D, before getting into a real and more complex problem with HEC.RAS 5.0. From this practical comparison, this paper aims to obtain conclusions regarding the two-dimensional performance of river floods of HEC-RAS 5.0 next to an already developed two-dimensional model such as Delft3D.

Initial data

The ideal case has been fully created for the purpose of this document. It consists of a prismatic channel with big floodplains at both sides. Its topography has been created with Delft3D RGFGRID and QUICKIN modules and can be visualised in the next figure.

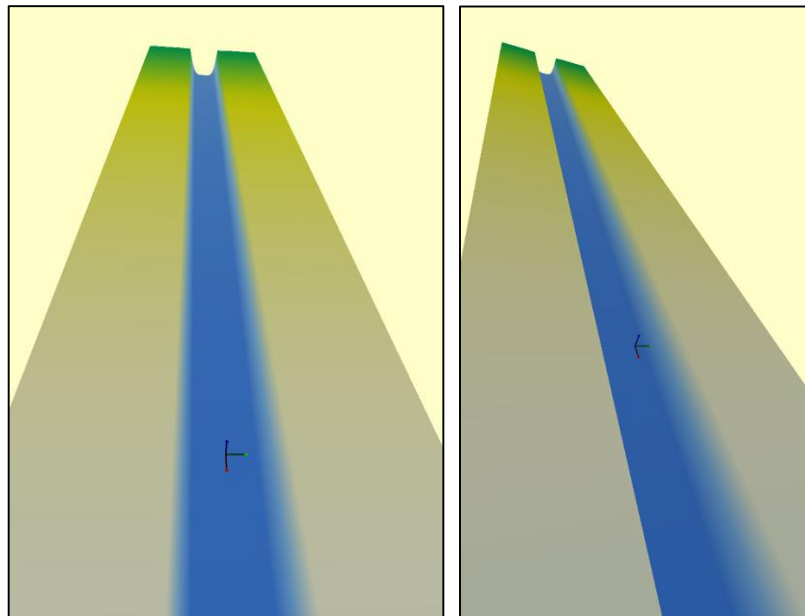


Figure 5.1.1.1. Created channel topography in three-dimensional view, with Delft3D

The data has been elaborated in order to fulfil the following conditions:

- M-type Channel (mild slope channel) $\rightarrow i < c_f$ (bed slope value must be smaller than friction coefficient)
- And, what is the same, in consequence: Slow regime $\rightarrow Fr < 1$
- Small value for CFL (Courant-Friedrichs-Lewy condition) in order to fulfil a proper simulation
 - o $CFL = u' \cdot \Delta t / \Delta x$, where Δt is time step, Δx is cell size and $u' = u + \text{sqrt}(g \cdot d_e)$
 - o For pure explicit numerical methods, CFL must be lower than 1
 - o However, since this is not the case for Delft3D and HEC-RAS, this is not a strict condition and the value can be higher, but one still needs to lower it as much as possible
 - o Delft3D requires a maximum CFL of 11
- Reasonable values for water depth d_e , flow velocity u , bed slope i , width B , time step Δt , total discharge Q , discharge over width q and Chézy coefficient C .

An Excel file is created in order to be able to change values and obtain different results depending on the input until the data fulfils the mentioned conditions and is possible for a steady flow channel.

Table 5.1.1.1. Created channel data, set in a simple Excel file

INPUT		
Grid definition		
Columns		499 u
Rows		49 u
Cell size		25 m
Channel characteristics		
Inner width	B_{int}	225 m
Outer width	B_{ext}	325
Height difference	Δz	1.25 m
Roughness coefficient	C_f	0.01 -
Water flow characteristics		
Total discharge	Q	200 m ³ /s
Others		
Time step	Δt	0.1 min
Acceleration gravity	g	9.81 m/s ²

OUTPUT		
Channel characteristics		
Domain length	Δx	12475 m
Domain width	Δy	1225 m
Channel depth	$\Delta z_{channel}$	2 m
Slope	i	0.0001 -
Levees slope	i_{levees}	0.04
Outer width water surface	$B_{ext, watersurf}$	319 m
Wet area	A	460 m ²
Water flow characteristics		
Discharge over width	q	0.889 m ² /s
Equilibrium depth	d_e	1.88 m
Flow velocity	u	0.43 m/s
Checking coefficients		
Chézy coefficient	C	31.68 -
Froude number	Fr	0.10 -
Courant number	CFL	1.14 -
Manning		
Slope for Manning	i	0.00015 -
Manning coefficient	n	0.035 -
Hydraulic radius	R_h	1.42 m

Therefore, the created data brings to the following channel:

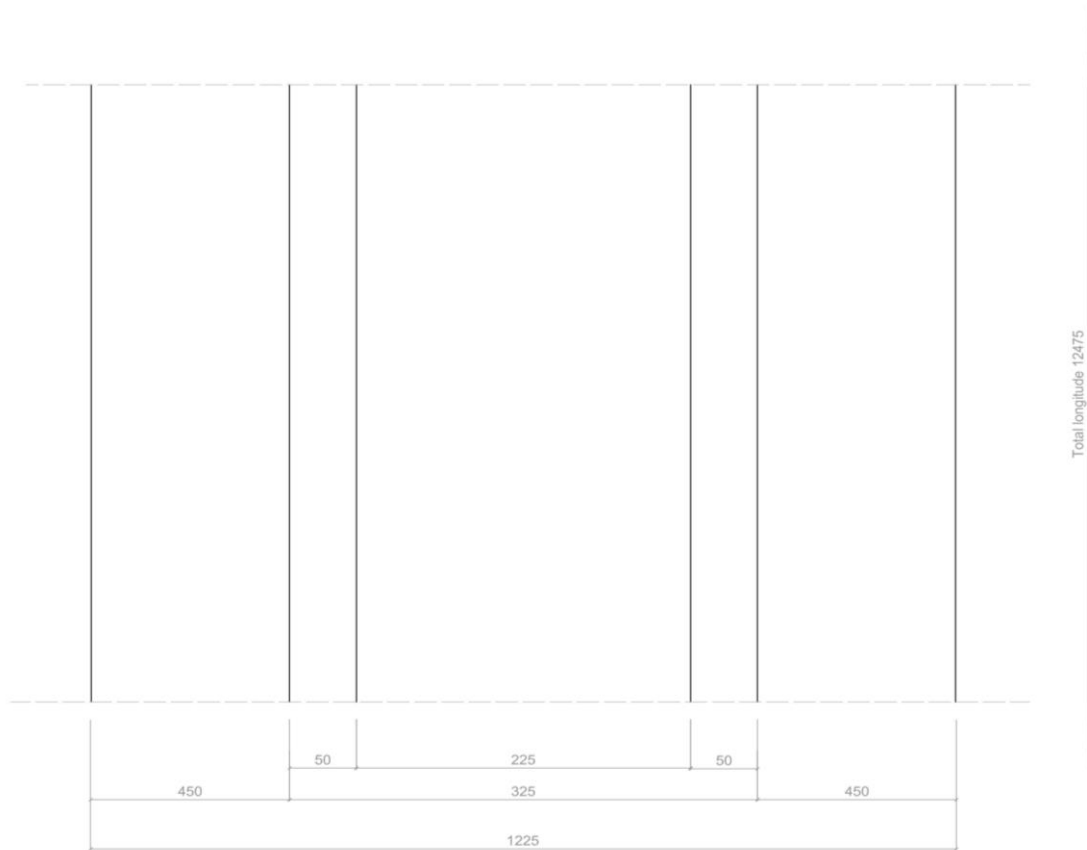


Figure 5.1.1.2. AutoCAD sketch of top and front view of the created channel. Sketch units in meters (m). Please note the sketch is not on scale.

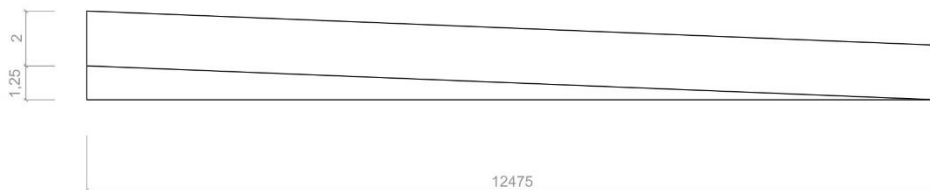


Figure 5.1.1.3. AutoCAD Sketch of longitudinal view of the created channel. Sketch units in meters (m). Please note the sketch is not on scale.

Two simulations have been performed for the ideal channel:

- A **steady flow simulation** in order to learn how to perform very basic simulations. The steady discharge applied is constant 200 m³/s, as the previous excel table shows. This way, it has been possible to check that predicted output data in the Excel file was correct.
- An **unsteady flow simulation** in order to perform a flood simulation, since this project is focused in this kind of phenomena. The discharge data for this simulation was also created only for the purpose of this case. In order to make the water reach the floodplains, the discharge was gradually increased from 200 m³/s (steady state) to 450m³/s, its peak flow, as *Table 5.1.1.2* shows.

Table 5.1.1.2. Hydrological data created for the purpose of the unsteady flow simulation of the ideal channel

Time	Discharge
<i>dd mm yyyy hh mm ss</i>	<i>m³/s</i>
01 01 2000 00 00 00	200
01 01 2000 04 00 00	200
01 01 2000 06 00 00	210
01 01 2000 08 00 00	220
01 01 2000 10 00 00	250
01 01 2000 12 00 00	300
01 01 2000 14 00 00	360
01 01 2000 16 00 00	410
01 01 2000 17 00 00	450
01 01 2000 18 00 00	410
01 01 2000 19 00 00	360
01 01 2000 21 00 00	320
01 01 2000 23 00 00	300
02 01 2000 01 00 00	270
02 01 2000 03 00 00	250
02 01 2000 06 00 00	230
02 01 2000 09 00 00	220
02 01 2000 12 00 00	200
02 01 2000 20 00 00	200

5.1.2. CONSIDERATIONS

Grid

The grid created for both models is a rectangular grid that perfectly fits with the topography data created with RGFGGRID and QUICKIN. This is, a 500x50 cells grid with 25m cell size.

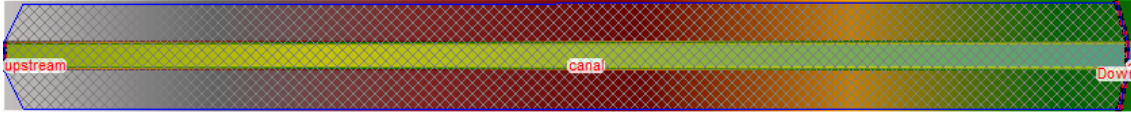


Figure 5.1.2.1. Rectangular grid created for HEC-RAS 5.0 channel performance

Delft3D is capable to create curvilinear grids with different cell sizes, which is most of the times an advantage in terms of details and computational time. However, for this channel case the created grid is a rectangular grid with squared shaped cells (25 m cell size) in order to do a very similar comparison to HEC-RAS 5.0, which can only work with rectangular grids. Thus, its dimensions are 500x50 cells.

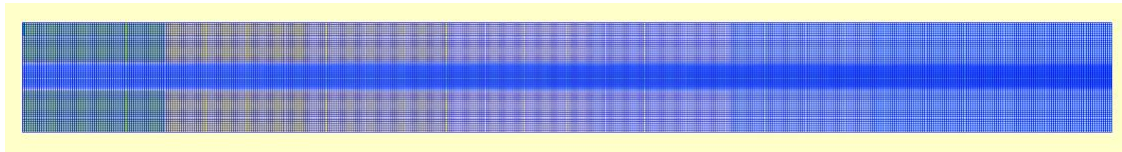


Figure 5.1.2.2. Rectangular grid created for Delft3D channel performance

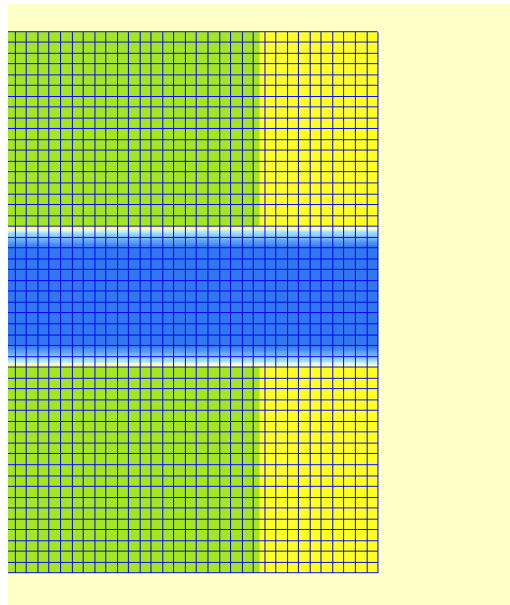


Figure 5.1.2.3. Close view of the rectangular grid used in Delft3D, with 25x25m² cells

Latitude for Coriolis

It is assumed that the channel is located at the equator (Latitude 0), for simplification reasons.

Roughness coefficient

Manning's coefficient of roughness has been assumed $n=0.035$ for both the river bed and floodplains, for simplification issues. This a reasonable value that could perfectly be found in nature.

Downstream boundary condition

The downstream boundary condition has been set to 1.88 m for both Delft3D and HEC-RAS 5.0 simulations since this is the value obtained for the equilibrium depth in the excel and in order to apply the exact same data for both models.

In order to let the water flow outside the domain at the end, the downstream boundary condition has been extended to the full width of the domain, only for the unsteady flow case, also for both Delft3D and HEC-RAS 5.0 simulations. This was not necessary at all for the steady case since the water was not flowing outside the river channel to the floodplains.

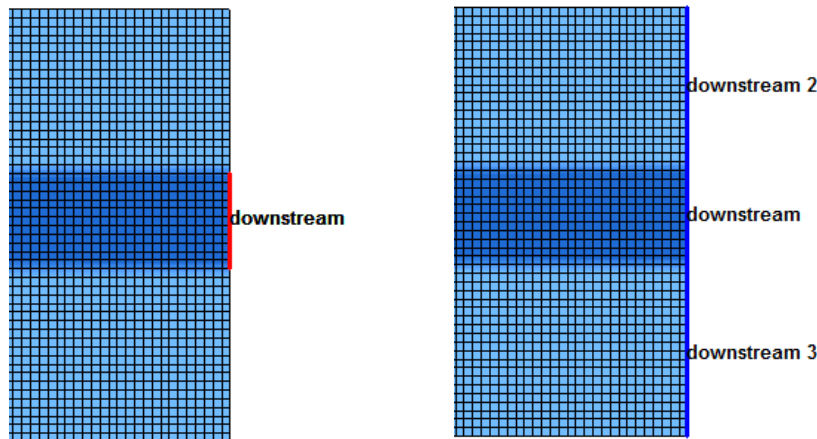


Figure 5.1.2.4. Extension of the downstream end boundary condition for the unsteady case (left: steady case; right: unsteady case). Example with Delft3D model

Equations used

In order to contrast in a more effective way the Delft3D and the HEC-RAS simulations, one would rather use the same equations. As previously studied, HEC-RAS 5.0 can work with Diffusive Wave or with Full Momentum. Since Delft3D is working with Full Momentum, those are the equations chosen, as shown in the figure below. Note that the use of Diffusive Wave is simpler and that would lead to a decrease in computational time.

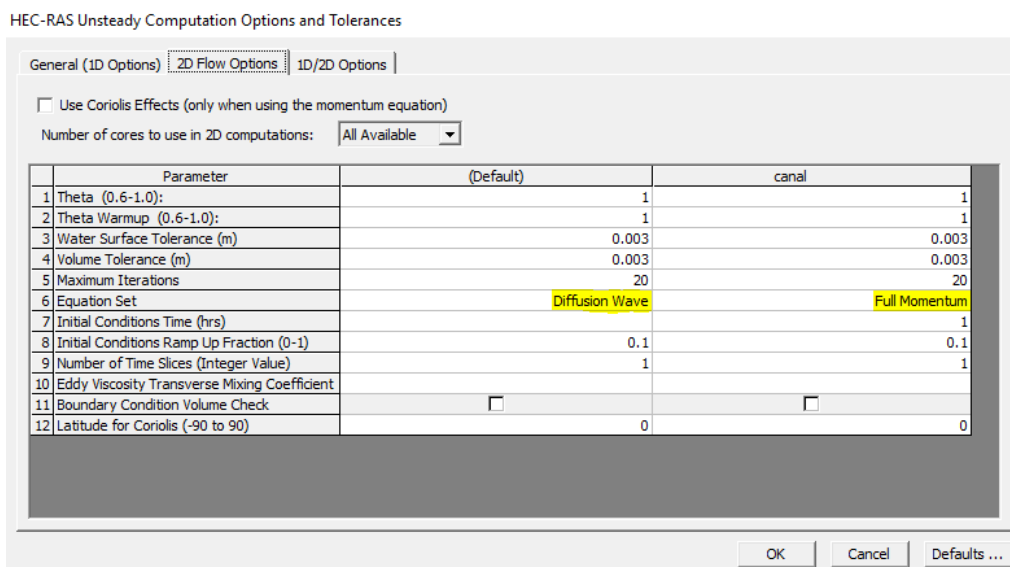


Figure 5.1.2.5. HEC-RAS Interface with previous default options and chosen options for the performance of the ideal channel simulation

One can also note that the latitude is set at the equator (Latitude 0), as previously mentioned.

5.1.3. PROBLEMS FOUND

During the performance of the ideal case simulation, some obstacles that led to an increase of the expected work time were found.

Regarding data input:

- Since this is a hypothetical ideal case, the data was not originally provided. Thus, this data had to be created with RGFGRID and QUICKIN, Delft3D modules. The initial lack of background on the workability of those two modules on how to create bathymetries was a hard barrier to overcome.
- The mentioned data had to be created regarding some conditions, such as the Courant-Friedrichs-Lewy condition or a Froude number $Fr < 1$. Those conditions were not fulfilled by the first trials, so they had to be recreated again more than once.

Regarding program workability:

- It can be considered that HEC-RAS has a little error when using Spanish as the interface language. The problem is the following: when the user set the time frame, has to write the initial and final simulation date in a determined format: for instance, 21OCT2008, meaning 21st October 2008. Then, when writing months that are differently written in Spanish and English, such as January (JAN) and Enero (ENE), the program does not understand the input and the model cannot run. This problem led to a significant loss of time when the channel was set in a time frame starting on 1st January 2000, since finding the origin of the problem was more difficult than expected. Once noticed, the time frame was finally switched to 20th October 2008 in order to perform the simulation properly.
- Delft3D showed problems when trying to simulate from a completely dry domain. Thus, an initial conditions file was needed. This file contains the information for the initial water level elevation in order to let the model know from which situation the simulation must be performed. Since this file was not initially provided and there is no explanation in Delft3D Manual about how to create it, this issue represented a really big loss of time.

5.1.4. RESULTS

5.1.4.1. HEC-RAS 5.0 SIMULATION

As already mentioned, the channel performance has been carried out for two different flows: steady and unsteady. In this first results section, the results for those two simulations for HEC-RAS 5.0 are presented.

Steady flow case results:

For this first steady flow case, the results are expected to be very similar to the output in the excel file previously showed.

The following figures show the channel water depth. As expected, the water depth is constant for all time and space. There are only small variations between 1.87 m and 1.89 m.



Figure 5.1.4.1.1: Channel water depth in steady conditions, with HEC-RAS 5.0

With the new RAS-Mapper interface, it is easy to handle the output data. For instance, the following graph clearly shows the depth over time for the two pink points, located at separated points of the reach. In both cases, the water depth tends to 1.88 metres, as expected for the data set.

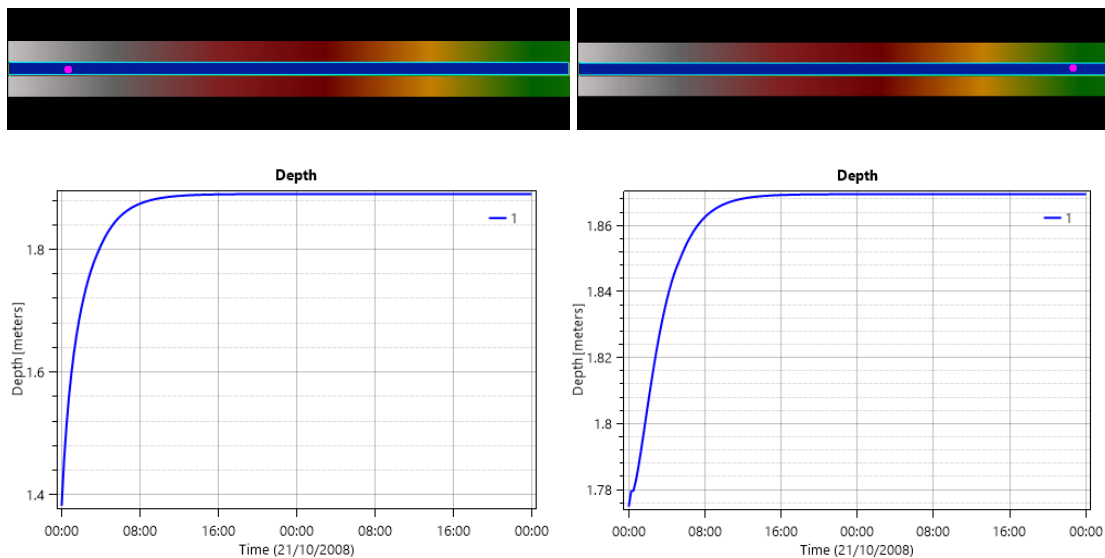


Figure 5.1.4.1.2. Location and depth over time graphs for two representative points in the channel reach, for steady conditions, with HEC-RAS 5.0

As expected in the calculations, the water velocity is very close to 0.43 m/s with only little variations:

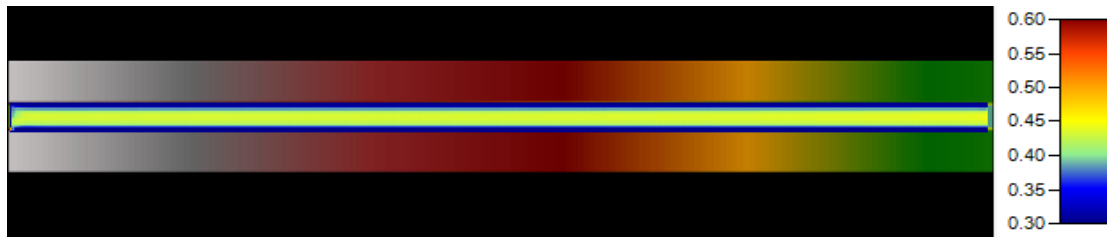


Figure 5.1.4.1.3. Channel water velocity all over the reach for steady conditions, with HEC-RAS 5.0

The following pink point shows the location for the velocity-time graph. As one can see, the hyperbolic curve tends to 0.43 m/s, as expected.

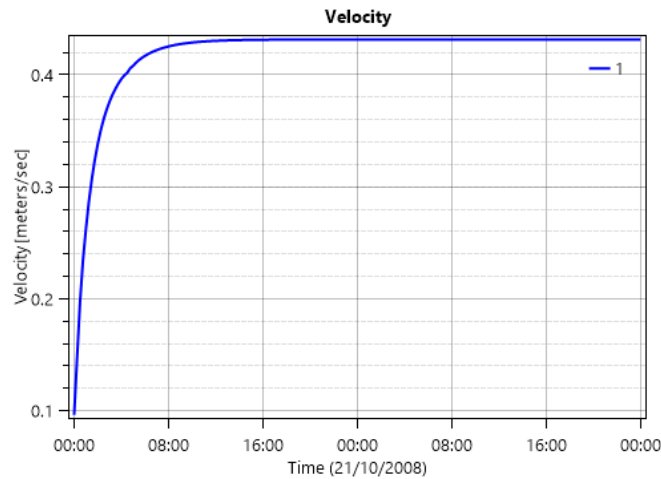
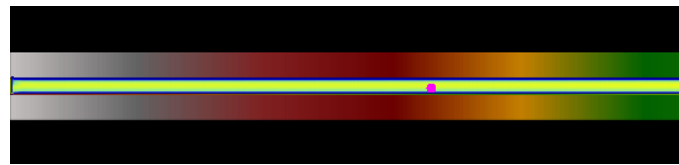
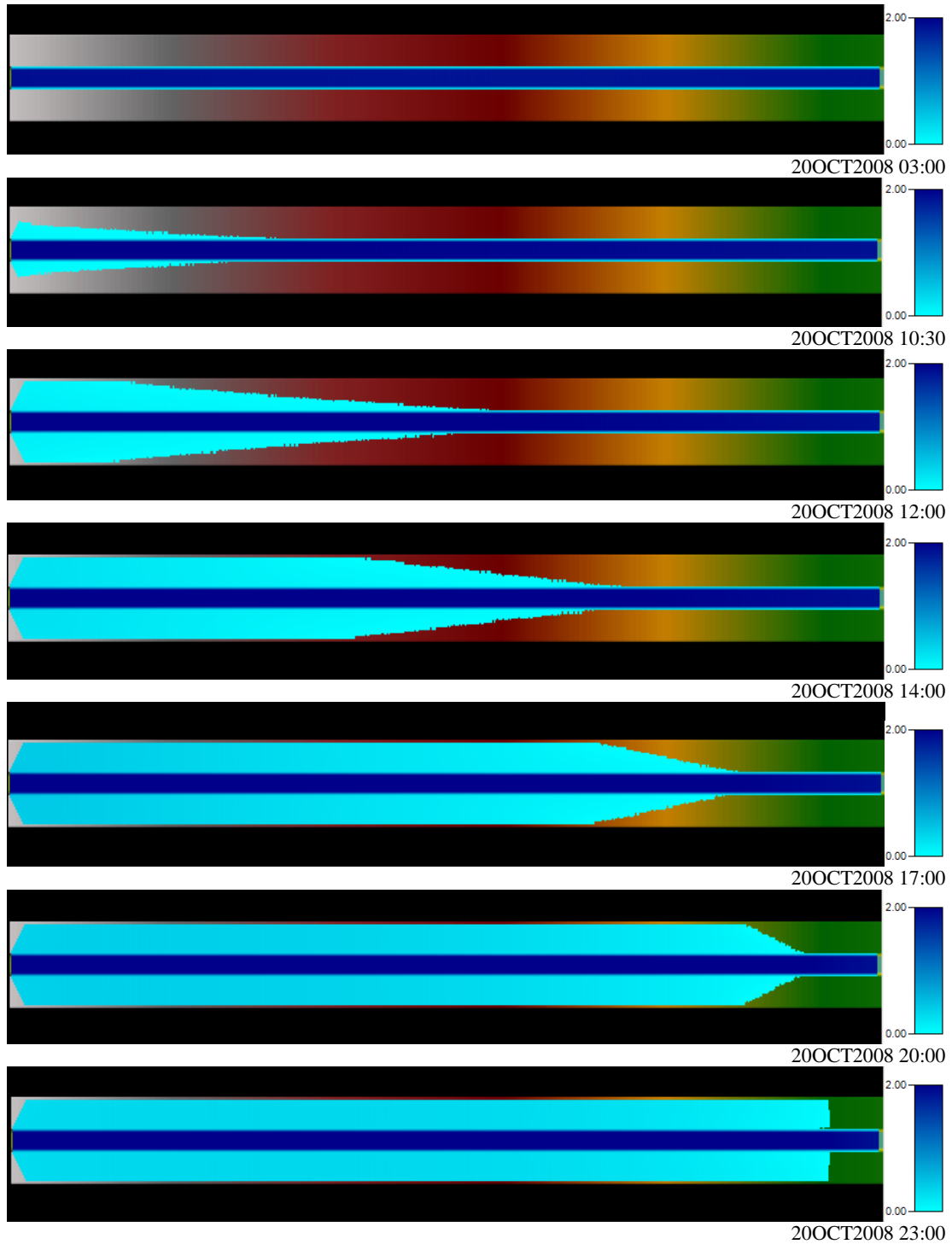


Figure 5.1.4.1.4. Location and velocity over time graph for selected point of the ideal channel, in steady conditions, with HEC-RAS 5.0

Unsteady flow case results (flood simulation):

For the purpose of modelling a flood simulation, the channel has been object of the created hydrological data mentioned in the case description section, which starts in a steady state (200m³/s) and has a peak discharge of 450m³/s before coming back to the steady state again at the last part of the time period.

The process of the flow modelled with HEC-RAS 5.0 is the following (units: depth in metres):



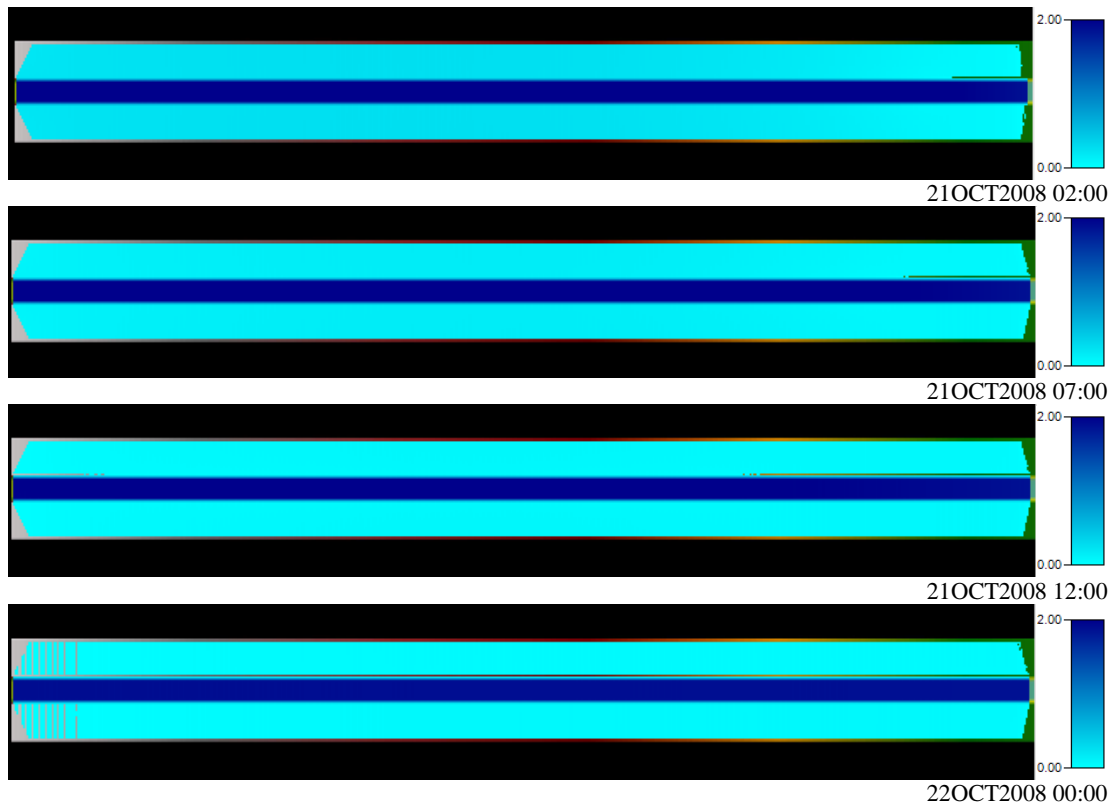


Figure 5.1.4.1.5. Flooding flow behaviour series of the ideal channel for the unsteady hydrological data created, with HEC-RAS 5.0

In sum, the flow starts behaving steadily (20OCT2008 03:00) and then turns unsteady, flooding the floodplains from the top to the downstream end. After that, the discharge diminishes again and that's why the domain starts to dry out (noticeable at the upstream end side in picture 22OCT2008 00:00).

However, a little instability has been noticed. The fact is that two thin longitudinal dry areas, which were not expected, appear in the slope change between the floodplains and the main channel when the flow reaches to the downstream region. This is observable in the previous pictures, from 20OCT2008 23:00 to 22OCT2008 00:00. One can see that those areas are first short, but start extending until they reach the upstream end.

The cause of this issue could probably be the combination of two facts. First, the water depth at the flooded areas is really small at the end of the simulation time (less than 10 centimetres), which can lead to wetting-drying problems, this is, how the program distinguishes whether a cell is considered wet or not when the water depth value is really small. Second, the area of the problem is exactly when the channel wall slopes appear. This is obviously an area which is likely to have instability problems, since its slope is not constant.

The next image shows the area of the problem from a closer point of view.

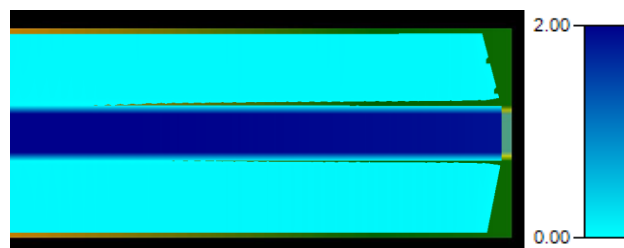


Figure 5.1.4.1.6. Close view of the area at the downstream end of the reach at time 21OCT2008 10:45

Regarding the water depth and velocity of the flow, two points have been chosen to be analysed at the same representative reach height but one in the main channel and another in the floodplains. These are the results:

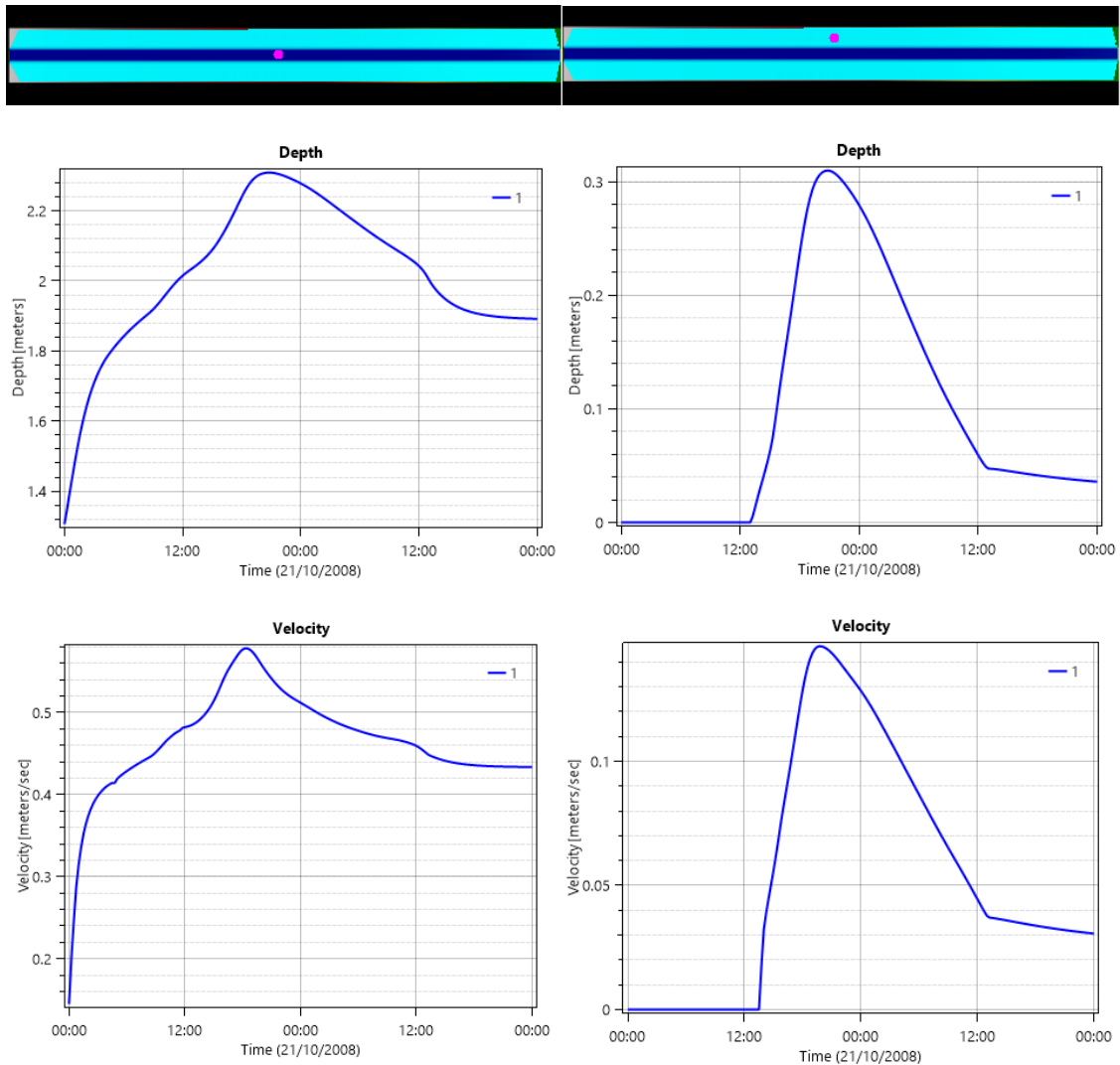


Figure 5.1.4.1.7. Location, water depth over time graph and velocity over time graph of the two points chosen for analysis in the flooded channel situation, with HEC-RAS 5.0

Regarding water depth:

The maximum depth value for the first point, located at the centre of the reach and at the centre of the main channel, is 2.31 metres. At the end of the simulation, the water depth comes back to the equilibrium, this is, 1.88 metres.

The second point, located at the centre of the reach and at the north floodplain, reaches its maximum water depth a little later than the first point. This time difference is the time that the flood water front needs to move from one point to the other. Its maximum water depth is 0.31 metres.

It is observable that the difference between both maximum water depths is 2.00 metres, the exact height of the channel. This makes perfect sense, since once the domain is flooded the water surface is the same for the channel and the floodplains, so the depth difference must be the channel height.

Regarding flow velocity:

The first point has its maximum in 0.58m/s while the second has it in 0.15m/s. One also needs to take into consideration the fact that the water in the channel moves much more longitudinally than the water in the floodplains, which also moves laterally in order to flood the dry areas. This is shown in more detail in the Delft3D results.

The magnitude velocity difference between main channel and floodplains can be observed in the following image. Units in m/s.

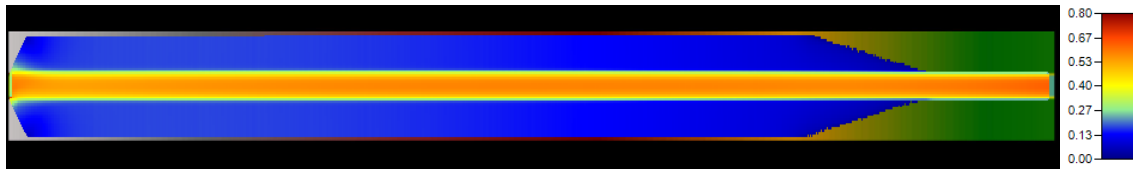


Figure 5.1.4.1.8. Water flow velocity difference between the main channel and the two floodplains in the flooded channel situation (velocity units in m/s), with HEC-RAS 5.0

5.1.4.2. DELFT3D SIMULATION

In the present section, the results for steady and unsteady simulations for the ideal channel with Delft3D are presented.

Steady flow case results:

The steady case results with Delft3D are also notably satisfactory. All the predicted data can be considered correct.

The following figures show the channel water depth. As expected, the water depth is constant for all time and space. For this reason only one figure is enough to show the water depth behaviour in this steady case. On it, one can see the dry floodplains and a water depth of around 1.88 in the main channel.

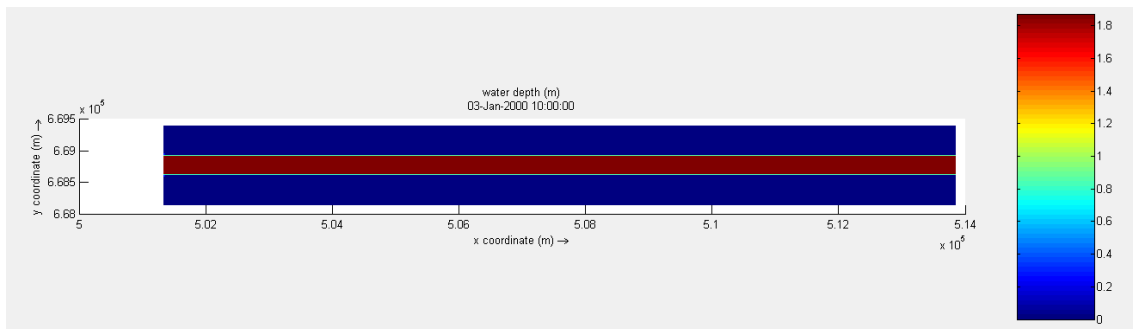


Figure 5.1.4.2.1. Channel water depth all over the reach in steady conditions, with Delft3D

Or, which is the same, the water level is steady for all simulation times:

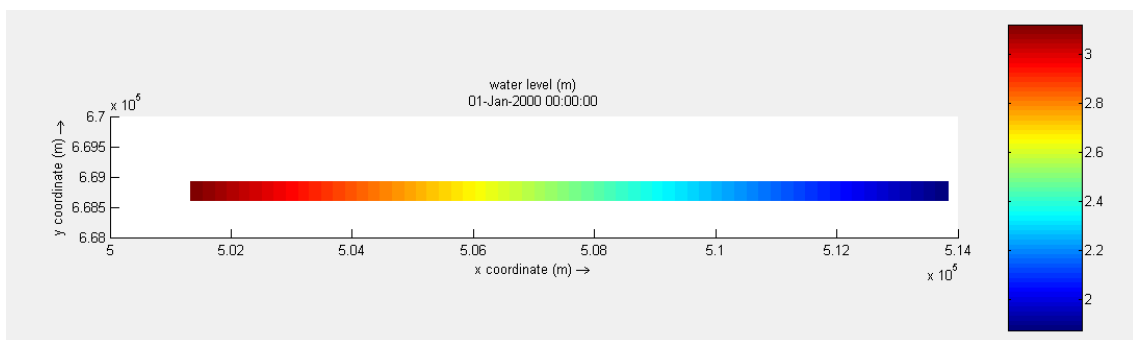


Figure 5.1.4.2.2. Channel water level all over the reach in steady conditions, with Delft3D

Velocities are analysed by means of observation points set along the channel reach. In this case, three observation points are set for results. The exact location of this points is not of relevant importance in this case since the results need to be steady for all of them.

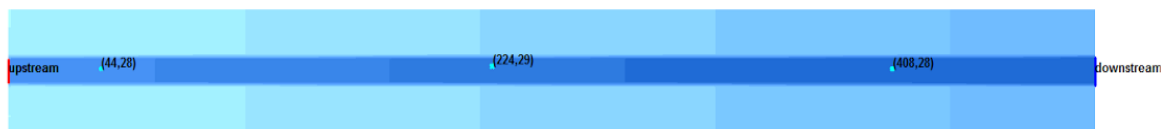


Figure 5.1.4.2.3. Situation of the three observation points for the steady flow performance in the channel, with Delft3D

The first observation point (44,28) computes a velocity in x-direction (component 1) of 0.42-0.43 m³/s, while the previous calculations are about 0.43 m³/s. Thus, those calculations can be considered really accurate.

The second component of the velocity is negligible, as it was assumed in the beginning since the channel is straight, the flow is steady and the initial transversal velocity input is negligible.

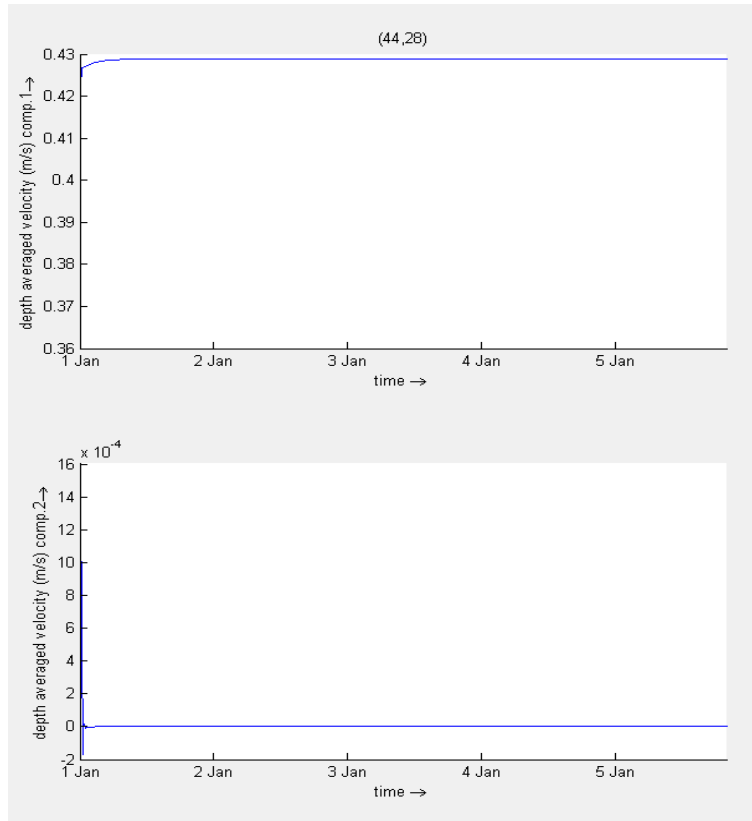


Figure 5.1.4.2.4. Graph showing the two water velocity components over time in the unsteady channel simulation with Delft3D for point (44,28)

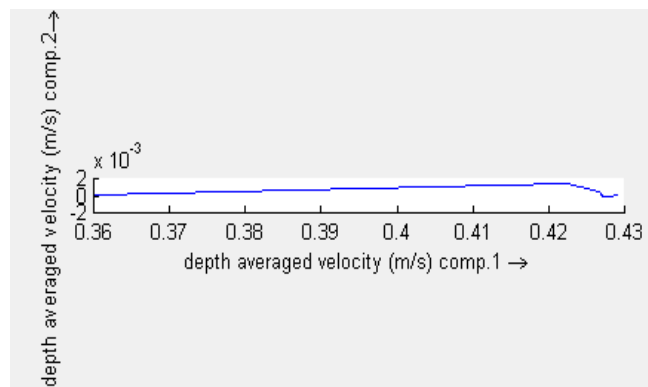


Figure 5.1.4.2.5. Graph showing the magnitude difference between both velocity components in the unsteady channel simulation with Delft3D for point (44,28)

Similar results can be observed for the other two observation points, (224,29) and (408,28):

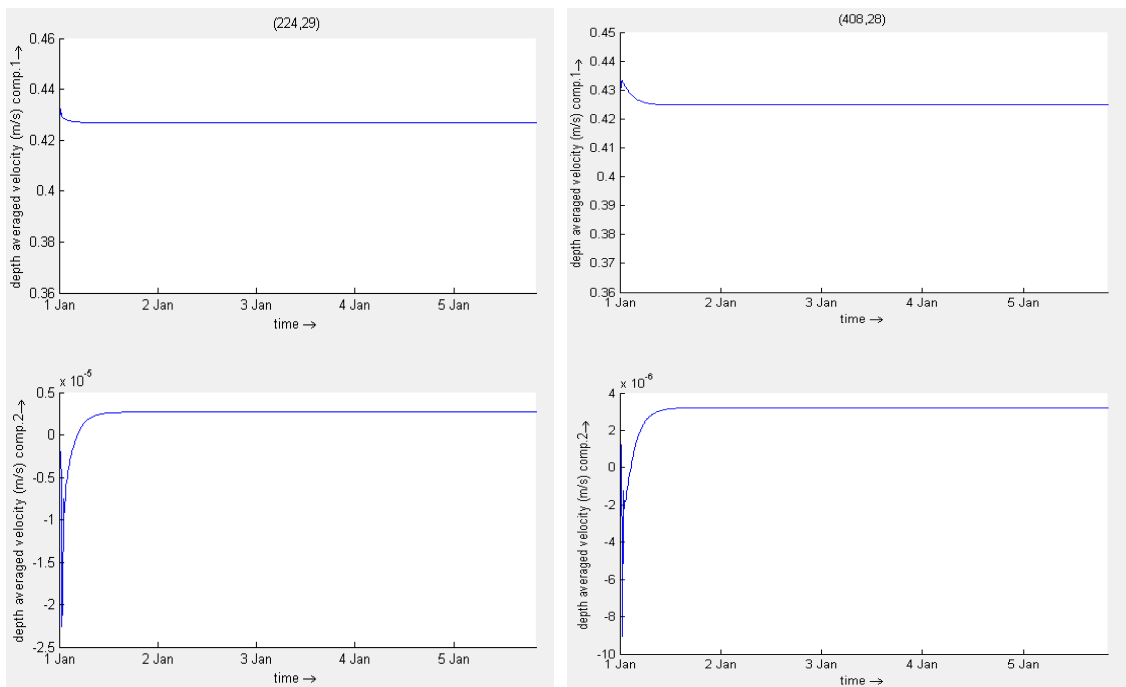


Figure 5.1.4.2.6. Graph showing the two water velocity components over time in the unsteady channel simulation for points (224,29) and (408,28)

The water depth in the channel is also very close to the expected. However, it is 2-3 centimetres smaller.

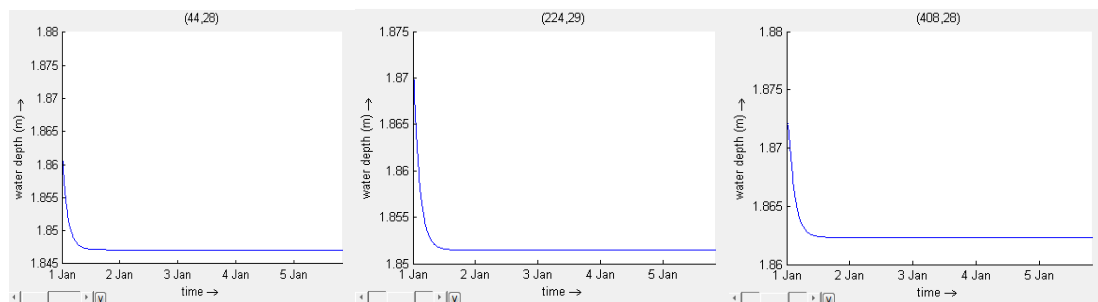


Figure 5.1.4.2.7. Water depth in the channel for steady flow for the three observation points set

Delft3D is able to show output figures with the computed Froude number at each time and space. Those results show that the approximation made is very accurate. Let us remind that the initial Excel calculation shows a Froude number $Fr=0.10$, and the following results give values between 0.09 and 0.10.

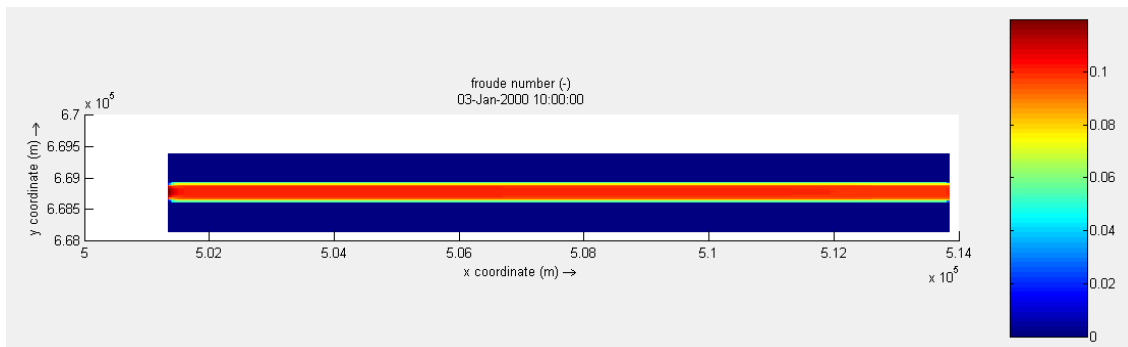
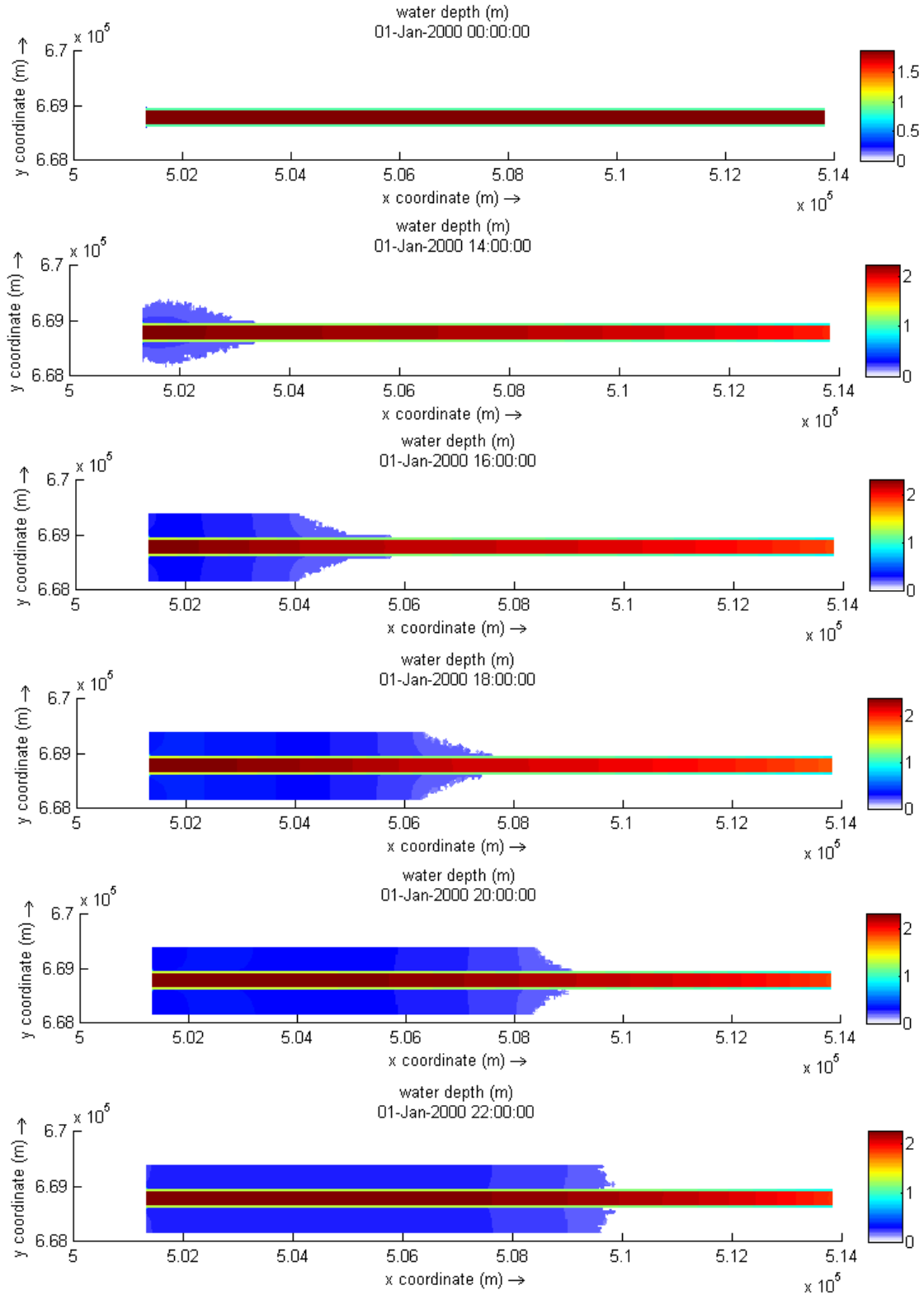


Figure 5.1.4.2.8. Graph showing the Froude number all over the reach simulated with Delft3D for the steady channel situation

Unsteady flow case results (flood simulation):

The following series of figures represent the water depth on the channel reach. As expected, the water flows outside the main channel and reaches the floodplains. It is noticeable that the maximum discharge is released between 16:00h and 18:00h on the 1st of January. It is from that moment when the floodplains start being seriously flooded.



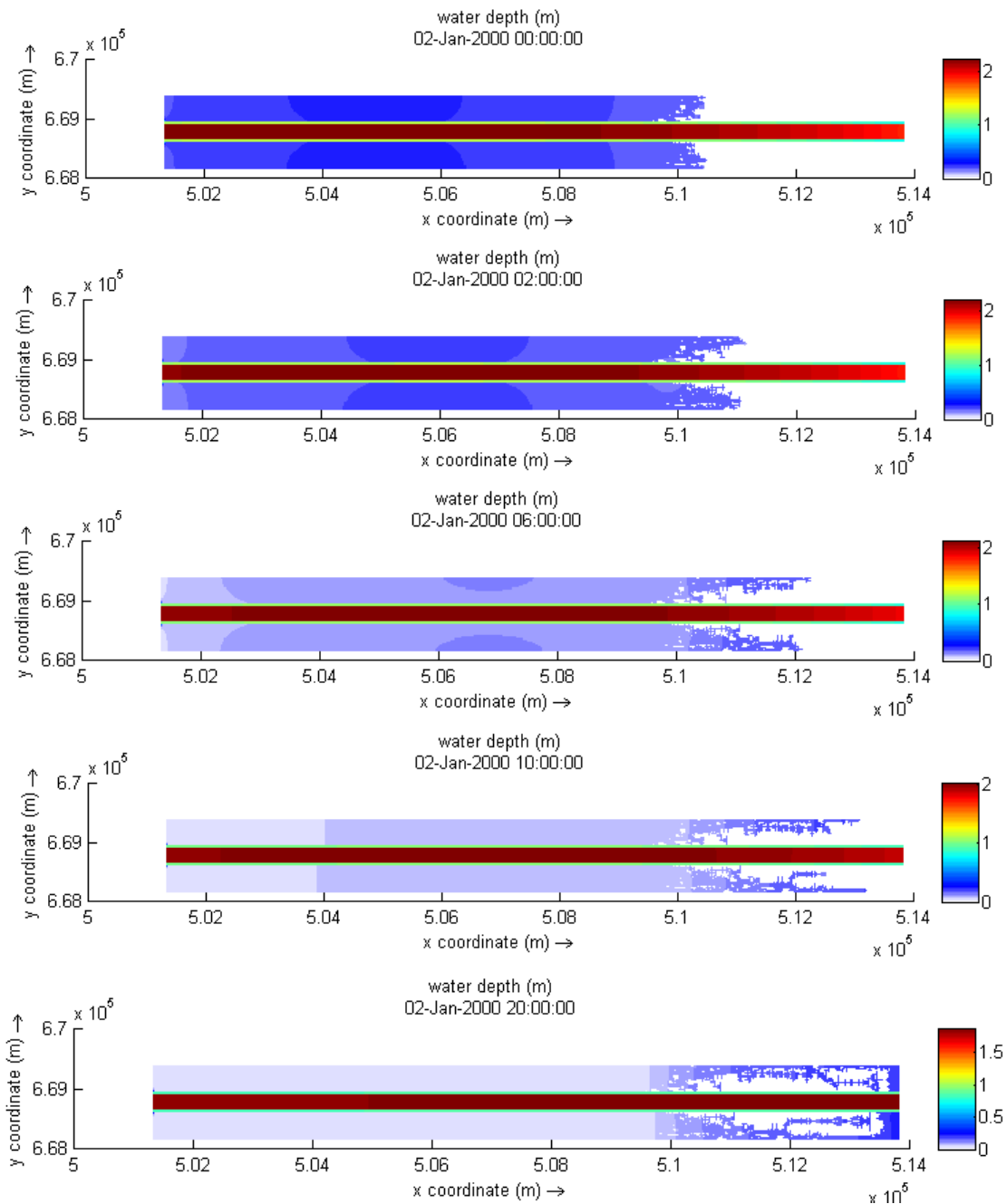


Figure 5.1.4.2.9. Flooding flow behaviour series of the channel for the unsteady hydrological data created, with Delft3D

One can easily see that the behaviour at the last third of the reach is different. This is due to the fact that when the water reaches this area, the front wave (maximum discharge released) is already stabilized, so the water flow that gets there has much less energy and is not flooding the floodplains so severely. The white area is area which is never considered wet in the whole process.

This fact can lead to controversy about the reliability of both Delft3D and HEC-RAS 5.0 models, since slight different results appeared. However, this is very likely to be a mere tolerance issue, this is, one model has different value than the other for considering a cell to be wet or not. Could be that HEC-RAS 5.0 considers 2mm depth enough to define that a cell is wet, but Delft3D uses 4mm for that purpose. This leads to differences in terms of results although the calculations are the same.

In order to better analyse the behaviour of the different features of the flow at exact points in the floodplain, six extra points have been added to the three already used for the previous steady simulation.



Figure 5.1.4.2.10. Situation of observation points over the channel reach and floodplains for unsteady results with Delft3D

Regarding water depth results, points (224,43), (224,29) and (224,17) will be analysed. Those points are especially chosen because they have similar locations to the points in the river reach analysed for the HEC-RAS 5.0 case.

Water depth results for observation point (224,29) are presented in *Figure 5.1.4.2.11*.

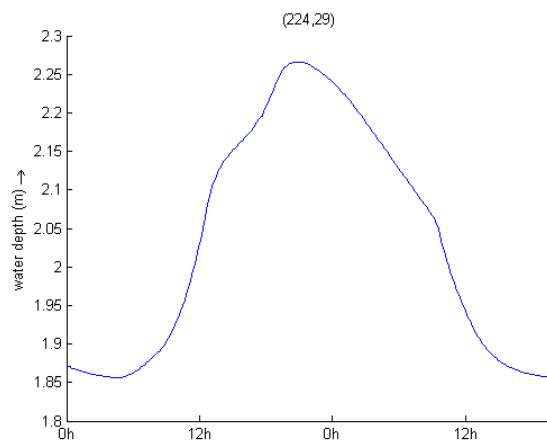


Figure 5.1.4.2.11. Water depth over time graph of point (224,29) for the flooded channel situation, with Delft3D

As examples for the floodplains, results on water depth for points (224,43) and (224,12) in the floodplains are presented below.

One should note that those points are at the same domain height but at opposite floodplains, one in each side of the main channel. Therefore, symmetric results may be expected for those points in terms of depth and velocity, taking into account the symmetry of the domain. Regarding to the depth in particular, the values must be the same at the same time, as follows:

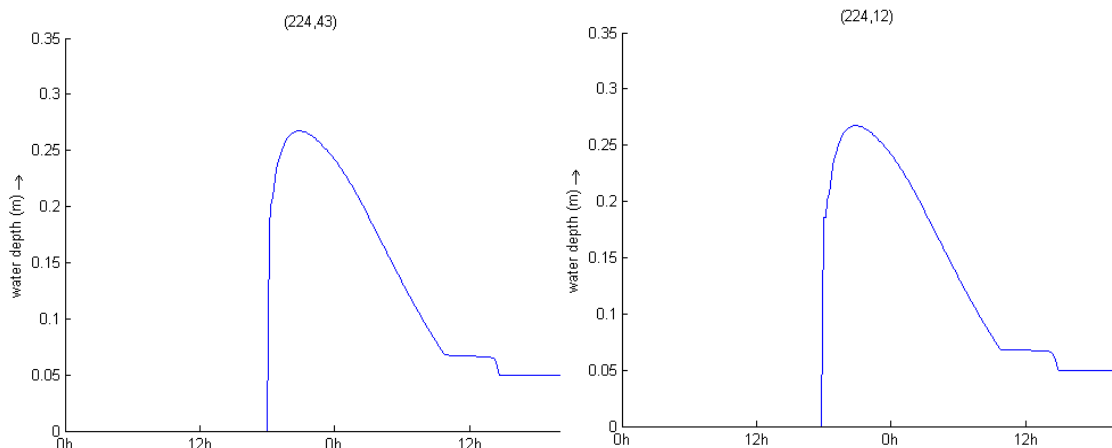


Figure 5.1.4.2.12. Water depth over time graph of points (224,43) and (224,12) for the flooded channel situation, with Delft3D

Regarding the depth averaged velocity results, those can be represented in QUICKPLOT interface, with arrows that show the magnitude and direction of the water flow.

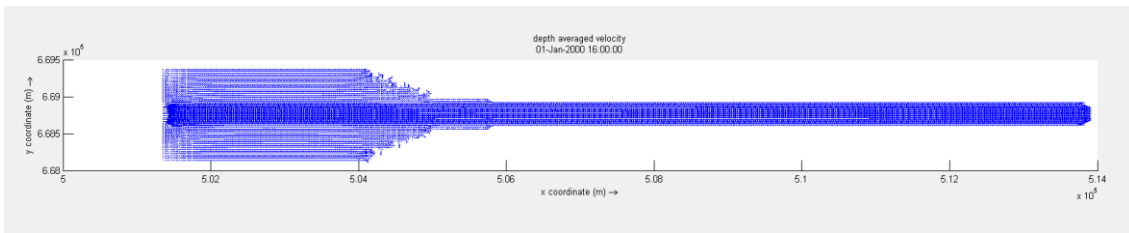


Figure 5.1.4.2.13. Flow velocity general results for unsteady channel case, with Delft3D

From a closer viewpoint:

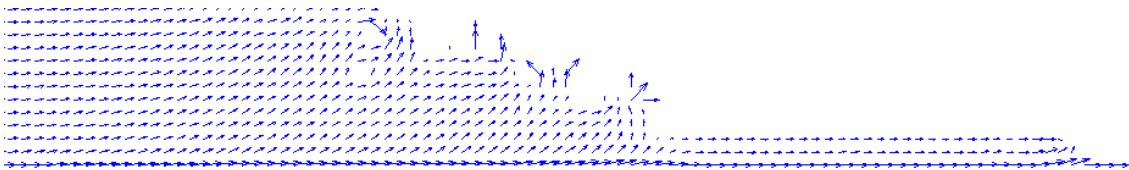


Figure 5.1.4.2.14. Close view of flow velocity general results for unsteady channel case, with Delft3D

Those views, though, are not very clear and are difficult to analyse. In order to properly analyse the velocity results in the floodplains, one is more interested in analysing the six extra observation points that have been placed in the area.

As examples, results on velocity for points (224,43) and (224,12) in the floodplains are presented on the next page. As said, those points are chosen because they have similar locations as the points in the floodplains analysed for the HEC-RAS 5.0 case. Their graphs show that the velocity is zero until the floodplain is flooded, as expected. One can also observe that the transversal velocity component is not negligible as it was happening in the steady flow case, because in this case the water is flowing laterally too, in order to cover the dry area of the floodplains.

As expected, due to the symmetry of the domain and the opposite position of the points in the floodplains, the results show same values for the longitudinal velocity component (component 1) over time and, for the lateral velocity component (component 2), same value magnitudes but with opposite sign, since the direction of the flow is north for the northern floodplain and south for the southern floodplain.

The mentioned graph results are shown in the next page.

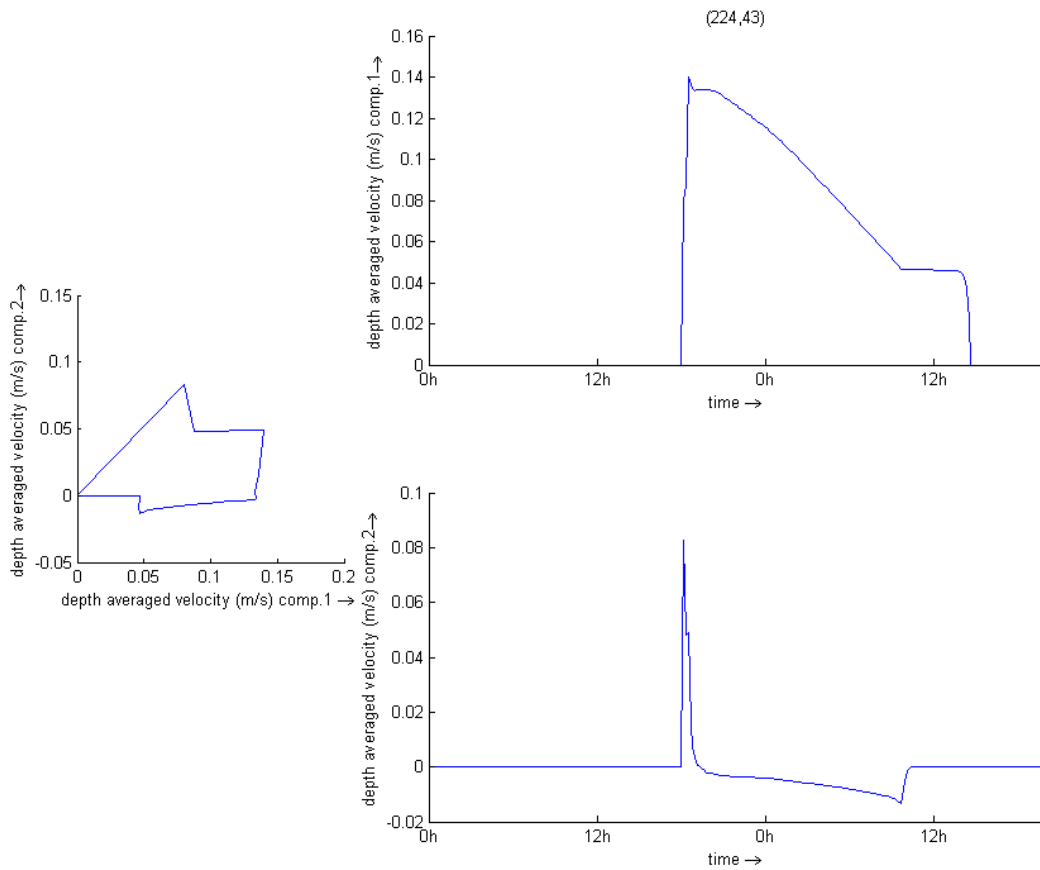


Figure 5.1.4.2.15. Graphs showing the two water velocity components over time and the relation between them, in the unsteady channel simulation, for point (224,43), with Delft3D

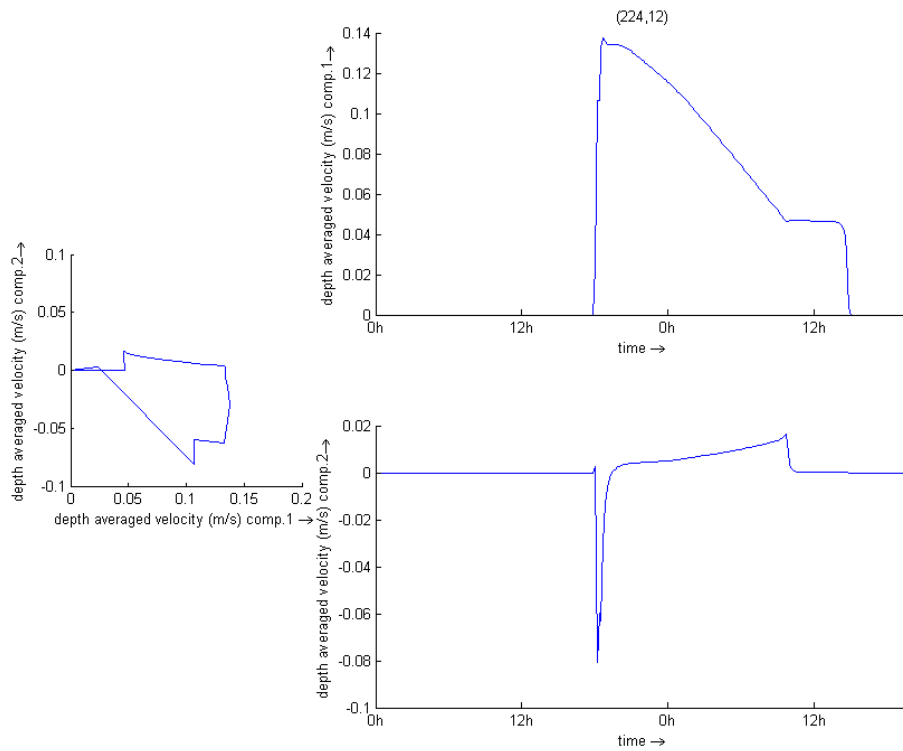


Figure 5.1.4.2.16. Graphs showing the two water velocity components over time and the relation between them, in the unsteady channel simulation, for point (224,12), with Delft3D

It is noticeable the difference between these points, in the floodplains, and the observation point (224,29), placed in the main channel. As one can observe in the next figure, in comparison to the previous, the water flow in the points in the main channel has negligible transversal velocity component (component 2) compared to longitudinal velocity component (component 1). This makes perfect sense since the main channel flow behaves straight and the flooding water has to move laterally in order to cover the floodplains with water.

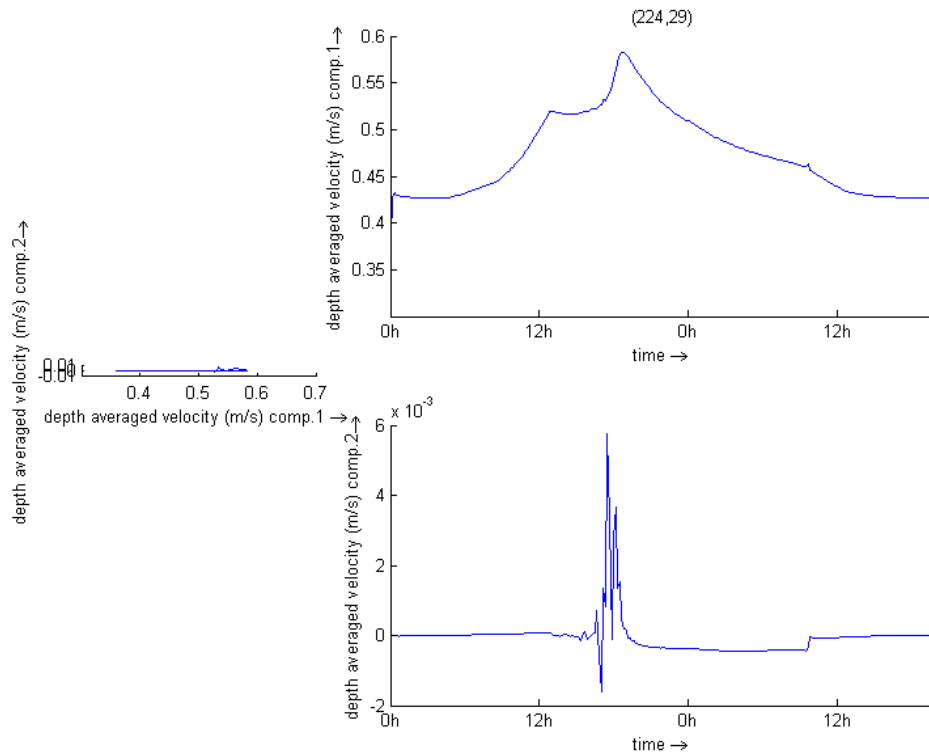


Figure 5.1.4.2.17. Graphs showing the two water velocity components over time and the relation between them, in the unsteady channel simulation, for point (224,29), with Delft3D

Regarding the Froude number, results show that in any case it exceeds 0.4, which makes sure the simulation has been fully performed in subcritical flow and that there are no instabilities due to supercritical flow. The next figure shows the instant when highest Froude number is computed.

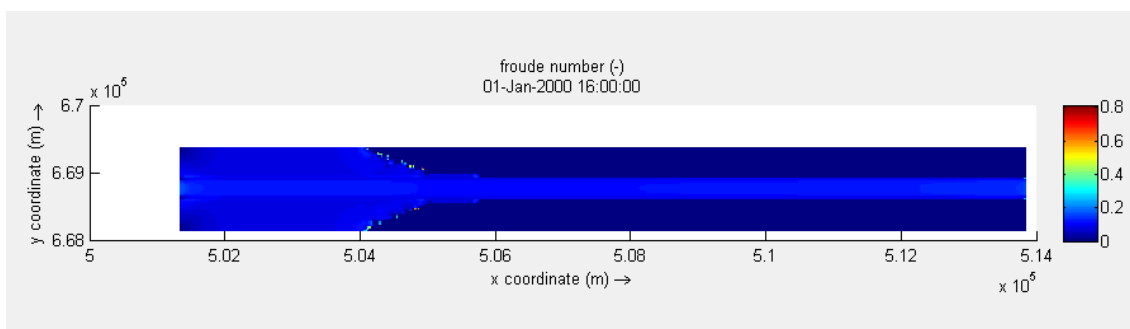


Figure 5.1.4.2.18. Graph showing the Froude number all over the reach simulated with Delft3D for the unsteady channel situation

5.1.5. EXTRA TESTS: M1 AND M2 CURVES

Some more extra tests with HEC-RAS 5.0 have been performed in order to check its workability when the water surface defines curves M1 and M2 (mild slope curves).

The following figure shows the shape that every type of M curves present:

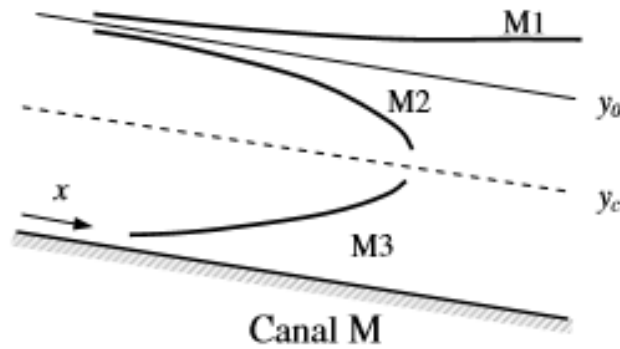
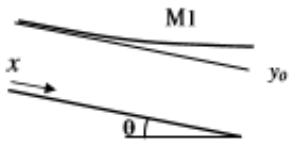
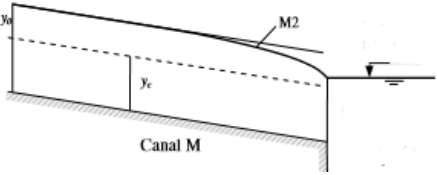


Figure 5.1.5.1. M-type curves (Gutiérrez, 2014)

where y_0 is the normal water depth and y_c is the critical water depth

For this purpose, the same previous steady case data has been applied, with the only difference of varying the downstream boundary condition. Since the critical depth has been proved to be 1.88 metres, one would need a higher value in order to get an M1 curve and a smaller value for an M2 curve. Those values have been set as 2 m and 1 m respectively.

Table 5.1.5.1. Boundary conditions set for the M1 and M2 curves in the channel, with HEC-RAS 5.0

	M1 CURVE	M2 CURVE
Upstream BC	Steady discharge: 200 m ³ /s	Steady discharge: 200 m ³ /s
Downstream BC	Water depth 2 m	Water depth 1 m
Curve searched		

M1 curve results

The results show the expected gradient of water depths, starting from around 1.89 - 1.88 metres (very close to the normal depth for the discharge applied and critical depth at the same time) at the upstream end and growing up the level until 2 metres water depth at the downstream end.

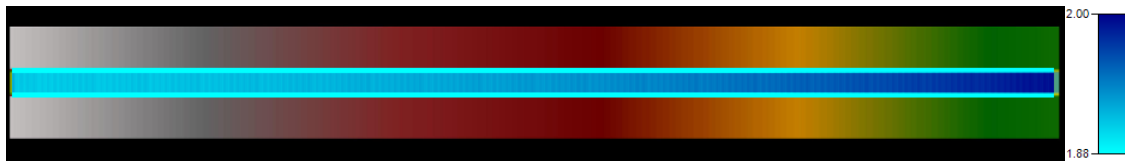


Figure 5.1.5.2. Water depth in the case of M1 curve in the channel. Units in metres.

Therefore, if depth increases in downstream direction, flow velocity must decrease in the same direction, according to the equation $u = \frac{q}{d}$, where u is the flow velocity, q is the discharge over width and d is the water depth. The following figure with the flow velocity results are showing exactly this phenomena:

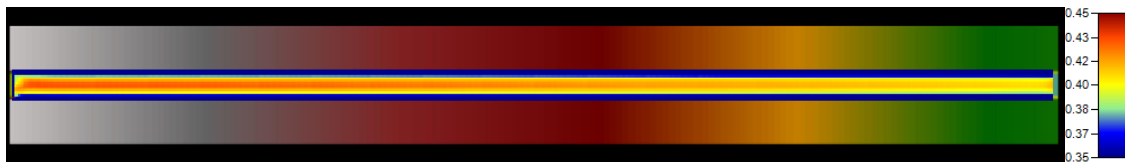


Figure 5.1.5.3. Flow velocity in the case of M2 curve in the channel. Units in metres.

M2 curve results

The results show the expected gradient of water depths, starting from 1.88 metres (normal depth for the discharge applied and critical depth at the same time) at the upstream end and lowering the level until 1 metre water depth at the downstream end.



Figure 5.1.5.4. Water depth in the case of M2 curve in the channel. Units in metres.

Therefore, if depth decreases in downstream direction, flow velocity must increase in the same direction. Again, the following figure with the flow velocity results are showing exactly this phenomena:

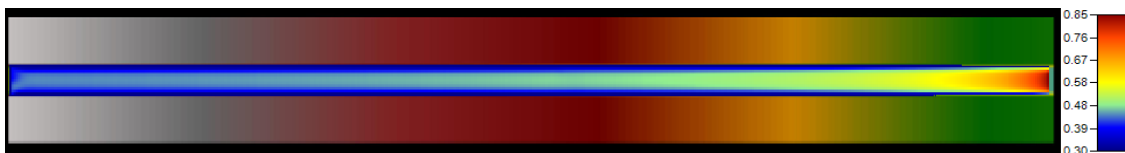


Figure 5.1.5.5. Flow velocity in the case of M2 curve in the channel. Units in metres.

In sum, these extra tests regarding M-type curves have led to the expected results.

After this series of simulations, it is concluded that the workability basics with HEC-RAS 5.0 have been learnt and that the next sections can already handle more complex simulation scenarios.

5.2. REAL CASE: FLUVIÀ RIVER

Once the workability of HEC-RAS 5.0 new version has been tested next to Delft3D, a more complex problem is presented. The following sections describe a two-dimensional hydrodynamic study based on a small reach of Fluvià River, with HEC-RAS 5.0.

5.2.1. CASE DESCRIPTION

Contextualization

Fluvià river basin is located in the Catalan province of Girona, in Spain. This basin has a total surface of almost 1000km² and comprises other sub basins such as the Gum, the Riera de Bianya, the Llierca, the Borró and the Ser basins. Also, Fluvià river basin is considered inside a bigger system, so-called Sistema Nord de les Conques Internes de Catalunya (CIC). The basin is limited by the Pyrenees and Pre-Pyrenees in the north, Serralada Transversal Mountains in the west, Centenys, l'Aire and Ventalló in the south and by the Mediterranean Sea in the east. (ACA, 2015)

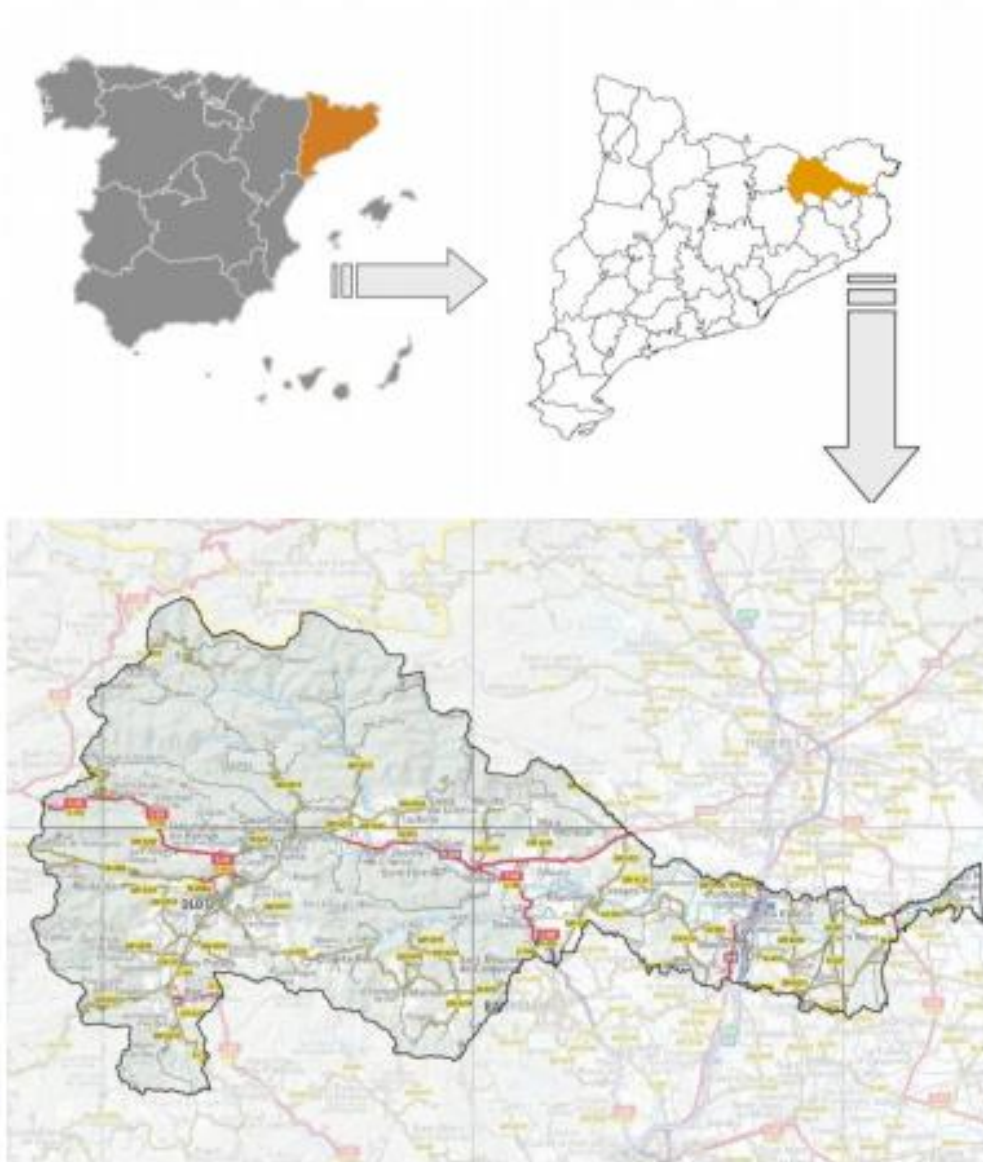


Figure 5.2.1.1. Fluvià River basin location in Spain (ACA, 2015)

Fluvià River longitude is 100km, originating in La plana d'en Bas, at 920m altitude, and ending up at the sea, in Gulf of Roses, close to the small village of Sant Pere Pescador. Its trajectory passes by close to Olot, Sant Joan de les Fonts, Castellfollit de Roca, Besalú, Esponellà and Torroella de Fluvià, this is, mainly Garrotxa, Pla de l'Estany and Alt Empordà regions. (ACA, 2015)

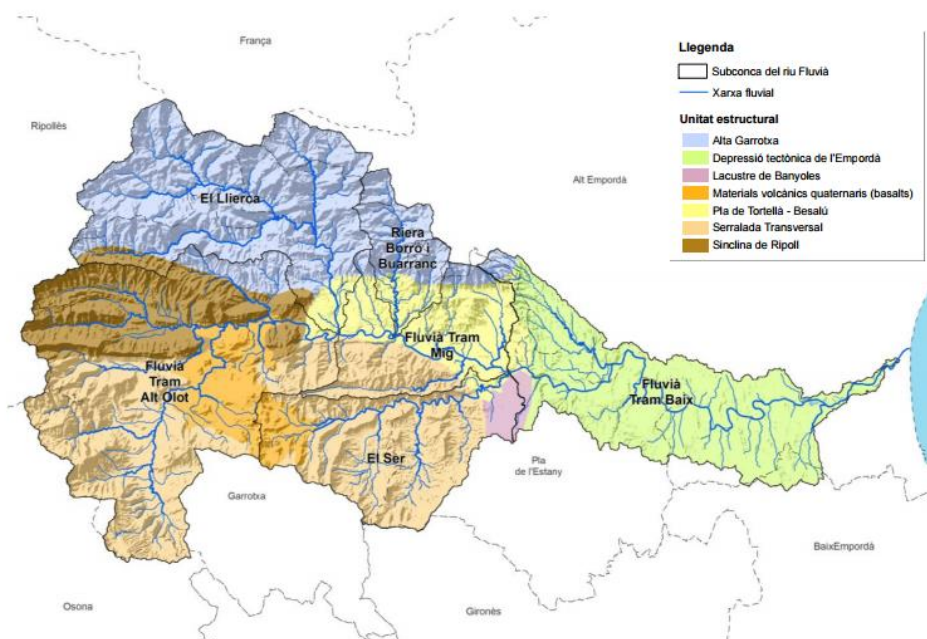


Figure 5.2.1.2. Fluvià River reaches and sub basins (ACA, 2015)

Nevertheless, the area of study is only a little reach of Fluvià River, located next to Torroella de Fluvià. The following image shows in more detail the investigation site.



Figure 5.2.1.3. Domain studied, top view satellite image (Google Maps, 2015)

Initial data

The initial data for the Fluvià river reach simulation consists in:

- The topography of the domain (see picture in the previous page), which consists in a text file (.txt) with data of $5 \times 5 \text{m}^2$ cell size that covers the full domain (546 columns and 249 rows). Thus, the domain measures are $2730 \times 1245 \text{m}^2$.
- Hydrological data, based on the total discharge data at the upstream end, given by Agència Catalana de l'Aigua (ACA, Catalan Water Agency) in July 2009.

Some problems appeared due to the upstream end hydrological data. At first, this data was given for a return period of 500 years (peak total discharge of $3400 \text{m}^3/\text{s}$). However, when running the program, an error appeared, saying that the water level was rising to more than 25 meters in a very short period of time, which is not possible in a realistic performance. The problem was that this discharge was definitely too severe for the small domain and the consequence was that, when the flood reached the domain limits, those limits behaved like walls and the full domain was filled with water, like a swimming pool.

Once the problem was noticed, the hydrological data was changed from 500 to 10 years of return period (with a peak discharge of $400 \text{m}^3/\text{s}$). This new discharge first resulted in a proper flooding simulation with a time step of 1 minute, which let us think the simulation would be definitive. However, after contrasting HEC-RAS 5.0 and an IBER simulation performed by the director of this project, Martí Sánchez-Juny, it was noticed that the time step was too high and that the result was not realistic, since the mentioned discharge would not be enough to flood the area. The time step value was then set to 0.25 minutes (15 seconds) and, as expected, a non-flooded situation was the result. Those “erroneous” simulations are also present in the results section for a better understanding of the reader about the process.

Finally, the discharge data was changed again in order to flood the area. This time, the return period chosen was of 50 years, relative to a maximum total water discharge of around $1200 \text{m}^3/\text{s}$. This discharge magnitude was definitely more appropriate for the case, since no conceptual errors appeared and the domain was flooded as expected. The results were successfully checked again with IBER.

In the results sections, not only the definitive simulation ($T=50$ years) but also the non-flooded ones ($T=10$ years) are analysed. Thus, in the end, three simulations are presented:

- Simulation 1: $T=10$ years, $\Delta t=1$ minute. “Erroneous” simulation.
- Simulation 2: $T=10$ years, $\Delta t=0.25$ minute. “Non-flooded” simulation.
- Simulation 3: $T=50$ years, $\Delta t=0.25$ minute. “Flooded” simulation.

The hydrological data obtained for the performance of the mentioned simulations follows in the next page.

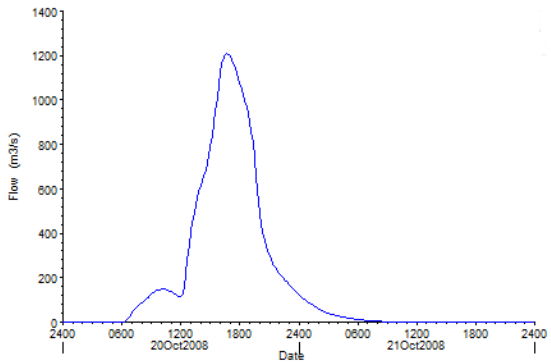
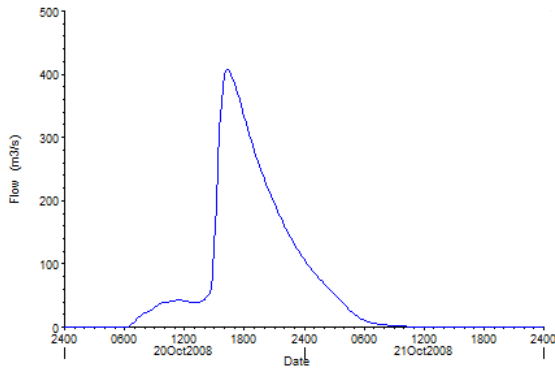


Figure 5.2.1.4. Fluvià hydrograph for T=10 years **Figure 5.2.1.5.** Fluvià hydrograph for T=50 years

Table 5.2.1.1. Hydrograph data for T=10 years (ACA, 2009)

Date	Time	Discharge (m3/s)
20-oct-08	0:00	0
20-oct-08	7:00	8.3
20-oct-08	8:00	21.8
20-oct-08	9:00	30.2
20-oct-08	10:00	39.1
20-oct-08	11:00	41.9
20-oct-08	12:00	41.6
20-oct-08	13:00	38.9
20-oct-08	14:00	43.9
20-oct-08	15:00	129.3
20-oct-08	16:00	397.2
20-oct-08	17:00	386.4
20-oct-08	18:00	332.5
20-oct-08	19:00	279.7
20-oct-08	20:00	234.1
20-oct-08	21:00	195
20-oct-08	22:00	161.2
20-oct-08	23:00	131.8
21-oct-08	0:00	106.9
21-oct-08	1:00	86.2
21-oct-08	2:00	68.5
21-oct-08	3:00	52.4
21-oct-08	4:00	36.1
21-oct-08	5:00	19.7
21-oct-08	6:00	10.3
21-oct-08	7:00	5.8
21-oct-08	8:00	3.5
21-oct-08	9:00	2.1
22-oct-08	0:00	0

Table 5.2.1.2. Hydrograph data for T=50 years (ACA, 2009)

Date	Time	Discharge (m3/s)
20-oct-08	0:00	0
20-oct-08	7:00	38.6
20-oct-08	8:00	84.9
20-oct-08	9:00	126
20-oct-08	10:00	147.7
20-oct-08	11:00	136.2
20-oct-08	12:00	115.2
20-oct-08	13:00	404.4
20-oct-08	14:00	612.8
20-oct-08	15:00	789.5
20-oct-08	16:00	1123.6
20-oct-08	17:00	1197
20-oct-08	18:00	1075.4
20-oct-08	19:00	900.6
20-oct-08	20:00	489.4
20-oct-08	21:00	299.7
20-oct-08	22:00	221.5
20-oct-08	23:00	168.5
21-oct-08	0:00	123.8
21-oct-08	1:00	88.5
21-oct-08	2:00	60
21-oct-08	3:00	39.6
21-oct-08	4:00	26.8
21-oct-08	5:00	18.6
21-oct-08	6:00	12.3
21-oct-08	7:00	7.1
21-oct-08	8:00	3.8
21-oct-08	9:00	2
21-oct-08	0:00	0

5.2.2. CONSIDERATIONS

The case study site has some characteristics and considerations that must be understood before reading the results of the simulation performance.

Roughness coefficient

Manning's coefficient of roughness has been considered $n=0.035$. This value has been extracted from a morphodynamic study of "Planificació de l'espai fluvial de la conca del Fluvià", by ACA. The same value is applied to both the river bed and floodplains, for simplification issues.

Downstream boundary condition

With HEC-RAS 5.0, the user can set a "Normal depth" in the downstream boundary condition. This feature works by means of a "warming up time", formally called initial conditions time, in which the model "warms up" for some time in the beginning of the simulation in order to set a normal depth at the downstream end. This methodology has been applied in this case, with an initial conditions time of one hour.

Thin dam

The reach of study contains a thin dam, located in the centre of the domain. Some hydrodynamic models include the option to add thin dams to the simulation reach. This is possible, for instance, in models like Delft3D. However, not only this feature has not been applied in the case simulation, but also it would have been wrong to apply it, since the topography data is already considering the terrain elevation at the dam points, so the program already takes that into account.

Bridge

There is a road bridge that crosses the reach of study. Sometimes, for very precise simulations, one can consider the influence of the bridge piles in the water flow. This can be applied in models like Delft3D using the option Dry points, for instance. However, for simplification, this effect has been considered negligible in the simulations of this document.

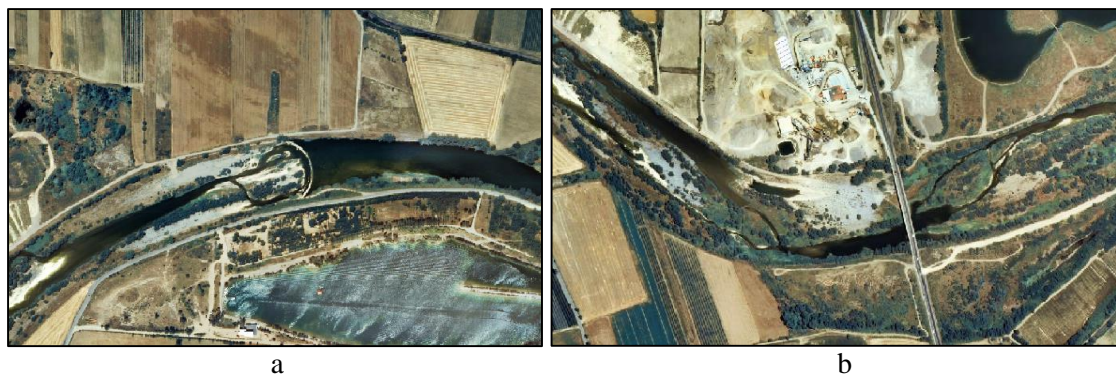


Figure 5.2.2.1. a) Thin dam top view (Google Maps, 2015)
b) Bridge top view (Google Maps, 2015)

Latitude for Coriolis

In order to take into account the Coriolis forces, the real value for the latitude of the real case study is set, this is, 42.17 degrees.

5.2.3. PERFORMANCE

HEC-RAS 5.0 simulation functionality

In brief summary, the steps applied for HEC-RAS 5.0 simulation are the following:

- Input topography from text file with RAS Mapper
- Grid creation with Geometry data window
 - o Define area
 - o Define cell size: 5x5m₂
 - o Define Boundary condition lines
- Flow definition in Unsteady flow data edition
 - o Flow hydrograph at upstream boundary condition
 - o Normal depth at downstream boundary condition
- Run simulation
- Analyse results

Calculation grid

The calculation grid of study is a rectangular grid with by 5x5m² squared cells. In this case, the mesh has been created with 82328 cells. This is a notably detailed mesh taking into account the small domain and the apparent simplicity of the problem.

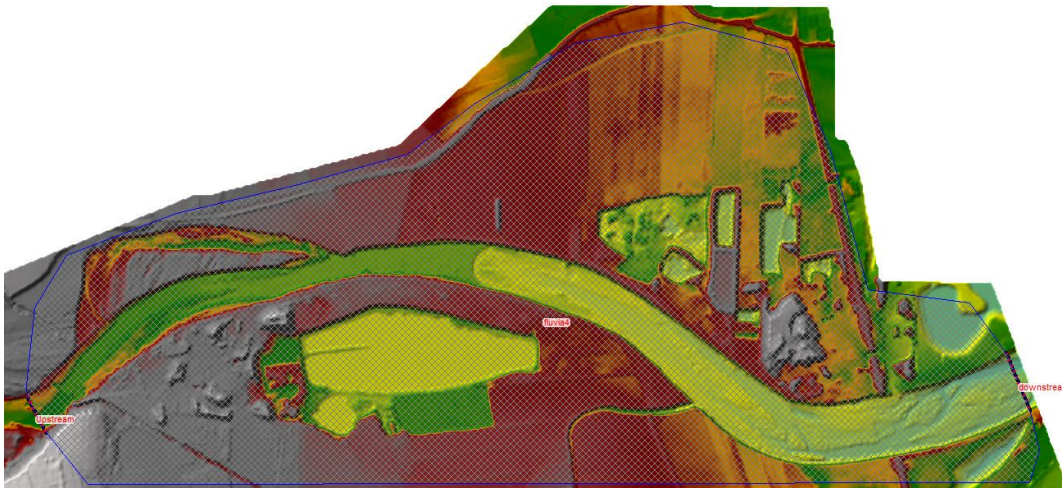


Figure 5.2.3.1. Terrain with the mesh and boundaries applied, with HEC-RAS 5.0

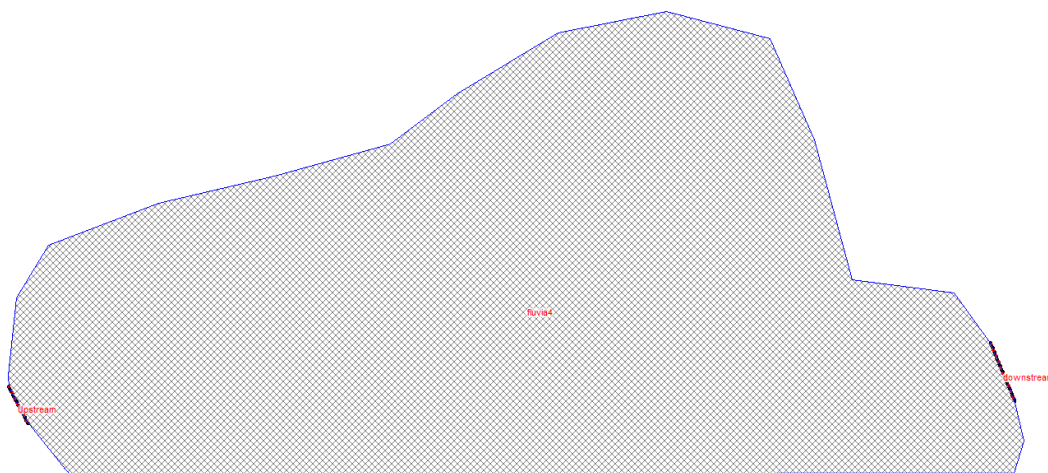


Figure 5.2.3.2. Mesh and boundaries used for Fluvia River reach, with HEC-RAS 5.0

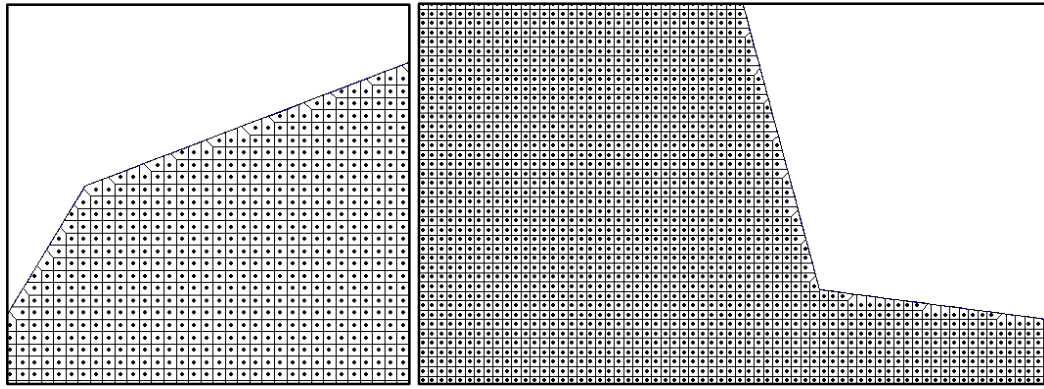


Figure 5.2.3.3. Detailed view for mesh with squared cells used

5.2.3.1. PROBLEMS FOUND

During the performance of the real case simulation, some obstacles that led to an increase of the expected work time were found.

Regarding data input:

- The data initially received consisted of the topography of the area and the hydrograph for a return period of 500 years. As previously explained, since the total discharge for 500 years of return period is huge, the water was reaching the limits of the (small) domain. This would not be a problem if it was not because the program considers the limits as vertical walls by defect, so the resulting simulation was a “full swimming pool”, with no technical or hydrodynamic interest for us. Since it was difficult to notice what was happening, why did it show an error, this obstacle led to a big loss of time. The solution was to change the hydrological data from 500 to 10 years of return period, so that the domain was not completely filled with water. This data was finally changed again to a return period of 50 years.

Regarding simulation performance:

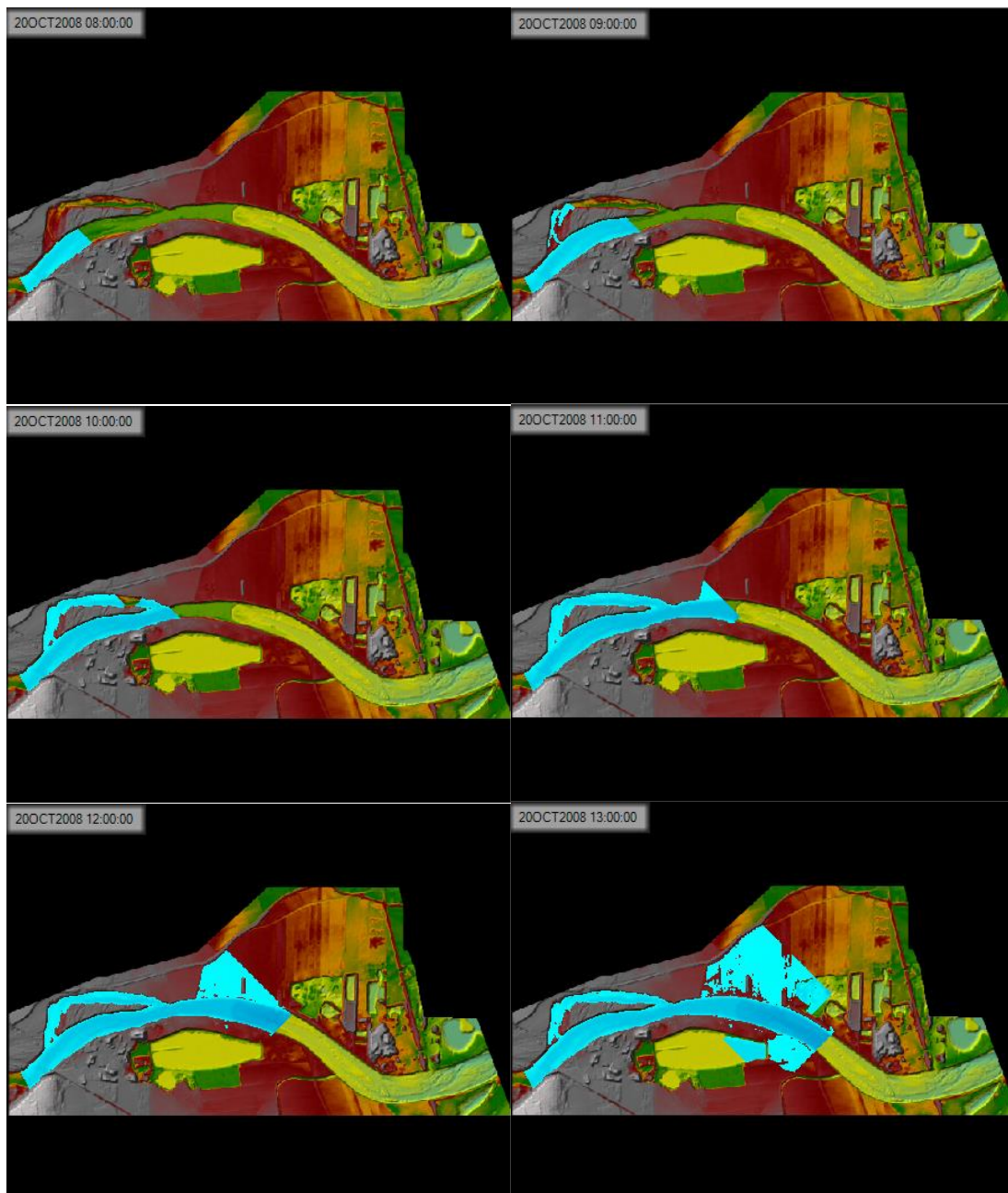
- The initial time step set was 1 minute. This led to a too high Courant number (CFL), situation in which lots of numerical instabilities arise. In consequence, Simulation 1 modelled a flooding scenario when there was actually no flood for the hydrological data introduced. As explained, the next simulation was performed with a time step of 15 seconds, which solved this instability problems.

5.2.4. RESULTS

Simulation 1: T=10 years, $\Delta t=1$ minute. “Erroneous” simulation.

As mentioned in section 3.2.2.1, at first, the flooded situation simulation was thought to be correct with hydrological data of a return period of 10 years. However, it was not, since the time step applied was 1 minute and had to be lowered until 0.25 minutes, this is, 15 seconds, which led to different results, showing flooding where, in reality, there was not. Although this can be considered a mistaken simulation, the results are shown for a better understanding about what happened.

The following series of images show the water depth behaviour for this simulation over time. One can easily distinguish a flooding behaviour of the flow.



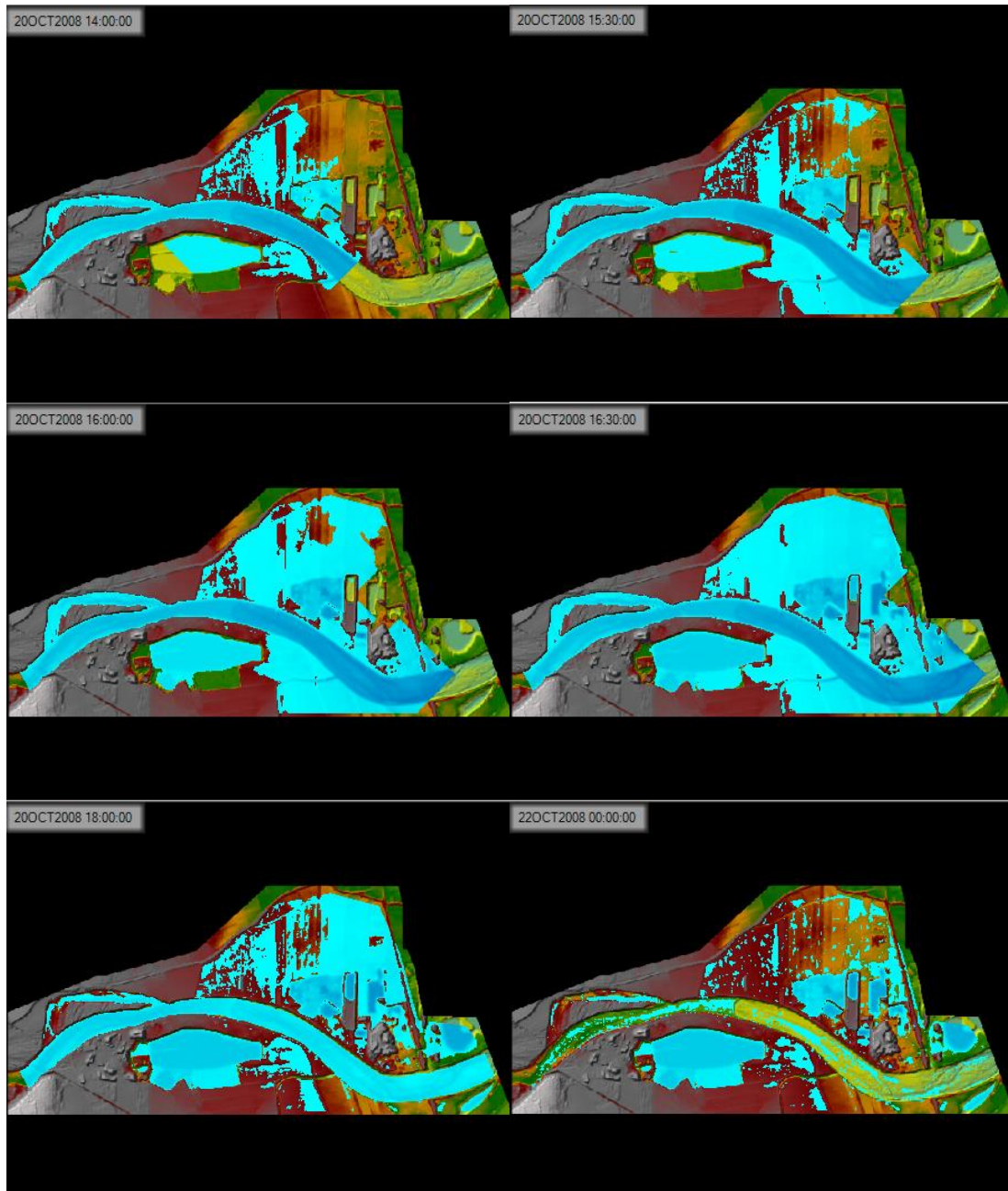


Figure 5.2.4.1. Flooding flow behaviour series of Fluvia River simulation 1 with HEC-RAS 5.0

According to IBER simulation checks, this observable flooding situation was not realistic, since the hydrological data applied, with a peak discharge of around $400\text{m}^3/\text{s}$ was not supposed to results in such a severe flood in the area.

It was then concluded that there were instabilities due to a too high Courant number (CFL). Thus, the time step was reduced for the next performances.

Simulation 2: T=10 years, $\Delta t=0.25$ minute. “Non-flooded” simulation.

After realising the previous simulation was erroneous, the time step was switched from $\Delta t=1\text{min}$ to $\Delta t=0.25\text{min}$. This change let us notice that the flow scenario for a hydrological data of a return period of 10 years was not at all a flood.

The following series of images show the water depth behaviour for this simulation over time. One can easily distinguish a non-flooding behaviour of the flow.

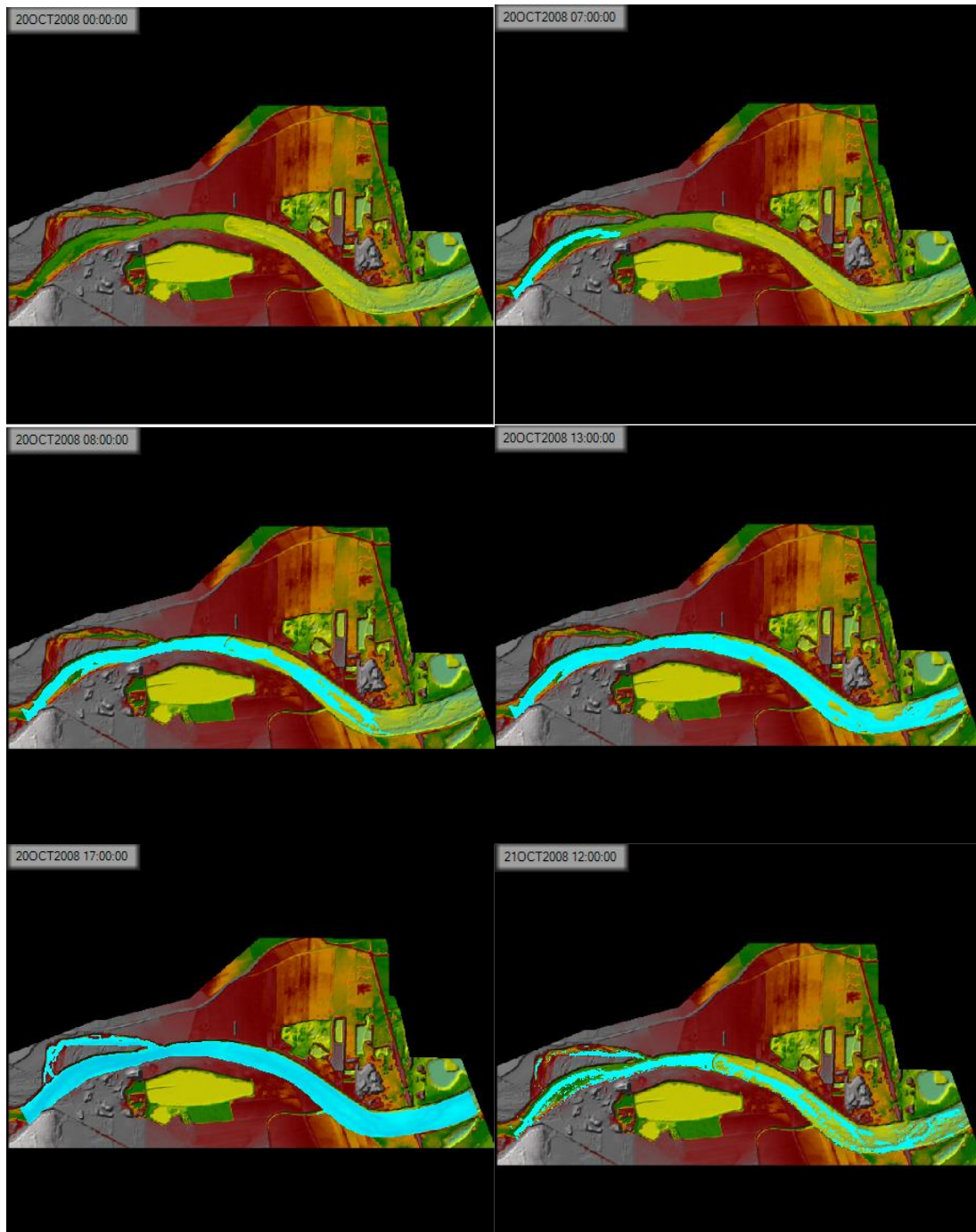


Figure 5.2.4.2. Non-flooding flow behaviour series of Fluvità River simulation 2, with HEC-RAS 5.0

The four first pictures show how the Fluvità River gets full of water in its main river channel. In the fifth, the peak water discharge fill it completely but, contrary to first expectations, cannot reach the floodplains. Finally, the last picture shows how the river dries out.

Simulation 3: T=50 years, $\Delta t=0.25$ minute. “Flooded” simulation.

After realising the previous simulation describes a non-flooding situation, the hydrological data has been changed in order to simulate a flood in the channel floodplains. The new hydrological data corresponds to a return period of 50 years, obtained by Agència Catalana de l’Aigua (ACA) in 2009. This is the definitive and previously wanted simulation: a realistic simulation of a flood situation in Fluvià River and the surrounding area.

Three main stages can be distinguished in the flow progress of Simulation 3.

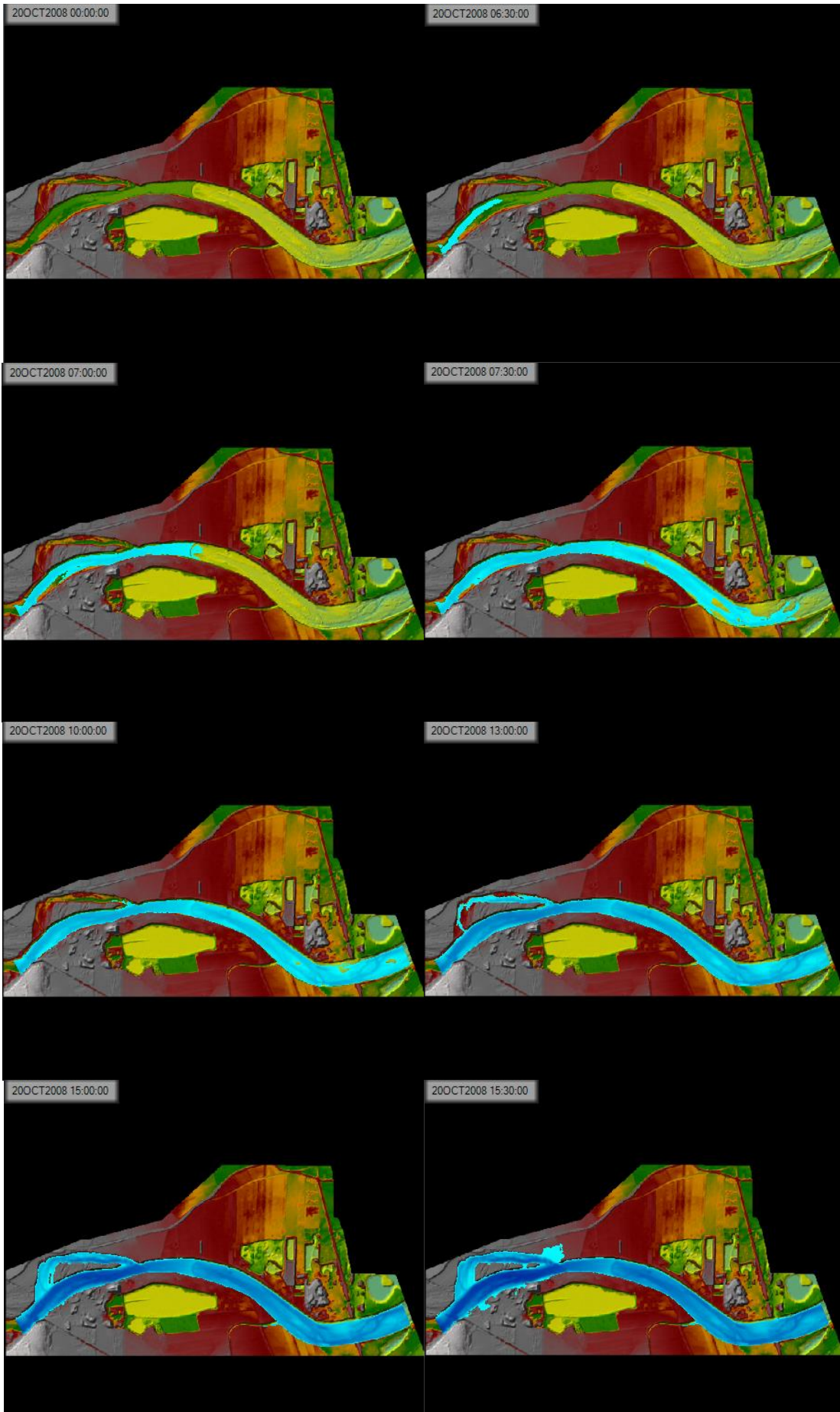
One first stage in which the water appears from the upstream end and fills the river main channel. This stage comprises the times from the simulation start time, 20OCT2008 00:00, to 20OCT2008 12:30, when the water flow starts flooding the floodplains.

The second stage is the flooding of the floodplains itself, the main objective of this simulation. The flooding stage develops from 20OCT2008 12:30 to 20OCT2008 19:00. This period of time is exactly when the most part of the total discharge is released. Thus, it makes perfect sense that the flood occurs by then. Also, it is noticeable that the northern floodplain is fully inundated but not the southern one. This may be because of topography issues, this is, the ground level in the northern side is slightly lower than in the south side, and also because of the river bend, that makes the water reach the northern floodplain more easily due to forces of inertia.

Since 20OCT2008 19:00 until the end of the simulation, the floodplain surfaces start drying out until most of the wet parts end up being dried, also in the main channel area. This drying out step is the third relevant stage of the simulation.

The following two pages show *Figure 5.2.4.3*, series of images where the water depth behaviour for this simulation over time can be observed. One can easily distinguish the flooding behaviour of the flow.

Furthermore, other aspects of the simulation results are explained in detail.



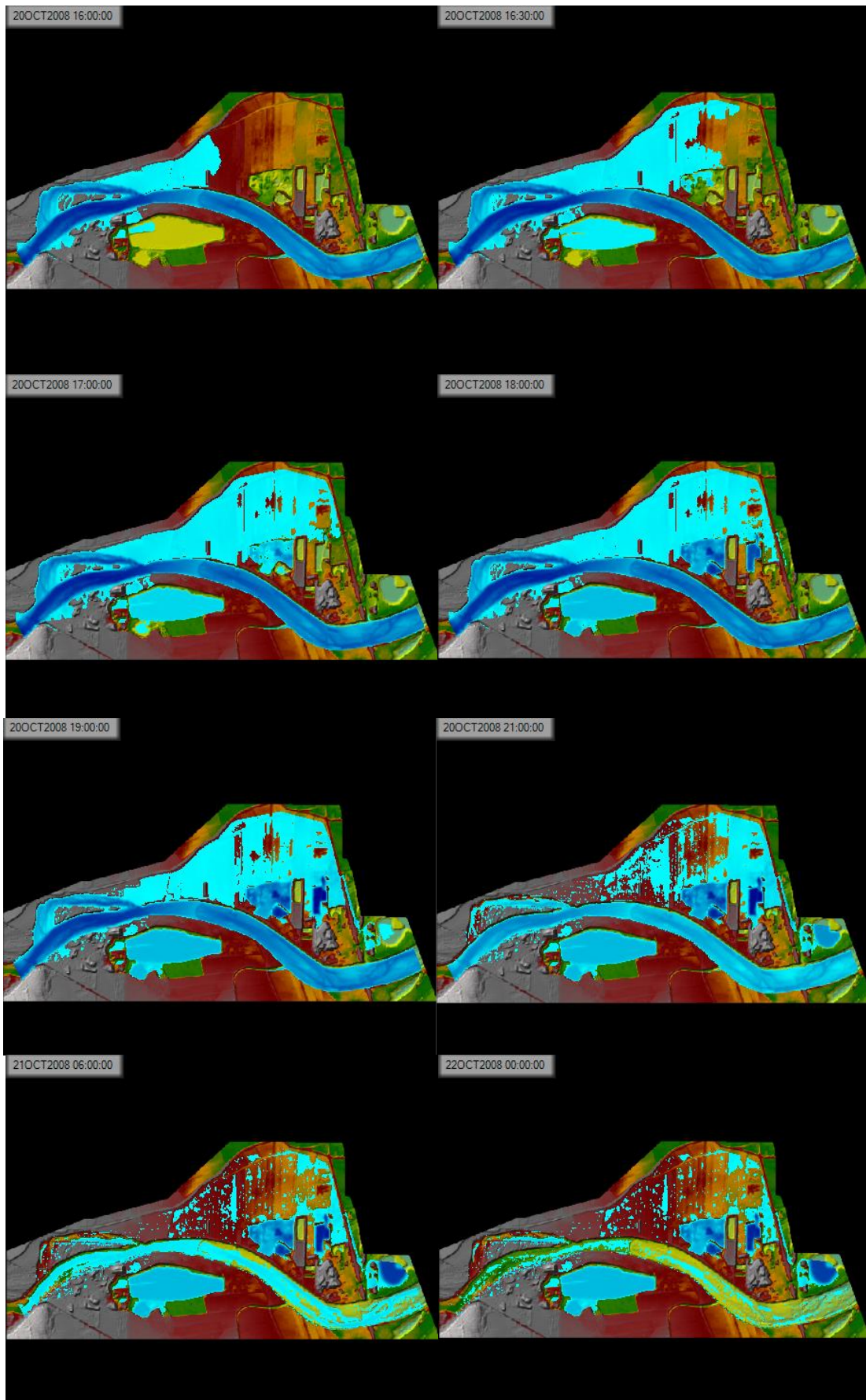


Figure 5.2.4.3. Flooding flow behaviour series of Fluvia River simulation 3 with HEC-RAS 5.0

Regarding the maximum depth, the floodplains are flooded until a depth of around 0.40 to 0.60 metres, which can be considered as a notable flood situation.

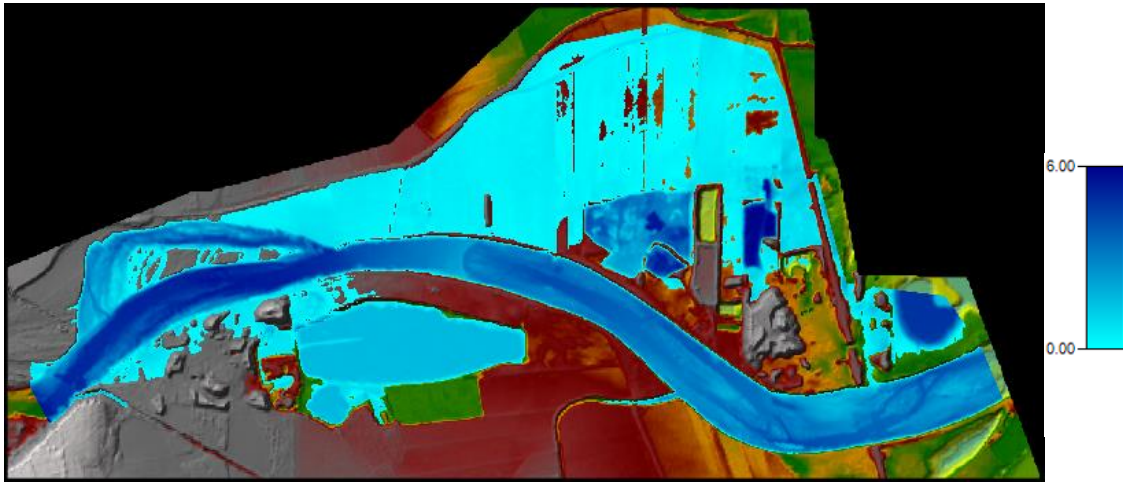


Figure 5.2.4.4. Maximum water depths at Fluvia River reach in Simulation 3, with RAS Mapper interface. Units in metres.

Regarding flow velocity, one can tell there have been some instability errors if one checks the maximum flow velocities with RAS Mapper interface. The results show, in some points, very high velocities, which are impossible in a real situation. Those errors arise when we found very small water depths, since the velocity calculation is $u = \frac{q}{d}$, where u is the flow velocity, q is the discharge over width and d is the water depth. Thus, for very small values of the water depth, the flow velocity becomes really high. Besides that, the velocity values along the reach are, in general, realistic.

Observation: note that this high unrealistic values of the velocity are shown, for instance, on top of the thin dam, which makes perfect sense since the water depth at those points is really low.

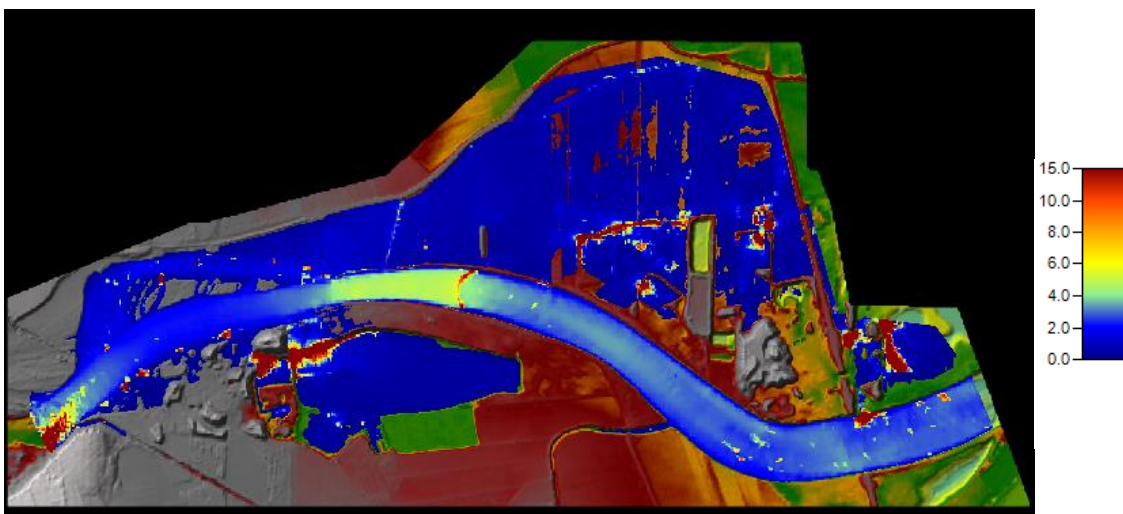


Figure 5.2.4.5. Maximum flow velocities at Fluvia River reach in Simulation 3 with RAS Mapper interface. Units in m/s.

In particular, some points are analysed. First, the water depth and the flow velocity are checked for two points in the main channel; one upstream and another downstream from the thin dam.

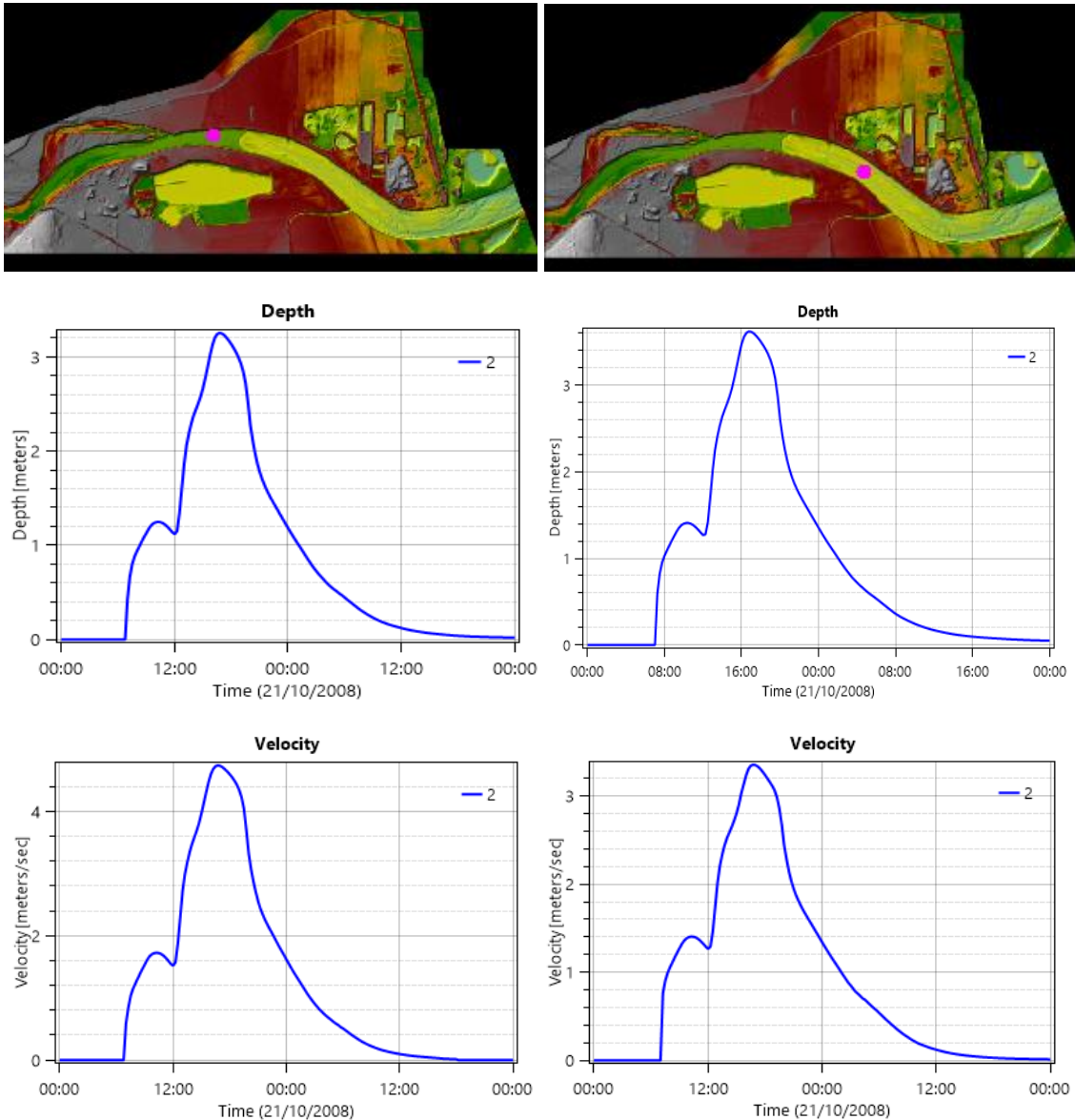


Figure 5.2.4.6. Location, water depth over time graph and flow velocity over time graph of two points in the main river channel in Fluvia River Simulation 3, with HEC-RAS 5.0

Very similar results are shown for both points in the main river channel. However, one can observe that the first point has higher flow velocity and lower water depth than the second. This makes perfect sense, taking into account the fact that both points have the same initial water discharge condition and that those parameters are defined by the formula presented before for an ideal channel: $u = \frac{q}{d}$. The fact that the velocity is higher in the first point than in the second is a consequence of the presence of the thin dam in between both points.

Also, two information points have been set in the floodplains in order to get some output about the flooding behaviour of this simulation. Both points are located at the northern floodplain since the opposite floodplain has not been fully flooded.

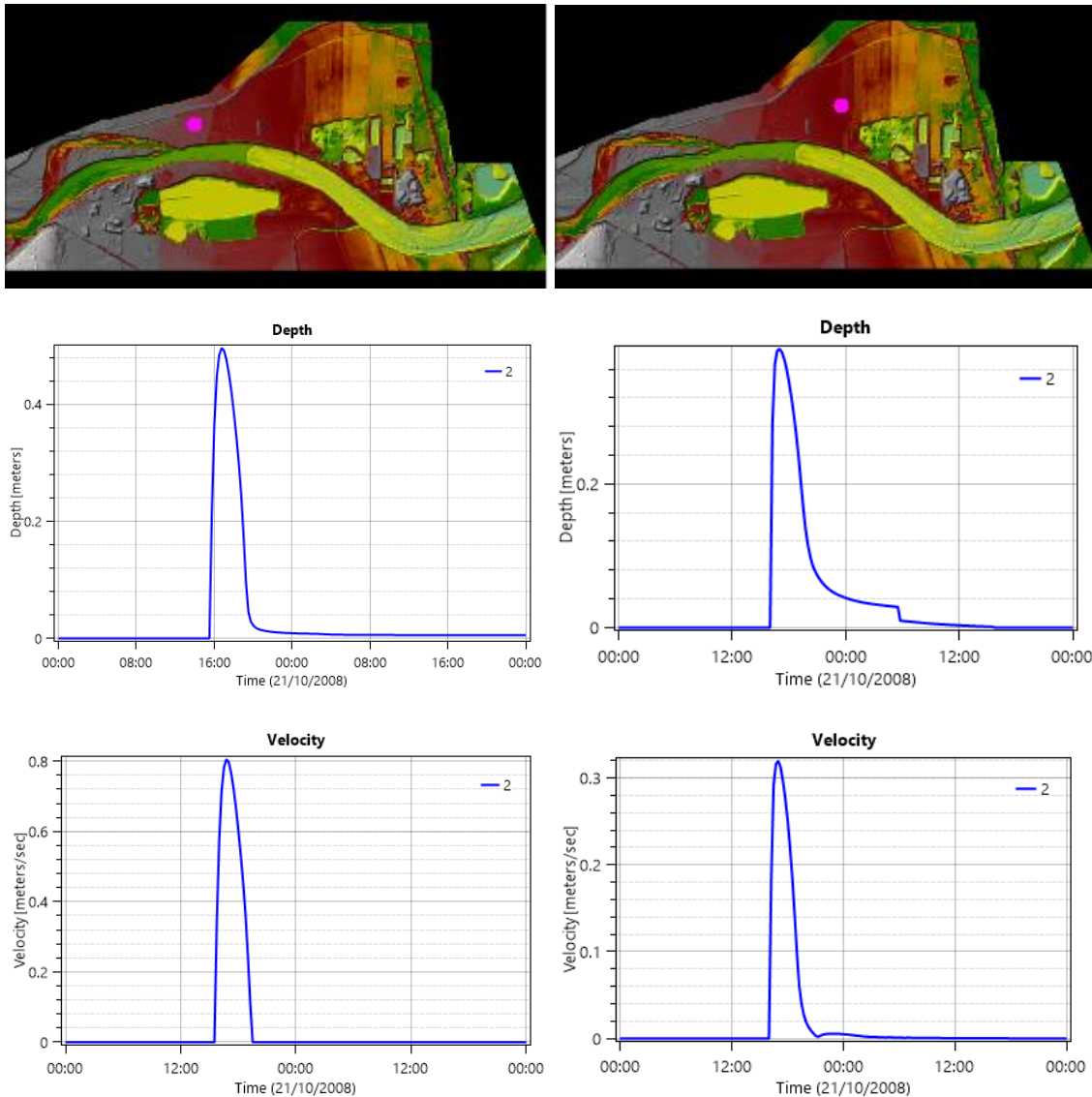


Figure 5.2.4.7. Location, water depth over time graph and flow velocity over time graph of two points in the northern floodplain in Fluvia River Simulation 3, with HEC-RAS 5.0

The results show negligible values until the water discharge reaches the area, which is a little after than in the main channel case, for obvious reasons. One can observe much smaller velocities and depths, which is characteristic in the floodplain regions. However, the depth is considerable during the flooding period, reaching until more than 0.5 metres in a considerable floodplain area.

Therefore, the studied reach can be considered as an easy-floodable area for hydrological data related to a return period of 50 years.

5.2.5. CONTRAST WITH IBER

All the previous simulation results for Fluvià River reach have been contrasted with simulation results made with IBER, obtained from the director of this project, Prof. Martí Sánchez-Juny. This IBER simulation has been performed with the only purpose of contrasting the results of this paper.

Of course, the boundary conditions applied are the same as in the HEC-RAS 5.0 simulation performed before, in order to obtain comparable results. A discharge related to the data obtained from ACA, regarding a return period of 50 years, has been applied at the upstream end condition, while the critical depth has been set as a downstream boundary condition.

One can compare this results to the HEC-RAS 5.0 simulation results and observe clear similarities. Again, the major part of the flooded area comprises the northern floodplain. Flow velocities are higher right before the thin dam, just as it was happening in the HEC-RAS 5.0 performance.

One can state that the last simulation results of this document have been successfully contrasted with another simulation of the same situation, performed by experts, with a comparable program, IBER. Therefore, the two-dimensional river flood simulation performed with HEC-RAS 5.0 in the Fluvià River reach for the obtained hydrological data related to a return period of 50 years is considered successful.

Figures with the results of maximum depths, maximum water levels and maximum velocities obtained with IBER are presented.

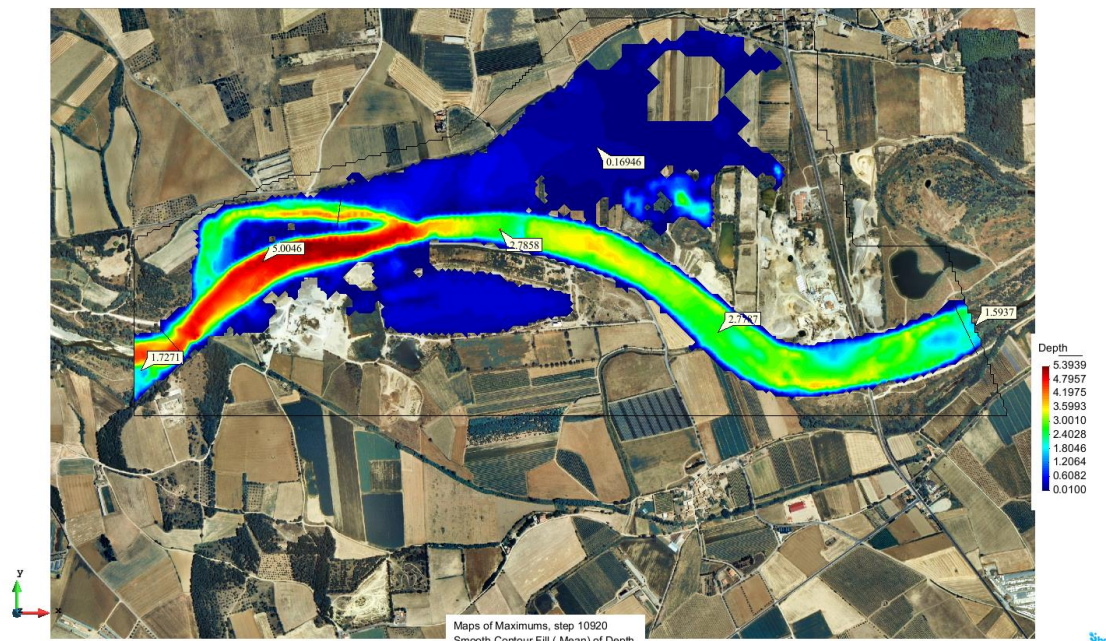


Figure 5.2.5.1. Maximum depths in Fluvià River simulation obtained with IBER

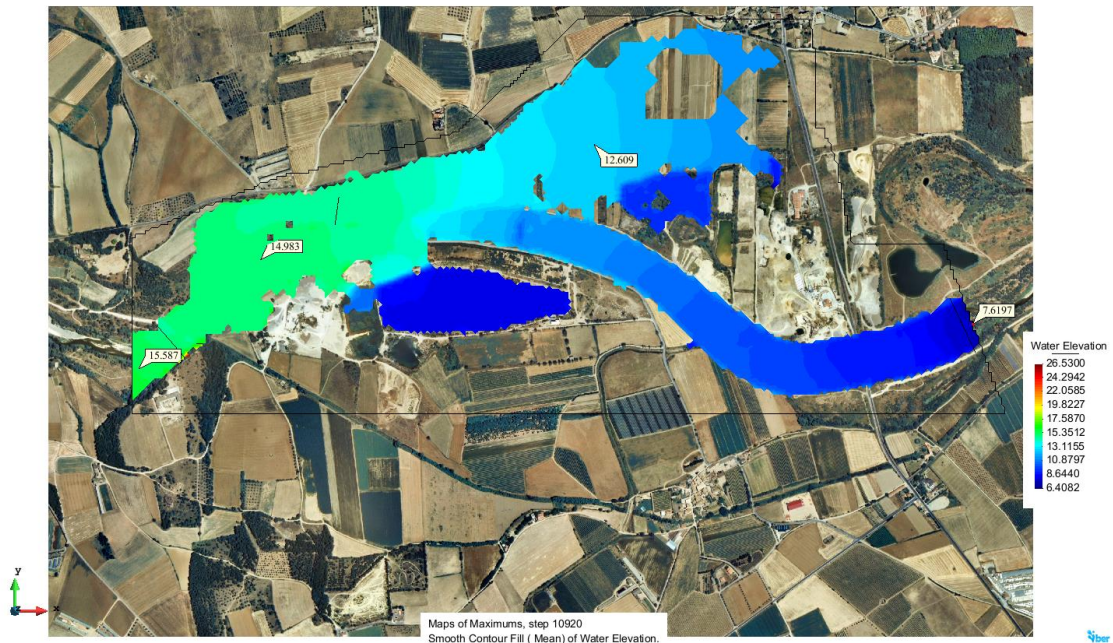


Figure 5.2.5.2. Maximum water elevations in Fluvia River simulation obtained with IBER

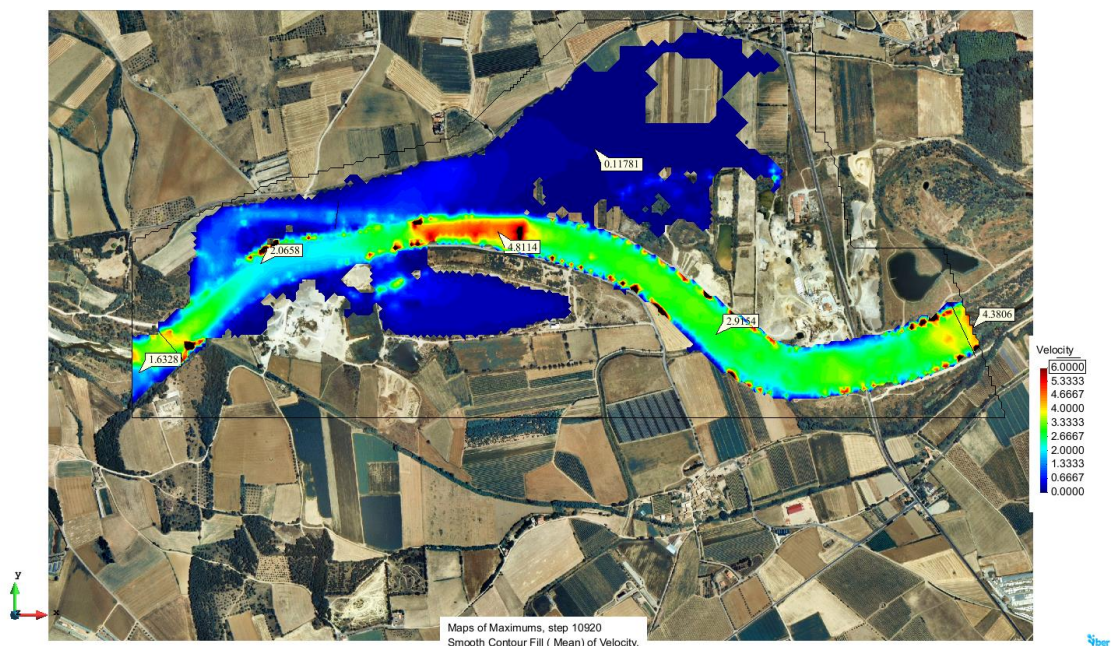


Figure 5.2.5.3. Figure X: Maximum velocities in Fluvia River simulation obtained with IBER

5.3. OVERVIEW OF THE SIMULATIONS PERFORMED

Once all the simulations have been successfully performed, a table of analysis has been considered useful in order to have an objective overview of the work.

Table 5.3.1. Overview table of the simulations performed

Case	Ideal case: Prismatic channel				Real case: Fluvia River		
	HEC-RAS 5.0		Delft3D		HEC-RAS 5.0		
Simulation	-	-	-	-	Simulation 1	Simulation 2	Simulation 3
Flow	Steady	Unsteady	Steady	Unsteady	Unsteady	Unsteady	Unsteady
Grid	Rectangular	Rectangular	Rectangular	Rectangular	Shaped	Shaped	Shaped
Cells	Squared 25x25m ²	Squared 25x25m ²	Squared 25x25m ²	Squared 25x25m ²	Squared 5x5m ²	Squared 5x5m ²	Squared 5x5m ²
Time step used	6s	6s	6s	6s	1 min	15s	15s
Initial situation	Use of warming time	Use of warming time	Initial conditions file	Initial conditions file	Use of warming time	Use of warming time	Use of warming time
Upstream BC	Created constant discharge 200m ³ /s	Created unsteady discharge (peak 450m ³ /s)	Created constant discharge 200m ³ /s	Created unsteady discharge (peak 450m ³ /s)	Hydrological data by APA T=10 years	Hydrological data by APA T=10 years	Hydrological data by APA T=50 years
Downstream BC	Water level 1.87 m	Water level 1.87 m	Water level 1.87 m	Water level 1.87 m	Normal depth	Normal depth	Normal depth
Roughness coefficient	Manning n=0.035	Manning n=0.035	Manning n=0.035	Manning n=0.035	Manning n=0.035	Manning n=0.035	Manning n=0.035
Equations	Full momentum	Full momentum	Full momentum	Full momentum	Diffusive wave	Full momentum	Full momentum
Latitude for Coriolis	0 deg	0 deg	0 deg	0 deg	42.17 deg	42.17 deg	42.17 deg
Flooding behaviour	No	Yes	No	Yes	Yes (erroneous)	No	Yes
Computational time	1h16min	1h17min	29min	14min	45min	4h05min	4h17min
Fr<1	Yes	Yes	Yes	Yes	Yes	Yes	Yes

6. CONCLUSIONS

Conclusions regarding the initial purposes and research questions can be extracted from the different parts of this paper.

From the intercomparison between the main hydrodynamic numerical models, this is, between HEC-RAS 5.0, Delft3D, IBER, SOBEK and 3Di, the following conclusions can be extracted:

- The most important features to consider when comparing hydrodynamic models are: dimensions, hydrodynamic equations, numerical equations resolution method, hydraulic roughness, turbulence submodels, suitability for supercritical flow, structures, combination with transport of substances and water quality, combination with sediment transport and morphological evolution, local running availability and open source availability.
- The most important features to consider when comparing hydrodynamic models regarding river flood modelling are: dimensions, hydrodynamic equations, numerical equations resolution method, hydraulic roughness, turbulence submodels, suitability for supercritical flow, structures and local running availability.
- HEC-RAS 5.0 is definitely comparable to the main hydrodynamic models in use.
- Delft3D and SOBEK were appropriate models to compare to HEC-RAS 5.0 from a practical approach in this paper.
- Although all the models studied are able to perform realistic river flood simulations, they all have different features and work differently.

From the study comparison in two-dimensional numerical modelling of the hydrodynamic behaviour of an ideal prismatic channel reach between HEC-RAS 5.0 and Delft3D, created for the only purpose of this document in an imaginary environment, with created hydrological data, the following conclusions can be extracted:

- HEC-RAS 5.0 presented a little instability in the unsteady flooding case, resulting in two thin longitudinal dry areas at the slope change between the floodplains and the levees. This is not considered a major error but it is of interest to report.
- Delft3D presented a notable dry area at the last third of the reach, in the floodplains, where there was supposed to be water with very small depth values. This can be due to tolerance issues with not further importance, as explained in the simulation results section.
- HEC-RAS 5.0 computational time is in general higher than for Delft3D for same exact situations.
- Both models performed realistic simulations of the two situations proposed, this is, for steady non-flooding and unsteady flooding cases for the same prismatic channel, although they have different workability and presented slightly different results.

From the study in two-dimensional numerical modelling of the hydrodynamic behaviour of Fluvità River reach in the environment of Torroella de Fluvità, for hydrological data concerning a period of return of 50 years, using HEC-RAS 5.0, the following conclusions can be extracted:

- The studied area is an easily-floodable terrain for 50 years of return period data.
- The maximum water depth range found in the floodplains is between 0.5 and 0.7 m, which is considerable taking into account the small magnitude of Fluvità River annual discharge and that the data is related to a return period of only 50 years.
- The maximum water velocity range found in the floodplains is between 0.7 and 1.3 m/s.
- The maximum water velocity range found in the river is between 4.5 and 5.5 m/s at the area before the thin dam. Downstream from the thin dam and in consequence of it, velocities decrease notably. Note: the error explained in the next point is not considered for these velocity results data.

- Due to very small values of water depth, the program output showed very high values for the flow velocity, which were obviously not possible. This small instability, though, was only happening at certain locations, such as the thin dam and the upstream end, and at certain small periods of time, so it did not affect the general development of the river flood simulation.
- Despite those small errors, HEC-RAS 5.0 was able to perform a very realistic river flood simulation, according to the similarity of results with the contrast study performed by experts with IBER.

From this, one can conclude that HEC-RAS 5.0 is definitely competitive with other hydrodynamic models regarding 2D river flood modelling when it comes to simple scenarios. However, other programs, like is the case of Delft3D, are far more advanced when it comes to very complex simulations that include features such as combination with transport of substances and water quality or combination with sediment transport and morphological evolution, which are not yet available in HEC-RAS 5.0 for two-dimensional simulations.

7. REFERENCES

ACA: Agència Catalana de l'Aigua. (2015). Sitio web: http://aca-web.gencat.cat/aca/documentos/ca/publicacions/espais_fluvials/publicacions/estudis_pef/c_fluvia/pef_fluvia.htm#fragment-01

Bladé, E., Cea, L., Corestein, G., Escolano, E., Puertas, J., Vázquez-Cendón, M.E., Dolz, J., Coll, A. (2014). *Iber: herramienta de simulación numérica del flujo en ríos*. Revista Internacional de Métodos Numéricos para Cálculo y Diseño en Ingeniería, Vol.30(1) pp.1-10

Bladé, E., Corestein, G., Cea, L., Lara, A., Escolano, E., Coll, A. (2014). *Iber, a river dynamics simulation tool*. Barcelona, Spain: UPC.

Bladé, E., Lluén, W. E. (2015). *Aplicación de la nueva herramienta HEC-RAS 5.0 para cálculos bidimensionales del flujo de agua en ríos*. Barcelona, Spain: UPC.

Bladé, E., Sánchez-Juny, M. (2010). *Estudi en model numèric bidimensional del funcionament hidràulic del riu Fluvià a l'entorn de Torroella de Fluvià considerant el condicionament de la carretera C-31*. Barcelona, Spain: FLUMEN, E.T.S. d'Enginyers de Camins, Canals i Ports, UPC.

Bladé, E., Sánchez-Juny, M., Sánchez, H.P., Gómez, M. (2009). *Modelación numérica en ríos en régimen permanente y variable. Una visión a partir del modelo HEC-RAS*. Barcelona, Spain: Edicions UPC.

Blom, A. (2015). *River Engineering Lecture Notes*. Delft, The Netherlands: Faculty of Civil Engineering and Geosciences, Technical University of Delft.

Brunner, G. W. (2014). *Combined 1D and 2D Modeling with HEC-RAS*.

Cáceres, E.D. (2006). *Modelación numérica del Río Huancabamba en la zona del Embalse Limón*. Piura, Perú: Universidad de Piura, UDEP.

Deltares. (2014). *Delft3D-FLOW User Manual*. Delft, The Netherlands: Deltares.

Deltares. (2016). *SOBEK, Hydrodynamic, Rainfall Runoff and Real Time Control User Manual*. Delft, The Netherlands: Deltares.

European Commission.(2015). EU Floods Directive. Website: ec.europa.eu/environment/water/flood_risk

Flumen, Grupo de Ingeniería del Agua y del Medio Ambiente. (2014). *Modelización bidimensional del flujo en lámina libre en aguas poco profundas*. Barcelona, Spain.

Gilles, D., Moore, M. (2010). *Review of Hydraulic Flood Modeling Software used in Belgium, The Netherlands and the United Kingdom*. Iowa, USA: University of Iowa, College of Engineering.

Google Maps. (2015) [*Map of Torroella de Fluvià and surroundings, Catalonia, Spain*]. Website: <https://www.google.es/maps>

Gutiérrez, C. (2014). *Apuntes de Hidráulica*. Barcelona, Spain: E.T.S. d'Enginyers de Camins, Canals i Ports, UPC.

Johansson, M. (2012). *Evaluation of RANS turbulence models for the hydrodynamic analysis of an axisymmetric streamlined body with special consideration of the velocity distribution in the stern region*. Stockholm, Sweden: KTH Royal Institute of Technology.

Moffatt and Nichol (2005). *Hydrodynamic modeling tools and techniques. South Bay Salt Pond Restoration Project*. California, USA: Coastal Conservancy.

NOAA Office of Coast Survey (2015). *How Hydrodynamic Models Are Used*. Website: http://www.nauticalcharts.noaa.gov/csdl/learn_models.html

O'Connor, J.E., Costa, J.E. (2004). *The World's Largest Floods, Past and Present: Their Causes and Magnitudes*. Denver, USA: U.S. Geological Survey.

Pedrozo-Acuña, A., Torres-Freyermuth, A. (2011). *Sobre el uso de las ecuaciones de Navier-Stokes con el promedio de Reynolds en el campo de la ingeniería de costas*. Yucatán, México: Instituto de Ingeniería, Universidad Multidisciplinaria de Docencia e Investigación.

The Ras Solution, The place for HEC-RAS members. (2016). Website: <http://hecrasmodel.blogspot.nl/>

UPC, Departament d'Enginyeria Hidràulica, M. i A. (2010). *Estudi morfodinàmic del riu Fluvià*. Agència Catalana de l'Aigua. Website: http://aca-web.gencat.cat/aca/documents/ca/publicacions/espais_fluvials/publicacions/altres_estudis/040P0001/aca_pef2015c_02B02_estudi_morfodinamic_v1.pdf

US Army Corps of Engineers. (2016). *HEC-RAS River Analysis System User's Manual, version 5.0*. California, USA.

US Army Corps of Engineers. (2016). *HEC-RAS River Analysis System Hydraulic Reference Manual, version 5.0*. California, USA.

US Army Corps of Engineers. (2016). *HEC-RAS River Analysis System 2D Modeling User's Manual, version 5.0*. California, USA.

US Army Corps of Engineers. (2016). *HEC-RAS 5.0.1 River Analysis System Release Notes*. California, USA.

US Army Corps of Engineers. (2016). *HEC-RAS River Analysis System Applications Guide, version 5.0*. California, USA.

3Di Waterbeheer consortium. (2014). *3Di explained*. Delft, The Netherlands

3Di Waterbeheer consortium (2015). Website: <http://www.3di.nu/en/product-information-2/>

